

Positive feedback in species communities

NIOO thesis 105
ISBN: 978-90-393-5824-5

Positive feedback in species communities

Positieve terugkoppeling in soortengemeenschappen

(met een samenvatting in het Nederlands)

Proefschrift

ter verkrijging van de graad van doctor aan de Universiteit Utrecht op gezag van de rector magnificus, prof.dr. G.J. van der Zwaan, ingevolge het besluit van het college voor promoties in het openbaar te verdedigen op woensdag 12 september 2012 des middags te 2.30 uur

door

Daniël Jakob Gerla

geboren op 31 mei 1977
te 's-Gravenhage

Promotoren: Professor Dr. E. van Donk
Professor Dr. W.M. Mooij

Co-promotoren: Dr. B.W. Kooi
Dr. M. Vos

Contents

1	General introduction	1
2	Alternative stable states and alternative endstates of community assembly through intra- and interspecific positive and negative interactions	7
3	Photoinhibition and the assembly of light-limited phytoplankton communities	27
4	Effects of resources and predation on the predictability of community composition	45
5	Alternative states and population crashes in a resource-susceptible-infected model for planktonic parasites and hosts	61
6	Synthesis	83
	Bibliography	89
	Summary	99
	Samenvatting	101
	About the author	103
	Publications	105
	Acknowledgements	107

Chapter 1

General introduction

1.1 Priority effects

In ecology, a community is a group of organisms belonging to different species whose populations potentially interact, for instance through competition or predation. Species communities do not come into existence instantaneously, but develop over time in the process of community assembly. Community assembly proceeds through the arrival and subsequent population growth of species. Communities are thus constructed through species invasions. An intriguing question is: when do the arrival times of species determine the abundance of the species in a community in the long run? If the arrival times matter, a *priority effect* occurs. Priority effects imply that assembly history determines species abundances. The question of when priority effects occur is not just intriguing for its own sake. It may have consequences for biodiversity patterns at the regional scale because places which are initially identical or very similar may develop different species communities because arrival times differ between places (Shurin et al., 2004). It may also have consequences for how communities function (Fukami et al., 2010). Furthermore, priority effects imply that restoring a habitat after disturbance does not necessarily restore the original species community (Suding et al., 2004). The question of when priority effects occur is at the heart of this thesis.

To study community assembly, ecologists develop community assembly models (e.g. Drake, 1990; Luh and Pimm, 1993; Law and Morton, 1993; Capitan and Cuesta, 2011). These models consider a pool of potentially invading species (the regional species pool) and a local community which they may attempt to invade. The regional species pool has a fixed species composition and one-by-one species are randomly drawn from it and added to the local community. This process of random selection and addition is repeated ad infinitum. At the beginning of the assembly process the community may be empty, meaning there are no species in it. As time progresses, species from the regional species pool are introduced into the community. Successful invaders become, at least for some time, members of the community (they become

residents), interacting with their own and other species. After a number of invasions the community may attain a state in which none of the species that are not already a member can invade. Community assembly has then arrived at an *endstate* (Morton and Law, 1997; Law, 1999), and there are no long lasting trends of change in the abundances of species in the community. For a given regional species pool, there may be several endstates of community assembly, so that it depends on the arrival times of the species which endstate is eventually attained. This means that different runs of an assembly model, with the same regional species pool and the same local conditions in each run, may yield different communities at the community assembly endstate because the times at which species from the regional pool invade the local community are different between model runs. If this is the case, priority effects determine the species composition of the local community.

In this way, the concept of priority effects is closely linked to the idea of alternative stable states. Alternative stable states (or coexisting attractors) mean that the state (i.e. the abundances of species) that the community eventually attains depends on the initial state of the community. If there are several endstates of community assembly, these endstates represent alternative stable states. These community states are stable in the sense that after a small deviation from the stable state the community returns to that state. For instance, a community that is at an endstate, may undergo a small perturbation by an invasion attempt of a species that is not present in the community endstate. However, since the community was at an endstate, the invader has a negative net population growth rate and its population will go extinct and the community will thus return to the endstate.

I should be clear about what I mean with the state of a community. With community state I mean the population abundances (either density or numbers) of the species that make up the community. It is sometimes convenient to include other types of attractors than just stable equilibria in the definition of stable state, such as limit cycles and chaotic attractors (as do Grover and Lawton, 1994). Using the term state to refer to species abundances is different from how Law (1999) uses the term in the context of community assembly, who defines the state of a community as the set of species that are present, i.e. that have a positive density. In this definition community state is synonymous to species composition *sensu* Grover and Lawton (1994) and Law (1999), i.e. the identity of the constituent species of the community. Law (1999) makes the proposition that when studying the dynamics of community assembly, the most appropriate way to characterize the community is by listing the identity of the constituent species. The state, or state variable, is then a set of species identities. This contrasts with the state variable in community dynamics, which is a set of species abundances. I do not agree that this shift from species densities to just the presence or absence of species, when shifting the attention from the internal community dynamics to the dynamics of community assembly, is always very useful. Communities can be very different, despite them having the same constituent species. Therefore, I will make a distinction between endstates at which the same species are present but at different densities.

Grover and Lawton (1994) define a priority effect as a form of alternative stable

states which differ in the presence and absence of species. This is, however, different from how ecologists use the term today. A more general definition is due to Fukami and Nakajima (2011):

A priority effect is the phenomenon of the effect of biotic interactions on species abundances depending on the order and timing of species immigration during community assembly.

Thus, a priority effect means that the abundance of species (as determined by interactions such as competition) depends on the times species arrive in the local community. The definition nicely captures how ecologists use the term in recent literature: priority effects imply that the outcome (in terms of population abundances) of species interaction depends on which species arrives first (and on how much earlier it arrives). The definition notably omits the time at which the outcome is to be determined. Obviously, species abundances are different at least for some time if one species arrives first instead of another species arriving first. However, initial differences between communities sharing a regional species pool that allows for only a single endstate will disappear after a long enough time. Thus, the definition allows for priority effects which do not imply alternative stable states. Instead, priority effects may lead to alternative transient states (Fukami and Nakajima, 2011). If the transients on the way to the endstate last for a long time, they may be biologically relevant. However, given enough time, these alternative states will eventually converge to a single state.

Given the definition above, priority effects may also occur during community assembly that has no endstate at all. This occurs in communities that exhibit neutrality. Neutrality means that individuals from different species have equal fitness, i.e. have an equal expected contribution to the future community through reproduction and survival. The dynamics in neutral communities are determined by chance and the composition of such communities is ever changing. Priority effects in neutral communities are stronger when population growth rates relative to immigration rates are higher, because then the species that happens to arrive first can build up a larger population before the others arrive. The priority effect is then stronger in the sense that the first arriving species attains a larger population size relative to the later arriving species (i.e. stronger *sensu* Urban and De Meester, 2009). The alternative states arising in this way are, however, merely transient and not stable. This thesis will focus on alternative states which are stable and are therefore potentially endstates of community assembly.

1.2 Positive feedback

How do alternative stable states and priority effects come about? It is often said that they are caused by positive feedback of population density on per capita growth rate. This is exemplified by the well known Lotka-Volterra competition model (Volterra, 1926; Lotka, 1932). This model models the growth of two competing species in a

phenomenological manner, that is, it models competition without specifying what the species compete for. This allows for conclusions which are more general in the sense that they apply both to, for instance, competition for resources and competition through direct interference between individuals (e.g. through aggression). The model is given by the following ordinary differential equations:

$$\frac{dN_1}{dt} = N_1 (r_1 - a_{11}N_1 - a_{12}N_2) \quad (1.1)$$

$$\frac{dN_2}{dt} = N_2 (r_2 - a_{21}N_1 - a_{22}N_2), \quad (1.2)$$

where N_i denotes the density of species i , r_i denotes the intrinsic growth rate, i.e. the per capita growth rate in the absence of intra- or interspecific interactions and a_{ij} denotes the competition coefficient which measures how much one unit of species j decreases the per capita growth rate of species i . The a_{ii} 's measure the strength of intraspecific competition and the a_{ij} 's measure the strength of interspecific competition. The necessary and sufficient condition for alternative stable states and a priority effects in this model is

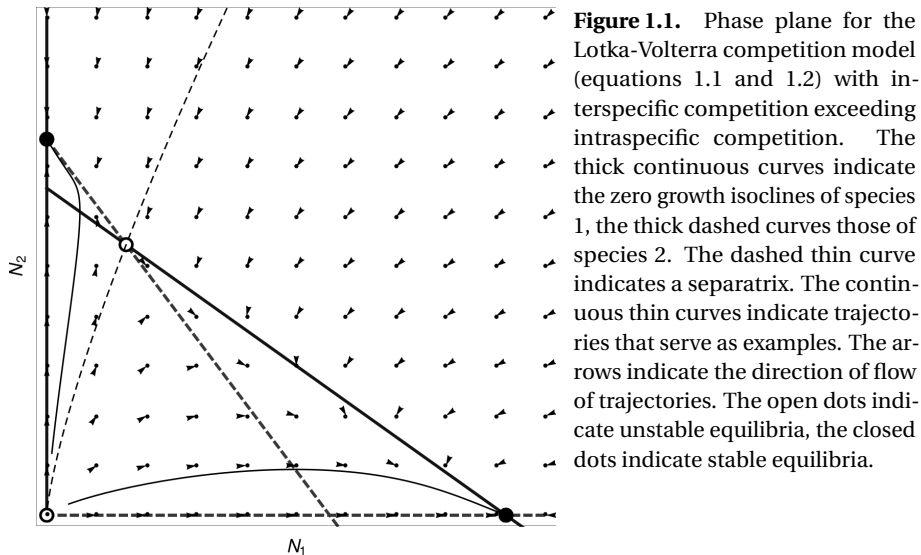
$$\frac{a_{12}}{r_2} > \frac{a_{11}}{r_1} \quad \text{and} \quad \frac{a_{21}}{r_1} > \frac{a_{22}}{r_2}, \quad (1.3)$$

which implies that for equal intrinsic growth rates interspecific competition should exceed intraspecific competition. This causes the positive feedback of species density on the per capita growth rate of a species. It is the text book example of an priority effect (e.g. Morin, 1999). An example where this condition is met is given in the phase plane of figure 1.1. In this figure, the density of each species is plotted along the axes and the black dashed curve separates initial densities for which the system is attracted to stable equilibrium with only species 1 or with only species 2, indicated with filled dots.

1.3 Thesis outline

The next four chapters of this thesis each deal with a model of population growth of interacting species. These community models are not formulated explicitly in terms of a regional species pool which supplies species to a local community through dispersal. A species pool is, however, implied. Each of the models exhibits alternative stable states, and thus positive feedback. Except for the model of chapter 2, each model models plankton populations.

Chapter 2 presents an abstract two species model that includes both positive and negative interactions within and between species. Here, positive and negative refer to whether a rise in density of a species increases or decreases the net reproduction of the own or the other species. This chapter focuses on the "higher level phenomena" (such as alternative stable states) and therefore the details of how positive or negative interactions come about are intentionally left out. This approach is similar to that of



the Lotka-Volterra competition model of the previous section. The model of chapter 2 addresses two issues. First, it presents conditions for when the combination of positive and negative interactions leads to priority effects and alternative endstates of community assembly. Second, it discusses how assumptions about the community assembly process determine the reachability of alternative stable states.

Chapter 3 deals with a model for population growth of phytoplankton that suffers from light stress. In most photosynthesising organisms light is an essential resource for growth, but if light is too strong, it may inhibit growth by damaging the photosynthetic machinery of cells. At low population densities, this may cause positive feedback of population density on population growth because increased population density causes shade protecting against damaging high light levels. The consequences of this for a community of phytoplankton species are determined.

Chapter 4 explores the effects of predation and food supply on the occurrence of alternative endpoints of community assembly in a community of two zooplankton species, sharing a single resource and a predator. One of the competitors interferes with the feeding of another species through the production of an inhibiting chemical.

Chapter 5 presents a model for a fungal parasite and its algal host. This model contains quite a lot of biological detail and exhibits some interesting phenomena including alternative stable states. It shows, among other things, what can happen if alternative stable states and cyclic population dynamics co-occur.

In the final chapter, Chapter 6, I discuss the results from the previous chapters to draw conclusions on when one may expect priority effects and alternative endstates of community assembly to occur. Furthermore, I suggest the existence of a general principle which states how the number of resources (or: the number of niches) species compete for limits the number of endstates of community assembly.

Chapter 2

Alternative stable states and alternative endstates of community assembly through intra- and interspecific positive and negative interactions

Daan J. Gerla and Wolf M. Mooij

Abstract. Positive and negative interactions within and between species may occur simultaneously, with the net effect depending on population densities. For instance, at low densities plants may ameliorate stress, while competition for resources dominates at higher densities. Here, we propose a simple two-species model in which conspecifics and heterospecifics have a positive effect on per capita growth rate at low densities, while negative interactions dominate at high densities. The model thus includes both Allee effects (intraspecific positive effects) and mutualism (interspecific positive effects), as well as intra- and interspecific competition. Using graphical methods we derive conditions for alternative stable states and species coexistence. We show that mutual non-invasibility (i.e. the inability of each species to invade a population of the other) is more likely when species have a strong positive effect on the own species or a strong negative effect on the other species. Mutual non-invasibility implies alternative stable states, however, there may also be alternative stable states at which species coexist. In the case of species symmetry (i.e. when species are indistinguishable), such alternative coexistence states require that if the positive effect exerted at low densities at the own species is stronger than on the other species, the negative effect at higher densities is also stronger on the own species than on the other species, or, vice versa, if the interspecific positive effects at low densities are stronger than the intraspecific effects, the negative effects at higher densities are also stronger between species than within species. However, the reachability of alternative stable states is restricted by the frequency and density at which species are introduced during community assembly, so that alternative stable states do not always represent alternative endstates of community assembly.

2.1 Introduction

How do positive and negative interactions between organisms combine to determine community composition and its dependency on initial population densities? This is an interesting question because evidence suggests that positive and negative interactions occur simultaneously, with the net effect depending on population densities. This is especially true in stressful environments, where organisms may ameliorate harsh conditions while at the same time competing for scarce resources (Bertness and Callaway, 1994; Stachowicz, 2001; Bruno et al., 2003). For instance, in semi-arid grasslands plants increase water availability by reducing evaporation (Maestre et al., 2003), in salt marshes reduced evaporation reduces salinity (Bertness and Yeh, 1994) and in phytoplankton communities under strong light self-shading reduces photoinhibition (Mur et al., 1977; Gerla et al., 2011). Such facilitation occurs both within and between species (Stachowicz, 2001; Fajardo and McIntire, 2011), and may cause alternative stable states through positive feedback, making community composition dependent on initial densities. If initial densities are important, places with very similar abiotic conditions and the same pool of potential colonizers may develop distinct communities because initial densities differ between places. This may have important consequences for restoration ecology (Suding et al., 2004; Young et al., 2005). Also, it may increase diversity between local communities and increase regional diversity even if abiotic heterogeneity is limited and the diversity of each local community is low (Chase, 2003). Thus, it is well justified to investigate the consequences of positive and negative interactions for the dependency of community composition on initial densities.

Initial densities are determined by the arrival times and densities of species. Thus, arrival times may have a long lasting effect on the species composition of the community, due to priority effects. In such priority effects, early arriving species inhibit the establishment of later arriving species and may cause a type of alternative stable states, where the alternative states are the different communities that eventually develop (Morin, 1999). The archetypal example of a priority effect occurs in the two species Lotka-Volterra competition model (Volterra, 1926; Lotka, 1932) in the case in which interspecific competition exceeds intraspecific competition. In this case, positive feedback of population density on relative fitness causes alternative stable states where in each state only one or the other species survives. Each of the two single species equilibria is stable against invasion by the species that is absent when it is introduced at a low density. This situation is called mutual non-invasibility and in the Lotka-Volterra competition model, mutual non-invasibility is a necessary and sufficient condition for alternative stable states through a priority effect.

To study how species combine to form communities, theoreticians have constructed assembly models (Drake, 1990; Luh and Pimm, 1993; Law and Morton, 1993, 1996; Capitan and Cuesta, 2011). These models model community assembly by randomly picking a species from a "regional species pool" and adding it to the community, which is then left to evolve through population growth and interactions

within and between populations. This process is repeated until none of the species from the regional pool that are absent in the community can invade. The community is then at an endstate (Law, 1999). For a given species pool, there could in principle be more than one endstate (alternative endstates, Law and Morton, 1993) due to priority effects. Often, assembly models make the simplifying assumptions that species are introduced at a low density and that introductions take place at a low rate relative to the rate at which the resident community develops. As we will show, these assumptions restrict the number of endstates that can be reached through the community assembly process. Therefore, as we will argue, it is important to take the reachability of a community state into account.

In another type of alternative stable states, the eventual outcome is also dependent on initial population densities. The archetypal example here may be the Allee effect (Allee, 1931), in the case where a population has a negative growth rate below a threshold density, and a positive growth rate above this threshold. Positive feedback of population density on the per capita growth rate of the population defines the Allee effect (Stephens et al., 1999). The Allee effect is called strong in the case that the population declines to extinction if it starts off below a threshold density, and weak if there is no such threshold but merely the positive feedback on population growth (Wang and Kot, 2001; Taylor and Hastings, 2005*b*). In the case of a strong Allee effect the alternative stable states correspond to extinction of the population and its survival.

Among the first to model the Allee effect were Vito Volterra (1938) and Vladimir Kostitzin (1940), who considered decreased fertility at low population densities in sexually reproducing species due to difficulty finding mates. Both Volterra and Kostitzin found a population density threshold: populations starting off below this threshold go extinct, above the threshold they survive. This implies a strong Allee effect. Since this pioneering work, many simple models of the Allee effect have been studied in the literature (for an overview, see Boukal and Berec, 2002). Studies of the Allee effect in competing species are relatively rare. The seminal paper of John Vandermeer (1973) seems to be the first to study the effects of low density positive intraspecific interactions (i.e. Allee effects), finding a multiplicity of stable states. Similar results were found by Wang et al. (1999) and Ferdy and Molofsky (2002), who found that in two-species communities, Allee effects may destabilize coexistence and lead to alternative stable states. In his purely graphical model, Vandermeer (1973) also considered low density positive interspecific interactions (i.e. mutualisms), again finding multiple stable states as well as oscillatory population dynamics. Since, authors studying two-species models have emphasized the stabilizing effect of mutualism on coexistence (Zhang, 2003; Zhang et al., 2007). It remains unclear, however, how positive and negative inter- and intraspecific interactions determine community composition when acting simultaneously and how they interact with negative interactions (specifically, competition).

In the present paper we propose a simple model to explore the effects of positive and negative intra- and interspecific interactions on community composition and its dependency on initial population densities. Here, positive and negative are defined

by the effect the interactions have on per capita growth rate, either of individuals of the same species or of another species. The strength of these interactions depends on population densities and turn from positive to negative as densities increase. The model exhibits both strong Allee effects and priority effects. We look for conditions under which these effects lead to alternative stable states, alternative endpoints of community assembly and coexistence. To assess how outcomes change as conditions change we vary the intrinsic growth rate of species from positive to negative values. Furthermore, we discuss how frequency and density of species introductions determine the reachability of alternative stable states and limit the number of community assembly endstates.

2.2 Model description

To study the effects of positive and negative interactions on community composition, we develop a simple model which is not explicit about the mechanisms that cause the positive and negative interactions. This level of abstractions allows us to arrive at more general conclusions and use graphical methods which illustrate our results. The model is defined as follows. For a community of n species, the population growth rate of the i th species is compactly given by

$$\frac{dN_i}{dt} = N_i \left(r_i + \sum_{j=1}^n N_j \left(b_{ij} - \sum_{k=1}^n N_k a_{ijk} \right) \right) \quad i = 1, \dots, n, \quad (2.1)$$

where t denotes time, N_i denotes the population density of species i , r_i denotes the intrinsic growth rate of species i , which is the per capita growth rate in the absence of con- or heterospecifics, b_{ij} measures how much the per capita growth rate of species i is increased by one population unit of species j and a_{ijk} measures how much this positive effect is reduced by one population unit of species k . We assume that all parameters are positive, except for the r 's, which may be positive, negative, or zero. In our model, the density of each species is measured in the same units. For simplicity, we will not mention units of measurement when specifying numerical values for the variables and parameters.

For the case of $n = 1$ species, (2.1) becomes, after dropping the subscripts,

$$\frac{dN}{dt} = N(r + bN - aN^2). \quad (2.2)$$

The case of $n = 1$ species was first studied by Vito Volterra (1938), who had $r < 0$. It is a simple model of the Allee effect, and in the case of a negative intrinsic growth rate and positive intraspecific effects strong enough to offset negative effects, of the strong Allee effect.

We now set n to $n = 2$ species, which gives the smallest community with which we

can study interaction between species. The population growth rates are now given by

$$\frac{dN_1}{dt} = N_1 (r_1 + b_{11}N_1 + b_{12}N_2 - a_{111}N_1^2 - (a_{112} + a_{121})N_1N_2 - a_{122}N_2^2) \quad (2.3)$$

$$\frac{dN_2}{dt} = N_2 (r_2 + b_{21}N_1 + b_{22}N_2 - a_{211}N_1^2 - (a_{212} + a_{221})N_1N_2 - a_{222}N_2^2). \quad (2.4)$$

Special cases of this model with the b 's smaller than zero have been studied by a number of authors, including Alfred Lotka (1925), Vito Volterra (1931), George Gause (1934) and Evelyn Hutchinson (1947), who considered only negative interactions.

2.3 Results

Zero growth isoclines

We analyse the two species model of equations (2.3) and (2.4) by means of invasion analysis and by drawing the phase plane with the zero growth isoclines. The phase plane is the plane with the density of species 1 along the x-axis and the density of species 2 along the y-axis. The zero growth isocline of a species is the set of points in the phase plane at which the population growth rate of the species equals zero. At the intersections of the isoclines of species 1 and 2, both species have a zero population growth and hence are at equilibrium.

To get the zero growth isoclines, we equate the left hand sides of (2.3) and (2.4) to zero, which gives two polynomial equations of degree 3. According to Bézout's theorem, two planar curves of degree n and m , have, unless the equations have a common factor, at most nm points in common. This means that the system of equations (2.3) and (2.4) has at most nine equilibria. The isocline for which $\frac{dN_1}{dt} = 0$ is given by

$$0 = N_1 \quad (2.5)$$

$$0 = r_1 + b_{11}N_1 + b_{12}N_2 - a_{111}N_1^2 - (a_{112} + a_{121})N_1N_2 - a_{122}N_2^2 \quad (2.6)$$

and the one for which $\frac{dN_2}{dt} = 0$ by

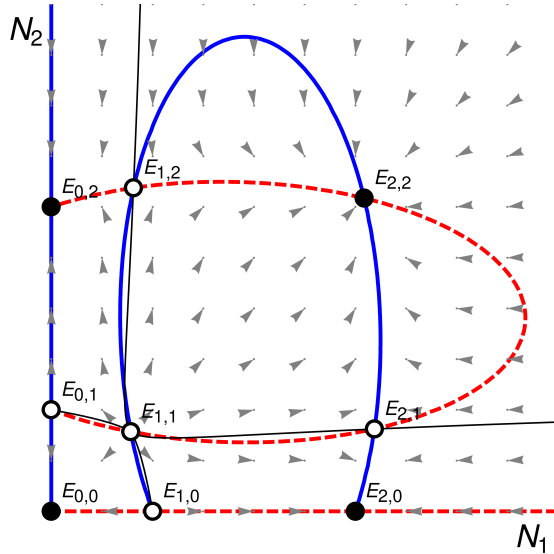
$$0 = N_2 \quad (2.7)$$

$$0 = r_2 + b_{21}N_1 + b_{22}N_2 - a_{211}N_1^2 - (a_{212} + a_{221})N_1N_2 - a_{222}N_2^2. \quad (2.8)$$

The graphs of (2.6) and (2.8) are, if they exist, conic sections. Whether they are ellipses, parabolas or hyperbolas depends on the signs of $D_1 = (a_{112} + a_{121})^2 - 4a_{111}a_{122}$ and $D_2 = (a_{212} + a_{221})^2 - 4a_{211}a_{222}$. For instance, if (2.6) has a graph, it is an ellipse for $D_1 < 0$ and a hyperbola for $D_1 > 0$. In any case, (2.6) and (2.8) intersect four times, twice or not at all; (2.6) and (2.7) intersect twice or not at all, as do (2.5) and (2.8). Together with the origin this gives nine, seven, five, three or one equilibrium.

We label the equilibria as in the figure 2.1. In the phase plane of this figure, the blue continuous curves are the zero growth isocline of species 1, the red dashed

Figure 2.1. Phase plane and zero growth isoclines with all equilibria feasible. At the blue continuous curves $\frac{dN_1}{dt} = 0$ and at the red dashed curves $\frac{dN_2}{dt} = 0$. The arrow heads indicate the direction of flow in the tip of the arrow head. Closed dots indicate stable equilibria, open dots unstable equilibria. The thin black curves are separatrices that separate domains of attractions. The axes extend to a population density of one unit. Parameter values: $r_1 = r_2 = -0.3$, $b_{11} = b_{22} = 2$, $b_{12} = b_{21} = 0.4$, $a_{111} = a_{222} = 2.5$, $a_{112} + a_{121} = 0.1$, $a_{122} = a_{211} = 0.5$.



curves are the zero growth isocline of species 2. The equilibria at the intersections are marked by a closed dot when stable, and by an open dot when unstable. (With stability we mean that densities tend to return to the equilibrium after a small perturbation. We call saddles unstable.) In figure 2.1 all nine equilibria exist and are feasible. (With feasibility we mean that the equilibrium densities are non-negative.) This means that for each species with the other species at a zero density there exist three equilibria, one stable equilibrium at which it has a high density ($E_{2,0}$ and $E_{0,2}$), one at which it has a low but positive density which is unstable ($E_{1,0}$ and $E_{0,1}$), and one in the origin which is stable ($E_{0,0}$). Furthermore, the isoclines cross four times in the interior of the phase plane, yielding three unstable equilibria ($E_{1,1}$, $E_{1,2}$, $E_{2,1}$ and $E_{2,2}$) and one stable equilibrium ($E_{2,2}$). Thus, depending on the initial densities, one of four things happens: extinction of both populations, survival of species 1 and extinction of species 2, extinction of species 1 and survival of species 2 or coexistence. Which initial densities lead to which equilibrium is indicated by the thin curves, which are separatrices separating the domains of attraction of each equilibrium.

Besides the phase plane of figure 2.1, where all equilibria are feasible, we have constructed series of phase planes where transitions between existence, feasibility and stability of the equilibria occur as the intrinsic growth rates vary. In figure 2.2, intraspecific interactions exceed interspecific interactions ($b_{11} > b_{12}$, $a_{111} > a_{122}$, $b_{22} > b_{21}$ and $a_{222} > a_{211}$). This figure is accompanied by the bifurcation diagram of figure 2.3, where equilibrium population densities are plotted as a function of intrinsic growth rate. In figure 2.4 the reverse inequalities hold ($b_{11} < b_{12}$, $a_{111} < a_{122}$, $b_{22} < b_{21}$ and $a_{222} < a_{211}$) and the accompanying bifurcation diagram is given in figure 2.5. The species in figure 2.2 resemble the Type II species of Vandermeer (1973), in the sense that they have a strong "positive low density *intraspecific effect*" (empha-

sis by DJG and WMM). This means that for low densities of a species, increasing this species density (while keeping the density of the other species constant) increases the growth rate of this species. For instance, the positive slope of the isocline of species 1 at low densities of species 1 in figure 2.2b means that an increase in the density of species 1 turns its growth rate from negative to positive as it crosses its isocline. Another way to look at this is that at low density of a species the "potential equilibrium value" of that species increases as its own density increases (with the density of the other species kept constant, Vandermeer, 1973). In figure 2.4, interspecific interactions are stronger and the reverse effect is more pronounced: at low densities of one species an increase in the density of that species benefits the other species (e.g. as in figure 2.4b). Hence, there is a positive low density *interspecific* effect and the species in figure 2.4 resemble more the Type I species of Vandermeer (1973).

Existence, feasibility, and stability of the border equilibria

We will now determine the existence, feasibility and stability of the border equilibria, that is, of the equilibria at which at least one species has a zero density. (With existence of an equilibrium we mean that the intersection of isoclines that is associated with that equilibrium actually exists.)

The criteria for existence, feasibility and stability of the border equilibria are easily derived. $E_{0,0}$ always exists and is of course always feasible. Criteria for its stability can be derived by means of invasion analysis. Stability requires that the growth rates of both populations are negative when their densities are close to zero, that is, for small N_1 and N_2 the right hand sides of equations 2.3 and 2.4 should be negative. For $N_1 > 0$ and $N_2 > 0$, the sign of the growth rate is determined by the expressions between the outer brackets in (2.3) and (2.4), which are the per capita growth rates. For small N_1 and N_2 the per capita growth rates are dominated by the r 's which are the intrinsic growth rates of the species. Thus, the condition for stability of the equilibrium at the origin is

$$r_1 < 0 \quad \text{and} \quad r_2 < 0. \quad (2.9)$$

Graphically, this condition is equivalent to the origin of the phase plane lying outside of the areas of positive growth delimited by the zero growth isoclines of (2.6) and (2.8), for instance, outside of the ellipses as in figure 2.1.

The other border equilibria do not necessarily exist, and non-existence can correspond to biologically meaningful situations. For instance, the ellipse of species 1 in figure 2.1 may be shifted upwards up to a point where $E_{1,0}$ and $E_{2,0}$ collide and then vanish in a saddle-node bifurcation, as happens on the transition between figures 2.2d and 2.2e when decreasing the intrinsic growth rate. This disappearance of the two border equilibria does not necessarily mean that the internal equilibria cease to exist, so coexistence may then still be possible. Survival of species 1 then depends on the positive effects it experiences from species 2. For instance, in figure 2.2e and figures 2.4d and e, the border equilibria of both species 1 and 2 do not exist, the coexistence equilibria do.

We will now give conditions applying to the border equilibria of species 1. Similar conditions exist for the border equilibria of species 2. The population densities at the equilibria with only species 1 present can easily be found by substituting 0 for N_2 in (2.6) and solving for N_1 :

$$E_{1,0} = \left(\frac{b_{11} - \sqrt{b_{11}^2 + 4a_{111}r_1}}{2a_{111}}, 0 \right) \quad \text{and} \quad E_{2,0} = \left(\frac{b_{11} + \sqrt{b_{11}^2 + 4a_{111}r_1}}{2a_{111}}, 0 \right).$$

The criterion for which these equilibria exist is

$$b_{11}^2 + 4a_{111}r_1 \geq 0. \quad (2.10)$$

Thus, if the intrinsic growth rate is positive, this criterion is always fulfilled. If it is negative, the single species equilibria exist if intraspecific positive effects are strong enough to make up for the negative intrinsic growth rate and the competitive effects measured by a_{111} . When existing, $E_{1,0}$ is feasible if $b_{11} \geq \sqrt{b_{11}^2 + 4a_{111}r_1}$, which is true when

$$r_1 \leq 0. \quad (2.11)$$

A feasible $E_{1,0}$ is always unstable, because if $r_1 < 0$, species 1 has a negative growth rate at low densities, and this growth rate changes sign at $E_{1,0}$. Feasibility of $E_{1,0}$ defines a strong Allee effect in species 1.

$E_{2,0}$ is always feasible when it exists and is stable if it cannot be invaded by species 2. This is the case if the per capita growth rate of species 2 is negative at $E_{2,0}$. Graphically, the condition is that the close vicinity of $E_{2,0}$ lies outside of the area of positive growth of species 2, delineated by the conic factor of its zero growth isocline (i.e. by equation 2.8):

$$\frac{b_{11} + \sqrt{b_{11}^2 + 4a_{111}r_1}}{a_{111}} \notin \left[\frac{b_{21} - \sqrt{b_{21}^2 + 4a_{211}r_2}}{a_{211}}, \frac{b_{21} + \sqrt{b_{21}^2 + 4a_{211}r_2}}{a_{211}} \right],$$

given that $E_{2,0}$ actually exists. Thus, $E_{2,0}$ must lie to the right of the right-most intersection of the species 2 isocline with the N_1 -axis (as in figure 2.2d), or $E_{2,0}$ must lie to the left of the left-most intersection (not shown), or the species 2 isocline must

Figure 2.2 (facing page). Phase planes with intraspecific interactions stronger than interspecific interactions, for several values of the intrinsic growth rate, r ($= r_1 = r_2$). For the meaning of used symbols etc., see figure 2.1. Parameter values: $b_{11} = b_{22} = 1$, $b_{12} = b_{21} = 0.4$, $a_{111} = a_{222} = 2$, $a_{112} + a_{121} = 0.2$, $a_{122} = a_{211} = 1$.

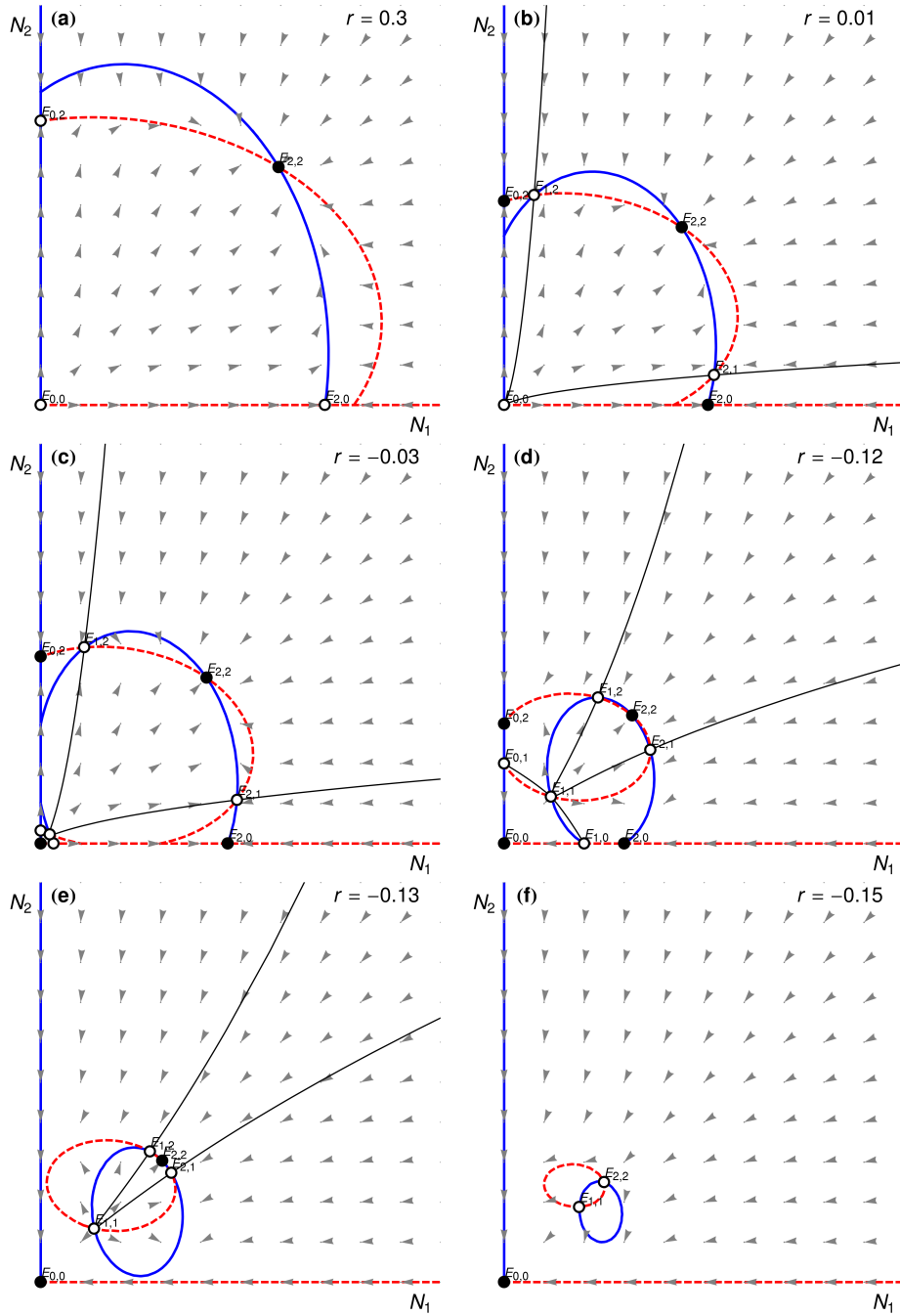
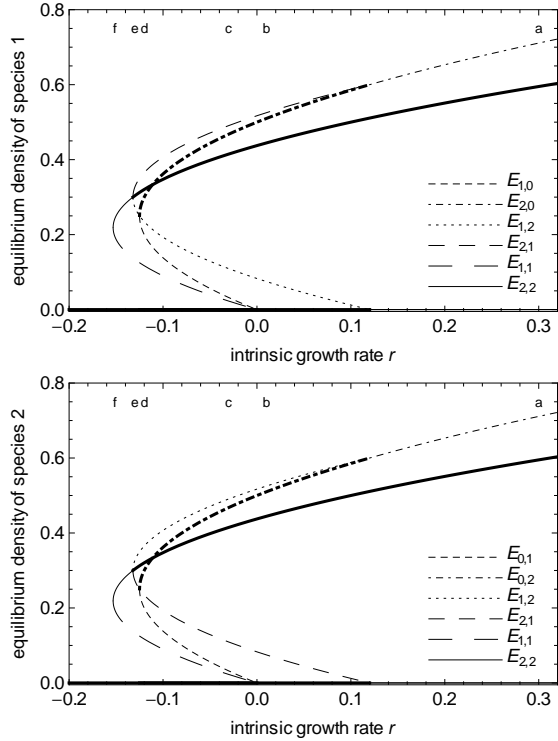


Figure 2.3. Equilibrium densities as a function of the intrinsic growth rate, r ($= r_1 = r_2$), with other parameters as in figure 2.2. Equilibria are plotted with a thick curve if stable, if unstable with a thin curve. The letters a to f indicate the r values of figure 2.2a to f. Other parameter values are as in figure 2.2.



not intersect the N_1 -axis at all (as in figure 2.1):

$$\frac{b_{11} + \sqrt{b_{11}^2 + 4a_{111}r_1}}{a_{111}} > \frac{b_{21} + \sqrt{b_{21}^2 + 4a_{211}r_2}}{a_{211}} \quad \text{or} \quad (2.12)$$

$$\frac{b_{11} + \sqrt{b_{11}^2 + 4a_{111}r_1}}{a_{111}} < \frac{b_{21} - \sqrt{b_{21}^2 + 4a_{211}r_2}}{a_{211}} \quad \text{or} \quad (2.13)$$

$$b_{21}^2 + 4a_{211}r_2 < 0, \quad (2.14)$$

Conditions (2.13) and (2.14) are never fulfilled if $r_2 > 0$. In that case, the condition for non-invasibility is given by (2.12). The left hand side of this inequality increases with b_{11} and decreases with a_{111} . The right hand side increases with b_{21} and decreases a_{211} (given that the intersection of the isocline of species 2 crosses the N_1 -axes).

Figure 2.4 (facing page). Phase planes with interspecific interactions stronger than intraspecific interactions, for several values of the intrinsic growth rate. For the meaning of used symbols etc., see figure 2.1. Parameter values: $b_{11} = b_{22} = 0.4$, $b_{12} = b_{21} = 1$, $a_{111} = a_{222} = 1$, $a_{112} + a_{121} = 0.2$, $a_{122} = a_{211} = 2$.

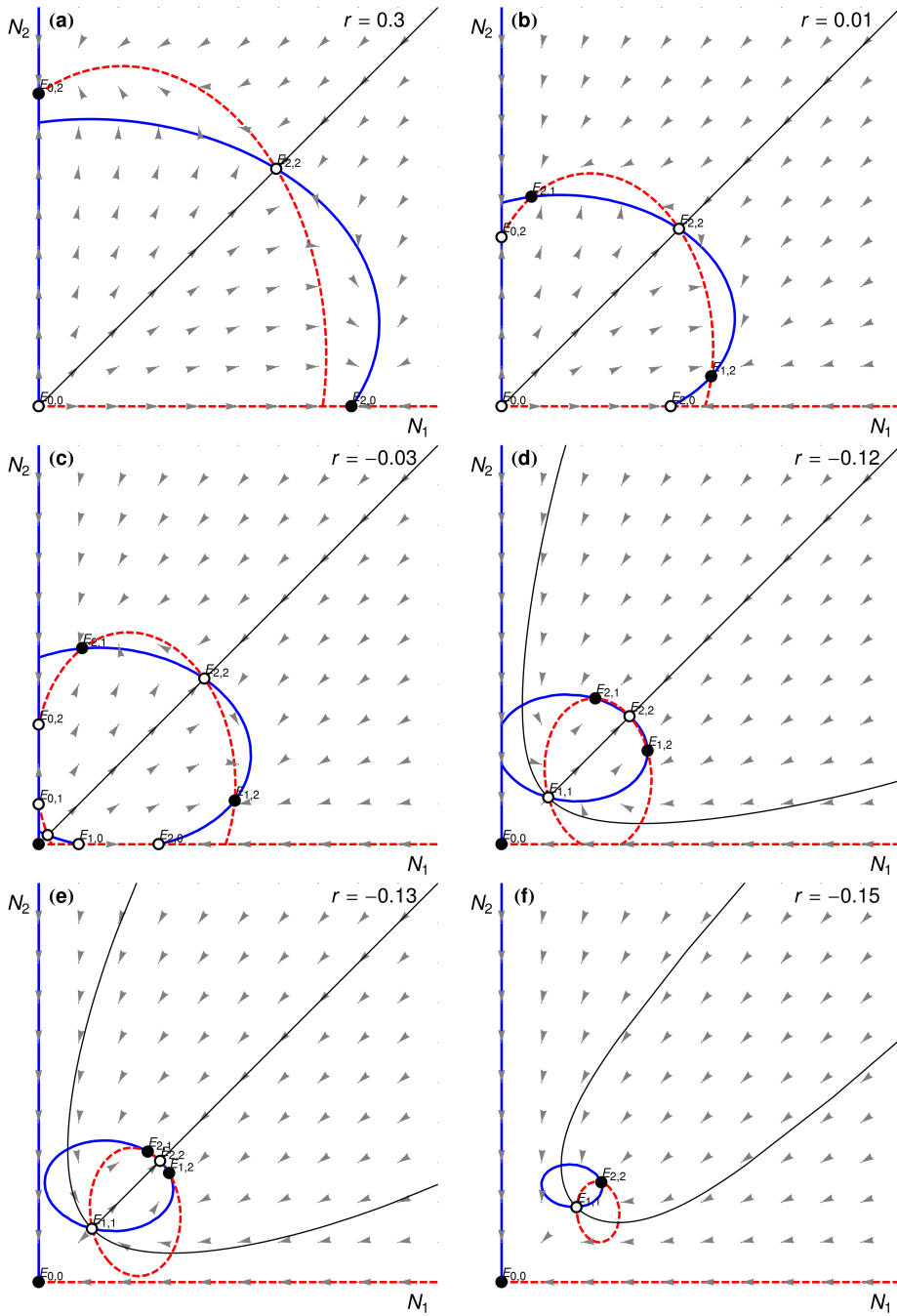
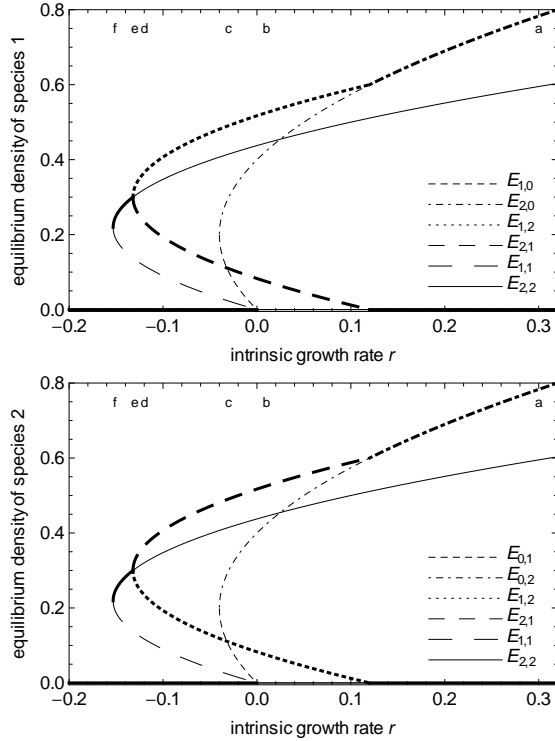


Figure 2.5. Equilibrium densities as a function of the intrinsic growth rate, r ($= r_1 = r_2$), with other parameters as in figure 2.4. Equilibria are plotted with a thick curve if stable, if unstable with a thin curve. The letters a to f indicate the r values of figure 2.4a to f. Other parameter values are as in figure 2.4.



Thus, if species 2 has a positive intrinsic growth rate, increasing the positive effect of species 1 on itself relative to the positive effect it has on species 2, or increasing the negative effect it has on species 2 relative to the negative effect it has on itself, makes non-invasibility of the monoculture of species 1 more likely.

Existence, feasibility, and stability of the interior equilibria in the case of species symmetry

Conditions for existence, feasibility and stability of the interior equilibria are not so easily derived. We did obtain expressions for the equilibria by equating the right hand sides of (2.3) and (2.4) to zero and solving for N_1 and N_2 , however, the obtained expressions for the internal equilibria are very large. Therefore, we now make the simplifying assumption that the species interactions are symmetric, that is, we assume that $r_1 = r_2 = r$, $b_{11} = b_{22}$, $b_{12} = b_{21}$, $a_{111} = a_{222}$, $a_{122} = a_{211}$ and $a_{112} + a_{121} = a_{212} + a_{221}$. The population growth rates are now given by

$$\frac{dN_1}{dt} = N_1 f(N_1, N_2) \quad \text{and} \quad \frac{dN_2}{dt} = N_2 f(N_2, N_1).$$

(Note the exchange of arguments from the first to the second equation.) The per capita growth rate f is given by

$$f(N_1, N_2) = r + b_{11}N_1 + b_{12}N_2 - a_{111}N_1^2 - (a_{112} + a_{121})N_1N_2 - a_{122}N_2^2. \quad (2.15)$$

We can find the equilibrium values of N_1 and N_2 by noting that $f(N_1, N_2) = f(N_2, N_1)$ (since $f(N_1, N_2) = 0$ and $f(N_2, N_1) = 0$). Solving the equation for N_2 using (2.15) gives two solutions:

$$N_2 = N_1$$

and

$$N_2 = \frac{b_{11} - b_{12} + (a_{122} - a_{111})N_1}{a_{111} - a_{122}}. \quad (2.16)$$

The first solution gives $f(N_1, N_1) = 0$. Since $N_2 = N_1$, this equation also gives the equilibrium values for N_2 :

$$E_{1,1} = \left(\frac{B - \sqrt{B^2 + 4Ar}}{2A}, \frac{B - \sqrt{B^2 + 4Ar}}{2A} \right) \quad \text{and} \quad (2.17)$$

$$E_{2,2} = \left(\frac{B + \sqrt{B^2 + 4Ar}}{2A}, \frac{B + \sqrt{B^2 + 4Ar}}{2A} \right) \quad (2.18)$$

where $A = a_{111} + a_{112} + a_{121} + a_{122}$ and $B = b_{11} + b_{12}$. These equilibria exist if

$$B^2 + 4Ar \geq 0. \quad (2.19)$$

This condition is always fulfilled if $r \geq 0$. If r is negative, it is more likely to be fulfilled if the positive interactions increase or the negative interactions decrease. If existing, $E_{2,2}$ is always feasible and $E_{1,1}$ is feasible if $r \leq 0$. The stability of these two equilibria can be determined using the slopes of the isoclines at the equilibria, in a manner similar as outlined in Vandermeer (1973). If species start off at equal densities, because of the symmetry assumption their densities will remain equal. At a feasible $E_{1,1}$, the population growth rates turn from negative to positive as densities increase along the line $N_1 = N_2$. This means that $E_{1,1}$ cannot be a stable equilibrium. Further more, at $E_{1,1}$ and $E_{2,2}$, the slope of the isoclines are each other's inverse, because of the species symmetry assumption and because at these equilibria $N_1 = N_2$. Thus, the slopes have the same sign. If the slopes are negative at $E_{2,2}$, stability requires that the slope of the isocline of species 1 is less than the slope of the isocline of species 2. If the slopes are positive, stability requires the reverse inequality. Using implicit differentiation to find the slopes and the fact that at $E_{2,2}$ the slopes are each others inverse, the stability criterion for $E_{2,2}$ reduces to

$$\left(\frac{b_{11} - (2a_{111} + a_{112} + a_{121})N_1}{b_{12} - (2a_{122} + a_{112} + a_{121})N_1} \right)^2 > 1, \quad (2.20)$$

where $N_1 = N_2$ is given by $E_{2,2}$ in (2.18). Thus, roughly, the stability depends on the balance between positive and negative intraspecific interactions relative to the

balance between positive and negative interspecific interactions. If the reverse inequality holds, $E_{2,2}$ is a saddle (i.e. is only stable along the line $N_1 = N_2$). Using similar reasoning, we find that $E_{1,1}$ is either a saddle, or unstable in any direction. Further more, oscillatory dynamics near $E_{1,1}$ and $E_{2,2}$ are ruled out.

The other two coexistence equilibria can be found using the second solution, equation (2.16):

$$E_{1,2} = \left(\frac{\beta - \sqrt{\beta^2 - 4\alpha\gamma}}{2\alpha}, \frac{\beta + \sqrt{\beta^2 - 4\alpha\gamma}}{2\alpha} \right) \quad \text{and} \quad (2.21)$$

$$E_{2,1} = \left(\frac{\beta + \sqrt{\beta^2 - 4\alpha\gamma}}{2\alpha}, \frac{\beta - \sqrt{\beta^2 - 4\alpha\gamma}}{2\alpha} \right), \quad (2.22)$$

where $\alpha = a_{112} + a_{121} - a_{111} - a_{122}$, $\beta = \frac{-\alpha(b_{11}-b_{12})}{a_{111}-a_{122}}$ and $\gamma = r + \frac{(a_{111}b_{12}-a_{122}b_{11})(b_{11}-b_{12})}{(a_{111}-a_{122})^2}$. (Looking at equation (2.16) or (2.22), one might think that if $a_{111} = a_{122}$ division by zero occurs. However, in that case $E_{1,2}$ and $E_{2,1}$ do not exist.) Existence of these equilibria can be inferred from the feasibility and stability of the border equilibria, if they exist, and from the stability of $E_{2,2}$. If the border equilibria and $E_{2,2}$ have the same stability (i.e. are all stable or unstable), the isoclines of species 1 and 2 must have additional intersections, implying that $E_{1,2}$ and $E_{2,1}$ exist. If the border equilibria and $E_{2,2}$ are stable, then $E_{1,2}$ and $E_{2,1}$ are unstable. If the border equilibria and $E_{2,2}$ are unstable, then $E_{1,2}$ and $E_{2,1}$ may be stable, or unstable, with either oscillatory or non-oscillatory dynamics near the equilibria. Furthermore, because $E_{1,2}$ and $E_{2,1}$ have the same stability (because of the species symmetry), existence of these equilibria implies the existence of $E_{2,2}$. A necessary – but not sufficient – condition for the feasibility of $E_{1,2}$ and $E_{2,1}$ follows from (2.16):

$$b_{11} \geq b_{12} \quad \text{and} \quad a_{111} > a_{122} \quad (2.23)$$

or

$$b_{11} \leq b_{12} \quad \text{and} \quad a_{111} < a_{122}. \quad (2.24)$$

Thus, feasibility of these equilibria is only possible if intraspecific interactions are consistently stronger or weaker at low and high densities. In other words: feasibility requires that if positive interactions at low density are stronger within species than between species, negative interactions at high densities are also stronger within species than between species (condition 2.23), or vice versa, that if low density positive interspecific interactions are stronger, that then also high density negative interspecific interactions are stronger (condition 2.24).

Transitions between qualitatively different phase planes

We have constructed the sequences of phase planes in figures 2.2 and 2.4 to show how existence, feasibility, and stability of the equilibria change as the configuration of isoclines changes. In these figures, the intrinsic growth rate ranges from positive to

negative values. These sequences of phase planes are accompanied by the bifurcation diagrams of figures 2.3 and 2.5, where equilibrium population densities are plotted as a function of the intrinsic growth rate. In the bifurcation diagrams, density is plotted with a thick curve if the equilibrium is stable and with a thin curve if unstable. The letters a to f indicate the values of the intrinsic growth rate used in the phase planes of figures 2.2 and 2.4.

In figure 2.2, intraspecific interactions are stronger than interspecific interactions, so that condition (2.23) is fulfilled. At $r = 0.3$ (figure 2.2a, corresponding to the far right of figure 2.3) there are two unstable (invadable) border equilibria and one stable interior equilibrium, which is a global attractor. This is the same situation as in the classical Lotka-Volterra competition model with coexistence of the competitors. Decreasing the intrinsic growth rate leads to the feasibility of two more interior equilibria, $E_{1,2}$ and $E_{2,1}$ (figure 2.2b). Here mutual invasibility has given way to mutual non-invasibility through two transcritical bifurcations. However, the coexistence equilibrium is still stable, so that there are three attractors. Decreasing r to negative values leads to the stability of $E_{0,0}$ and the feasibility of $E_{1,0}$ and $E_{0,1}$ (figures 2.2c and d). Further decreasing the intrinsic growth rate leads to the collision and disappearance of the single species equilibria $E_{1,0}$ and $E_{0,2}$ and of $E_{0,1}$ and $E_{0,2}$. These saddle-node bifurcations are apparent in figure 2.3 from the joining of the curves for the respective pairs of equilibria. After the saddle-node bifurcations, the single species equilibria have ceased to exist (figure 2.2e). Further decreasing r leads to a subcritical pitchfork bifurcation in which $E_{1,2}$ and $E_{2,1}$ disappear in $E_{2,2}$, leaving the $E_{2,2}$ unstable. After this bifurcation, the equilibrium in the origin is the only attractor (figure 2.2f).

A situation similar to figure 2.4d, but with a larger difference between intra- and interspecific interaction strengths, is depicted in the phase planes of figure 2.6. In figure 2.6a, the equilibria $E_{1,2}$ and $E_{2,1}$ are unstable, as opposed to figures 2.4b-e. In figure 2.6a, when species are introduced at densities close to $E_{1,2}$ or $E_{2,1}$, their densities will oscillate with increasing amplitude and eventually both species will go extinct. Increasing the intrinsic growth rate will lead to the birth of an unstable limit cycle in the equilibria $E_{1,2}$ and $E_{2,1}$ through two subcritical Hopf bifurcations. These limit cycles serve as separatrices, delineating the domains of attraction of the now stable $E_{1,2}$ and $E_{2,1}$ (figure 2.6b). Further increasing the intrinsic growth rate leads to a global bifurcation at which there is a heteroclinic connection between $E_{1,1}$ and $E_{2,2}$. For higher values of r , the unstable limit cycle disappears and the domains of attraction of $E_{1,2}$ and $E_{2,1}$ extend to high densities of the two species (figure 2.6c). These domains of attraction grow larger as r increases (figure 2.6d.)

2.4 Discussion

In the present paper we have proposed a two species model of positive and negative interactions, both within and between species. The model is a straight forward generalization to multiple species of the single species model first studied by Vito

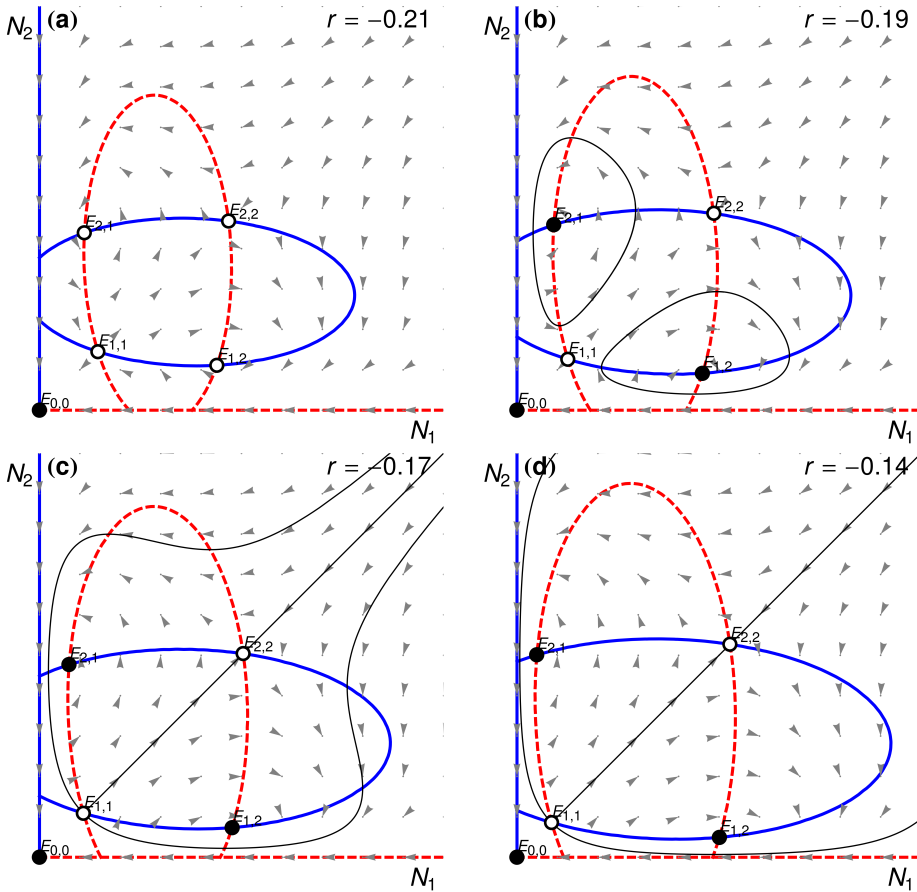


Figure 2.6. Phase planes with interspecific interactions stronger than intraspecific interactions, for several values of the intrinsic growth rate. In (b) there is an unstable limit cycle. For the meaning of used symbols etc., see figure 2.1. Parameter values: $b_{11} = b_{22} = 0.4$, $b_{12} = b_{21} = 1.5$, $a_{111} = a_{222} = 0.5$, $a_{112} + a_{121} = 0.1$, $a_{122} = a_{211} = 2.5$. 2.1.

Volterra (1938) (additionally relaxing the restriction that the intrinsic growth rate can only be negative). Previously, two species models of positive interactions have either modelled only intraspecific positive interactions (Allee effects) or interspecific positive interactions (mutualism). By simultaneously incorporating Allee effects and mutualism, we have assessed how the balance between these interactions and competition, leads to coexistence and alternative stable states. We have done so by determining conditions for existence, feasibility and stability of equilibria.

In our model, per capita growth rate is a second degree polynomial function of population densities, as in the single species model of Volterra (1938). In this respect our model differs from the class of models which are generalizations of the

single species model of Vladimir Kostitzin (1940), in which per capita birth rate is modelled as a rectangular hyperbola (Gyllenberg et al., 1999; Ferdy and Molofsky, 2002) or in which the benefit of mutualism is modelled in a saturating manner using a rectangular hyperbola (e.g. May, 1976). However, both classes of models have the conic sections as zero growth isoclines, so that our conditions for existence, feasibility and stability can be easily translated to conditions for the other class of models.

If both single species equilibria are stable against invasion of the species that is absent, we have mutual non-invasibility. Mutual non-invasibility, i.e. non-invasibility of a monoculture of species 1 by species 2 (condition 2.12-2.14) and non-invasibility of a monoculture of species 2 by species 1 (a condition analogous to 2.12-2.14), implies alternative stable states. In the case of positive intrinsic growth rates, this occurs if the *intraspecific* positive interaction coefficients are sufficiently large relative to *interspecific* positive interaction coefficients, or if *interspecific* negative interaction coefficients are sufficiently large relative to *intraspecific* negative interaction coefficients. Thus, if species help their own species more than the other species, or compete more strongly with the other species than with the own species, alternative endstates of community assembly are more likely. A simple example of mutual non-invasibility and alternative endstates occurs in figure 2.4a.

Whether mutual non-invasibility implies alternative endpoints depends also on the community assembly process and on the reachability of the single species equilibria. If community assembly proceeds through invasions from low density and if the single species equilibria are reachable, mutual non-invasibility does imply alternative endstates. However, the reverse is not necessarily true: alternative endstates do not imply mutual non-invasibility. For instance in figure 2.4b, where there are two stable coexistence equilibria, there is mutual invasibility, yet there are also alternative endstates. However, whether species arrival times determine community composition depends on how community assembly takes place. It is reasonable to assume that in most natural systems, species have a low density when they arrive. This severely restricts the number of community assembly endstates. For instance, if each species has a strong Allee effect, so that that population growth is negative for small populations, none of the species can establish itself and community assembly cannot proceed. This is the case in figure 2.1.

Community assembly also depends on the rate at which species are introduced. In natural systems, invasion attempts may be frequent or infrequent, depending on the system. This frequency may have consequences for the number of endpoints that can be reached, as in figure 2.2b, where each species has a stable single species equilibrium, there is a stable coexistence equilibrium and the species can invade the empty system. Here, if species introductions are infrequent and are at low density, so that the resident is close to its attractor when the invader is introduced, only the single species equilibria can be reached. On the other hand, if introductions are frequent, species are more likely to attain approximately equal densities, so that coexistence is the more likely outcome. Thus, sometimes the number of alternative endstates depends on the frequency at which species are introduced. Such outcomes were also observed during experimental community assembly with protists, in which some

communities could be assembled when species were introduced at equal densities at the same time, but not when they were introduced sequentially (Warren et al., 2003). Thus, even though some community states are stable in themselves, they may not be reachable through community assembly (Luh and Pimm, 1993; Warren et al., 2003; Capitan and Cuesta, 2011).

As noted before by Vandermeer (1973), positive interactions may lead to oscillatory dynamics. In figure 2.4, species densities approach the coexistence equilibria $E_{1,2}$ and $E_{2,1}$, when existing, with damped oscillations. In figure 2.6a, these equilibria are repellers, and starting off close to these equilibria, densities oscillate away from them with increasing amplitude, eventually ending up in the origin. In figure 2.6b, c and d, the equilibria are stable, in figure 2.6b, their domains of attraction are delimited by an unstable limit cycle. If the species start off at densities within the domains of attraction, they will oscillate towards the equilibria, from densities outside of them, they will go extinct. This result shows that if species oscillate away from an equilibrium, they may not end up coexisting on a limit cycle (figure 2.6a). Also, if a limit cycle exists, coexistence on that limit cycle may not be stable in the sense that the slightest deviation from the cycle may drive the species extinct (figure 2.6b). Furthermore, the domain of attraction of the coexistence equilibria may be small (figure 2.6b). Even if the domain of attraction is large, reaching very close to the borders of the phase plane, as in figure 2.6d, it depends on the community assembly process whether these equilibria can be reached.

If assembly proceeds through invasions from low density, how can alternative stable states that are not reachable be attained? This is an important question, because many ecological models exhibit alternative stable states, with one of the states being unreachable from low density (e.g. Courchamp, 1999). One answer is that parameters may gradually change over time in such way that an equilibrium is first reachable and later unreachable. The change in the parameters may take place through environmental change or through evolution. For instance, deterioration of the environment may turn intrinsic growth rates negative, making the stable equilibria unreachable from low density, as in figure 2.2d, after the community has settled on one of the stable equilibria when they were still reachable, as in figure 2.2b. This is also illustrated by the bifurcation diagrams of figures 2.3 and 2.5. Here, the stable equilibria become reachable from low density only when curves for the unstable equilibria intersect the r -axes at $r = 0$. Alternatively, a community state may be reachable if more species are considered, whereas it is unreachable if one only considers assembly with the species present at the community state in question. For instance, some species may facilitate the invasion of others, and become themselves extinct in the process. A nice example is the facilitation of phytoplankton inhibited in strong light by phytoplankton which is not so sensitive to strong light (Mur et al., 1977; Gerla et al., 2011). Such a case of species sorting is actually very similar to evolution, if one regards natural selection as a series of genotype invasions.

The conditions we have derived for existence and stability of the border equilibria do not depend on our assumption of species symmetry, however conditions for the coexistence equilibria do. This simplifying assumption is that each species

experiences the same per capita effect of the own species and of the other species on its per capita growth rate. This means species are indistinguishable and only differ by their name. This approach has also been adopted before by Gyllenberg et al. (1999) and Ferdy and Molofsky (2002). Although the assumption of exact species symmetry is probably never met in nature, pairs of species may be approximately symmetric, so that conclusions dependent on the symmetry assumption may be a good approximation.

One such conclusion is that feasibility of the additional coexistence equilibria (the ones at which $N_1 \neq N_2$, i.e. $E_{1,2}$ and $E_{2,1}$) requires that if at low densities positive interactions within species are stronger than between species, at high densities negative interactions within the species are stronger than between species (condition 2.23) or, the other way round, that both the positive and the negative interactions between species are stronger (condition 2.24). One would expect that, unless species interfere strongly with each other, competition within species is stronger than between species, because the niches of conspecifics completely overlap and the niches of heterospecifics only partially. In that case, the feasibility of the additional coexistence equilibria requires that positive effects are also predominantly intraspecific.

Models of single populations with a strong Allee effect come in many forms (Boukal and Berec, 2002). Often, these models are parameterized in terms of the population equilibria, as with the logistic growth equation which is most often stated in terms of the carrying capacity. The Allee effect models then also have a parameter for the lower unstable equilibrium, which is the 'Allee threshold' (e.g. Courchamp, 1999). Starting off below this density the population goes extinct, above it it will grow. The disadvantage of parameterizing the model like this, is that for no real-valued parameters one observes a saddle-node bifurcation at which the single species equilibria disappear. If one is only interested in situations in which the population can survive for at least some initial densities, it may make sense to parameterize the model in terms of the equilibria. However, when generalizing to more than one species, a species may be able to persist through coexisting with another while being unable to persist by itself because its single species equilibria do not exist.

To summarize, positive interactions may lead to alternative stable states, especially if positive interactions are stronger within species than between species. These alternative stable states may represent alternative endpoints of community assembly if these alternative states can be reached through the assembly process. This is not necessarily the case, especially if community assembly is limited by the density and frequency at which species are introduced. This is not only true for our model, but for all models in which alternative stable states of the strong Allee type occur. We therefore argue that it is important to acknowledge the assumptions about how species communities are formed when alternative stable states are found in ecological models.

Chapter 3

Photoinhibition and the assembly of light-limited phytoplankton communities

Daan J. Gerla, Wolf M. Mooij and Jef Huisman

Published in *Oikos* **120**:359-368 (2011)

Abstract. Photoinhibition is characterised by a decreasing rate of photosynthesis with increasing light. It occurs in many photosynthetic organisms and is especially apparent in phytoplankton species sensitive to high light. Yet, the population and community level consequences of photoinhibition are not well understood. Here, we present a resource competition model that includes photoinhibition. The model shows that, in strong light, photoinhibition leads to an increase of the specific growth rate with increasing population density due to self-shading. This so-called Allee effect can be either weak or strong. In monoculture, a strong Allee effect results in two alternative stable states. A low population density does not provide sufficient shade to protect itself against photoinhibition, such that the population goes extinct. Conversely, above a threshold population density the population may create sufficiently turbid conditions to suppress photoinhibition, so that the population can establish itself. When several species compete for light, a species which cannot establish itself due to photoinhibition can be facilitated by other species less sensitive to photoinhibition. If such facilitators are absent, photoinhibition may cause alternative stable states in community composition. Since each alternative stable state is dominated by a single species, photoinhibition does not favour species coexistence. The model predictions are consistent with published competition experiments, and illustrate the complex effects of photoinhibition on community assembly.

3.1 Introduction

Alternative stable states in species composition have important consequences for community structure. For instance, the presence of alternative stable states implies that habitats very similar in abiotic characteristics may develop distinct communities.

This may lead to differences in species composition between local communities, thereby increasing biodiversity at regional scales even when abiotic heterogeneity is limited (Chase, 2003; Shurin et al., 2004). Furthermore, the presence of alternative stable states may imply that restoring the abiotic characteristics of a habitat does not necessarily restore the species composition, which has important consequences for restoration ecology (Suding et al., 2004; Young et al., 2005).

One phenomenon that might be capable of causing alternative stable states in phytoplankton and plant communities is photoinhibition of photosynthesis. Photoinhibition is defined as a decrease in the rate of photosynthesis due to high light, and is caused by damage to the photosynthetic machinery of cells and by protective mechanisms to avoid this damage (Long et al., 1994; Takahashi and Murata, 2008). Here, we take photoinhibition to be a negative slope of the relation between photosynthetic rate and light intensity, as evident from a hump-shaped light-response curve (figure 3.1). Such hump-shaped light-response curves have been observed in many laboratory studies (e.g. Henley, 1993; Helbling et al., 2008; Moser et al., 2009) and are also evident from depressed rates of photosynthesis near the water surface (e.g. Belay, 1981).

Although many phototrophic organisms are vulnerable to photoinhibition, its population and community level consequences are not well understood. In phytoplankton populations suffering from photoinhibition, one would expect positive feedback of population density on growth rate, because a denser population provides shade that protects against inhibiting strong light. In population ecology, such a positive relation between per capita growth rate and population density is called an Allee effect (e.g. Stephens et al., 1999). When there is a threshold population density below which the population goes extinct, this Allee effect is said to be strong (Taylor and Hastings, 2005*a*). A strong Allee effect implies alternative stable states. In one state the population would disappear because it suffers from photoinhibition, while in the other state high population densities cast sufficient shade to protect against photoinhibition. If several species are involved, one might speculate that such alternative stable states may differ in species composition. For instance, each of two species may only be able to establish a population when it arrives before the other, because of a "priority effect" (Morin, 1999).

In a series of papers, Huisman and Weissing (1994, 1995) and Weissing and Huisman (1994) developed a theory on competition for light. They showed that, given a constant light supply and increasing light-response curve, competition for light among phytoplankton species in a well-mixed water column leads to competitive exclusion. The species with the lowest "critical light intensity" is the superior competitor for light. These theoretical predictions were confirmed by competition experiments (Huisman et al., 1999; Passarge et al., 2006; Agawin et al., 2007; Kardinaal et al., 2007). In subsequent work, the theory was extended to investigate implications of incomplete mixing (Huisman et al., 2004, 2006) and the underwater light spectrum (Stomp et al., 2004, 2007). Thus far, however, effects of photoinhibition on phytoplankton competition and community structure have not yet been investigated (but see Huisman, 1997).

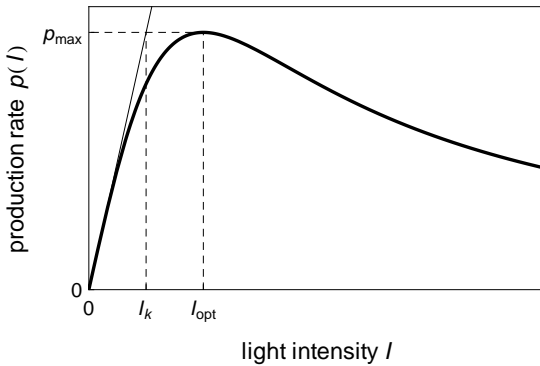


Figure 3.1. Specific production rate, $p(I)$, as a function of light intensity I , assuming photoinhibition. Here, p_{\max} is the maximum specific production rate, I_{opt} is the light intensity at which p_{\max} is reached, and I_k is the light intensity at which p_{\max} would be attained if the initial slope of the p - I curve would be maintained.

In the current work, we develop a general tractable model of phytoplankton competition that includes photoinhibition, we identify the conditions under which strong Allee effects and alternative stable states in species composition may arise, and we show that some species may overcome these alternative stable states through the shade cast by their competitors.

3.2 Competition model

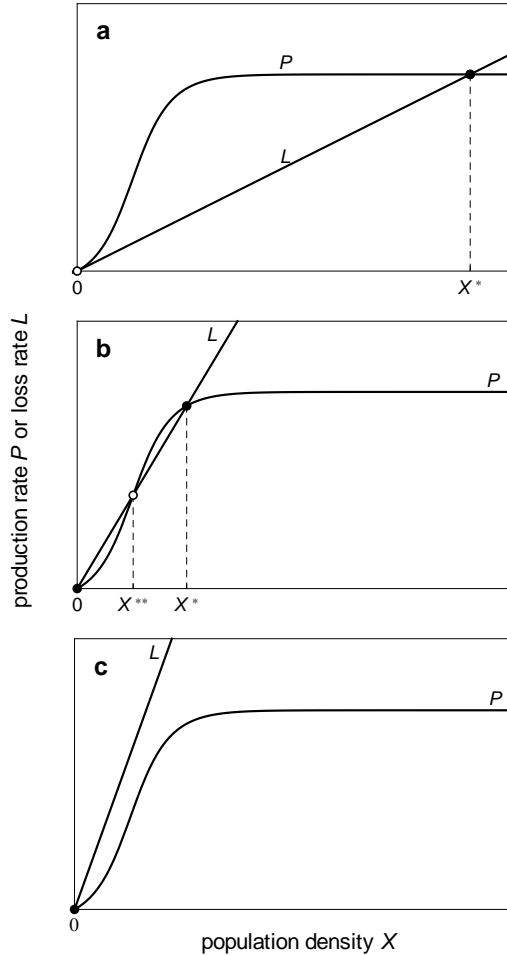
In our model we strive for a balance between realism, generality and tractability. We consider a vertical water column, in which a number of phytoplankton species compete for light. The model assumes that nutrients and carbon dioxide are in ample supply, so that light is the single factor that limits growth. We consider phytoplankton species that are of equivalent colour, so that there is no niche differentiation among species using different parts of the underwater light spectrum (Stomp et al., 2004, 2007). We further assume that there is no photoadaptation, i.e. the pigment concentration in cells is constant. Furthermore, we assume that the water column is well mixed. Mixing does not prevent the formation of a vertical light gradient: light is intenser at the top of the water column than at the bottom. These assumptions lead to the mathematical model developed by Huisman and Weissing (1994) and Weissing and Huisman (1994), which we extend by the incorporation of photoinhibition.

Let z denote the depth of the water column, where z runs from $z = 0$ at the water surface to $z = z_{\max}$ at the bottom of the water column. Let small x_i denote the population density of species i per unit volume of water, and let capital X_i denote its population density per unit surface area (i.e., $X_i = x_i z_{\max}$). The population growth rate of each species depends on the balance between its total production rate P_i and its total loss rate L_i :

$$\frac{dX_i}{dt} = P_i - L_i \quad i = 1, 2, \dots, n, \quad (3.1)$$

where n is the total number of phytoplankton species in the community.

Figure 3.2. Total production rate, P , and total loss rate, L , as functions of population density X , for a single species grown in monoculture. The total production rate, P , has an inflection point when $I_{\text{in}} > I_{\text{opt}}$. The slope of the total loss rate, L , is given by the specific loss rate, m . (a) If the specific loss rate is low, the stable equilibrium X^* is a global attractor. (b) An intermediate value of the specific loss rate yields a strong Allee effect. If the initial population density is below the unstable equilibrium X^{**} , the population goes extinct. If the initial population density exceeds this threshold value, the population will grow to the stable equilibrium X^* . (c) If the specific loss rate is high, the equilibrium at zero biomass is a global attractor. Closed dots indicate stable equilibria, open dots unstable equilibria.



Light is absorbed by phytoplankton, water, dissolved organic matter and other light-absorbing substances in the water column (Kirk, 1994). We therefore assume that light intensity decays exponentially with depth according to the law of Lambert-Beer:

$$I(z) = I_{\text{in}} \exp \left(- \sum_{j=1}^n k_j x_j z - K_{\text{bg}} z \right), \quad (3.2)$$

where I_{in} is the incident light intensity at the top of the water column, the k_j 's are the specific light attenuation coefficients of the phytoplankton species, and K_{bg} is the background turbidity due to light absorption by water, dissolved organic matter and other light-absorbing substances in the water column. We use I_{out} to indicate the

light intensity at the bottom of the water column:

$$I_{\text{out}} = I(z_{\text{max}}) = I_{\text{in}} \exp\left(-\sum_{j=1}^n k_j X_j - K_{\text{bg}} z_{\text{max}}\right).$$

Accordingly, an increase in the population densities of the phytoplankton species will absorb more light, hence reducing light availability penetrating to the bottom of the water column. Although Lambert-Beer's law offers a good approximation of the underwater light gradient, and will be used in all our simulations, it can be shown that a more general mathematical formulation as in Weissing and Huisman (1994) suffices for our main results.

The total production rate of species i is the integral of its local production rates over the depth of the water column:

$$P_i = \int_0^{z_{\text{max}}} p_i(I) x_i dz, \quad (3.3)$$

where $p_i(I)$ is the specific production rate of species i as a function of light intensity (i.e., the p - I curve). We assume that the specific production rate is a non-negative function. It is zero only in absolute darkness, increases with light intensity under low light, and decreases with light intensity at high light due to photoinhibition (figure 3.1). That is,

$$p(0) = 0, \quad \frac{dp}{dI} > 0 \text{ for } 0 \leq I < I_{\text{opt}}, \quad \frac{dp}{dI} < 0 \text{ for } I > I_{\text{opt}}, \quad (3.4)$$

where I_{opt} is the light intensity that gives the maximum specific production rate (i.e., $p(I_{\text{opt}}) = p_{\text{max}}$). Note we have dropped the subscripts i for readability. Several p - I curves proposed in the literature fulfill these assumptions (e.g., Steele, 1962; Peeters and Eilers, 1978; Platt et al., 1980; Han et al., 2000). For instance, based on a simple mechanistic model of photoinhibition, Eilers and Peeters (1988) derived the following equation:

$$p(I) = \frac{I}{aI^2 + bI + c}. \quad (3.5)$$

Equation (3.5) can be rewritten in terms of I_{opt} , the optimal light intensity for photosynthesis, I_k , the light intensity at which p_{max} would be attained if the initial slope of the p - I curve would be maintained, and p_{max} itself:

$$p(I) = \frac{p_{\text{max}} I}{\frac{I_k}{I_{\text{opt}}^2} I^2 + \left(1 - 2\frac{I_k}{I_{\text{opt}}}\right) I + I_k}. \quad (3.6)$$

The shape of this p - I curve is illustrated in figure 3.1. However, as in Weissing and Huisman (1994), our qualitative results do not depend on the specific mathematical formulation of the p - I curve. The assumptions of equation (3.4) are sufficient to derive our main results, while equations (3.5) and (3.6) serve as an example and for the construction of figures.

Finally, we assume that the total loss rate of a species is proportional to its population density:

$$L_i = m_i X_i \quad (3.7)$$

where m_i is the specific loss rate of species i , which includes losses through respiration, sedimentation, wash-out, cell lysis and grazing.

3.3 Results

Single species

First, we discuss the growth of a single phytoplankton species in the absence of other light absorbers (i.e., $K_{bg} = 0$), and we drop the unnecessary subscripts.

We are interested to see how the growth rate of this single species depends on its population density. It can be shown, using the Fundamental Theorem of Calculus, that the derivative of P with respect to X equals the specific production rate at the bottom of the water column (Weissing and Huisman, 1994):

$$\frac{dP}{dX} = p(I_{out}). \quad (3.8)$$

Since $p(I) > 0$ for all $I > 0$, this implies $dP/dX > 0$. Moreover, for large population densities, I_{out} approaches zero, and hence dP/dX approaches zero as well. Hence, the total production rate is an increasing and ultimately saturating function of population density. The second derivative is

$$\frac{d^2P}{dX^2} = \frac{d}{dX} p(I_{out}(X)) = \frac{dp}{dI_{out}} \frac{dI_{out}}{dX}. \quad (3.9)$$

The second term on the right-hand side, dI_{out}/dX , is negative. The first term, dp/dI_{out} , is positive at low light intensities but negative at high light intensities due to photoinhibition (see the inequalities in equation (3.4)). Thus, $d^2P/dX^2 > 0$ for $I_{out} > I_{opt}$. In the limit of low population density, $I_{out} \approx I_{in}$. Therefore,

$$\lim_{X \downarrow 0} \frac{d^2P}{dX^2} > 0 \text{ for } I_{in} > I_{opt}. \quad (3.10)$$

In other words, if the incident light intensity exceeds the optimal light intensity, the phytoplankton will suffer from photoinhibition. An increasing population density will cast more shade, thereby reducing light availability and diminishing the negative impact of photoinhibition. Equation (3.10) shows that, at low population densities, the total production rate P accelerates with increasing population density X . This implies that the per capita production rate, and hence the per capita population growth rate, increases with population density. That is, there is an Allee effect.

Based on these considerations, the total production rate can be sketched as a function of population density. In case of photoinhibition ($I_{in} > I_{opt}$), it will be an

S-shaped function (figure 3.2). According to equation (3.7), the total loss rate L is a linear function of population density, with slope m . The intersections of P and L define the equilibria of our dynamical system, at which $dX/dt=0$. We can distinguish three possible scenarios (figure 3.2). First, in figure 3.2a, the specific loss rate, m , is low. In this case, there are two equilibria, one at $X = 0$ and the other at $X = X^*$. The equilibrium at $X = 0$ is unstable, because $P > L$ for a slightly higher population density, so that the population will grow. The equilibrium at $X = X^*$ is globally stable, because $P > L$ for a lower population density while $P < L$ for a higher population density. Second, in figure 3.2b, the specific loss rate has an intermediate value. In this case, there is a third equilibrium (denoted X^{**}). The equilibria at $X = 0$ and $X = X^*$ are now both locally stable. In contrast, X^{**} is an unstable equilibrium and acts as threshold population density: a population starting below this threshold will decrease towards $X = 0$ and go extinct, whereas a population starting above the threshold will grow until it settles at $X = X^*$. Hence, there is a strong Allee effect, resulting in two alternative stable states ($X = 0$ and $X = X^*$). Third, in figure 3.2c, the specific loss rate is high. In this case, the loss rate exceeds the production rate irrespective of population density. The equilibrium at $X = 0$ is the only equilibrium and a global attractor for the dynamics.

Thus, the main result of this section is that photoinhibition causes an Allee effect. This Allee effect can be weak, meaning that the production rate exceeds the loss rate at low population density, such that photoinhibition does not prevent population growth (as in figure 3.2a). Or the Allee effect can be strong, meaning that there is a threshold population density below which the population goes extinct (as in figure 3.2b).

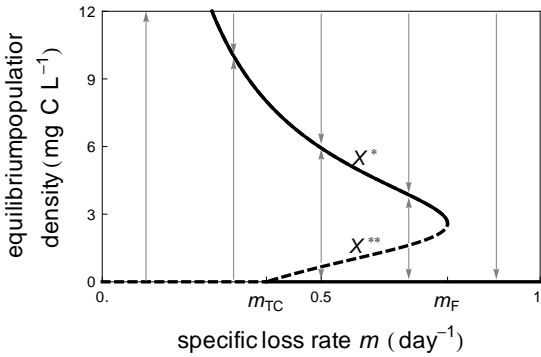
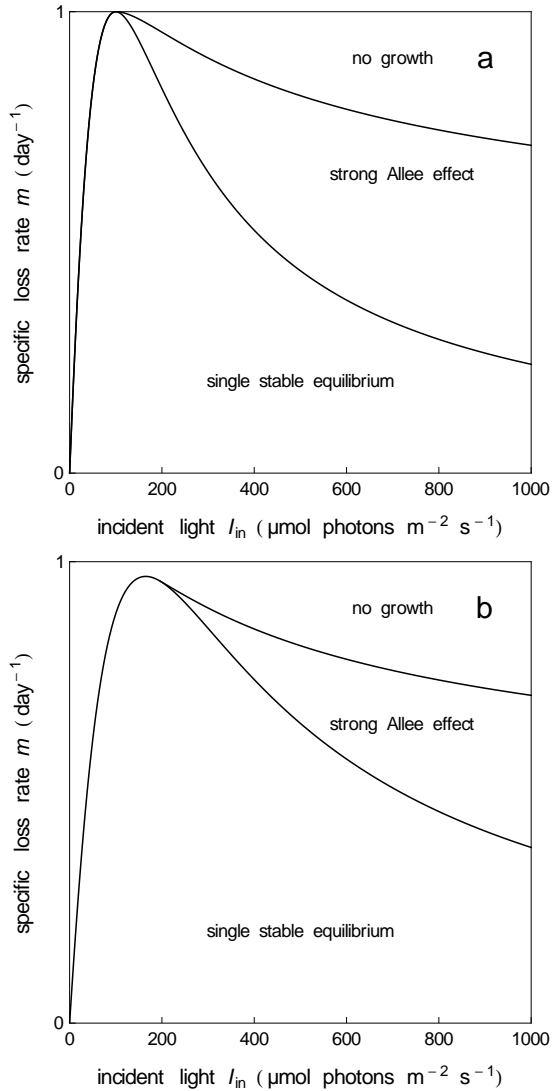


Figure 3.3. Equilibrium population densities of a species in monoculture, plotted against the specific loss rate m . Solid curves indicate stable equilibria, dashed curves unstable equilibria. A transcritical bifurcation occurs at m_{TC} and a fold bifurcation at m_F . Parameter values: $p_{\max} = 1 \text{ day}^{-1}$, $I_k = 40 \text{ } \mu\text{mol photons m}^{-2} \text{ s}^{-1}$, $I_{\text{opt}} = 100 \text{ } \mu\text{mol photons m}^{-2} \text{ s}^{-1}$, $I_{\text{in}} = 600 \text{ } \mu\text{mol photons m}^{-2} \text{ s}^{-1}$, $z_{\max} = 1 \text{ m}$, and $K_{\text{bg}} = 0 \text{ m}^{-1}$.

Effects of environmental conditions

It is interesting to investigate in further detail how the three possible scenarios sketched in figure 3.2 depend on environmental parameters such as the specific loss rate, the incident light intensity and the background turbidity. In figure 3.3, we have

Figure 3.4. Two dimensional parameter diagrams for a single species, indicating three regions with qualitatively different outcomes as function of the incident light intensity (I_{in}) and the specific loss rate (m). In the region with "strong Allee effects", there are two alternative stable states: the species either goes extinct or reaches its equilibrium population density. Panel (a) ignores background turbidity ($K_{bg} = 0 \text{ m}^{-1}$), while panel (b) includes background turbidity ($K_{bg} = 2 \text{ m}^{-1}$). Other parameter values: $p_{max} = 1 \text{ day}^{-1}$, $I_k = 40 \text{ } \mu\text{mol photons m}^{-2} \text{ s}^{-1}$, $I_{opt} = 100 \text{ } \mu\text{mol photons m}^{-2} \text{ s}^{-1}$, $z_{max} = 1 \text{ m}$.



plotted the equilibrium population densities X^{**} and X^* against the specific loss rate m . The point at which the unstable equilibrium X^{**} appears is called a transcritical bifurcation. It occurs at the specific loss rate m_{TC} . The point at which the unstable equilibrium X^{**} and the stable equilibrium X^* merge and disappear is called a fold bifurcation. This occurs at the specific loss rate m_F (figure 3.3).

To visualise how the incident light intensity affects the model predictions, we construct a parameter diagram with I_{in} and m along the axes and divide the I_{in} -

m plane into regions delineating the three possible scenarios (figure 3.4). If the background turbidity is negligible, the curve at which the transcritical bifurcation occurs is easily derived. The transcritical bifurcation occurs at the transition from figure 3.2a and b, when L is tangent to P at low population density (i.e., when L and P have equal slopes at the point $X=0$). Zero population density implies that I_{out} equals I_{in} and $p(I) = p(I_{\text{in}})$ at all depths in the water column. In view of equation (3.8), L and P have equal slopes at this point if

$$m_{\text{TC}} = p(I_{\text{in}}). \quad (3.11)$$

Thus, the specific loss rate m_{TC} at which the transcritical bifurcation occurs depends on the incident light intensity. More specifically, it is simply given by the curve $p(I_{\text{in}})$ (figure 3.4a).

Likewise, the curve describing the fold bifurcation in figure 3.4a can be derived. The fold bifurcation occurs at the transition from figure 3.2b and c, when the equilibrium population densities X^* and X^{**} merge. Let us call this population density \tilde{X} . At \tilde{X} , L is again tangent to P . That is, in view of equation (3.8),

$$m_{\text{F}} = p(I_{\text{out}}(\tilde{X})). \quad (3.12)$$

Thus, the specific loss rate m_{F} at which the fold bifurcation occurs is given by $p(I_{\text{out}})$ evaluated at the point \tilde{X} . This is implicitly a function of I_{in} . However, we do not have an exact expression for m_{F} as function of I_{in} , and we therefore used the software package AUTO-07p to calculate the fold bifurcation in figure 3.4a numerically. In the special case $I_{\text{in}} = I_{\text{opt}}$, we find $\tilde{X} = 0$. This implies $I_{\text{out}}(\tilde{X}) = I_{\text{in}}$, so then $m_{\text{F}} = m_{\text{TC}}$. If I_{in} increases from I_{opt} , \tilde{X} increases, I_{out} becomes less than I_{in} , and we get $m_{\text{F}} > m_{\text{TC}}$. Thus, for $I_{\text{in}} > I_{\text{opt}}$, there exists a window of specific loss rates, ranging from m_{TC} to m_{F} , for which the system exhibits alternative stable states (figure 3.3a).

In the above, light is absorbed by phytoplankton only, while background turbidity is assumed to be negligible. However, in reality, light absorption by water and dissolved substances contributes significantly to the total light absorption of aquatic ecosystems (Kirk, 1994). Therefore, we now add background turbidity (figure 3.4b). The curve at which the fold bifurcation occurs does not change position, although the fold bifurcation now becomes feasible only at a higher light supply. The curve at which the transcritical bifurcation occurs shifts upwards and to the right. That is, light absorption by background turbidity partly protects phytoplankton cells from photoinhibition, thus making the region with alternative stable states smaller (compare figures 3.4a and b).

Multiple species

We will now look at the growth of two or more species competing for light. In this context, it is useful to rewrite the total production rate, P_i , of each species from an integral over depth into an integral over light intensity. More specifically, using

Lambert-Beer's law, equation (3.3) can be rewritten as (Huisman and Weissing, 1994; Weissing and Huisman, 1994):

$$P_i = \frac{k_i X_i}{\sum k_j X_j + K_{bg} z} \int_{I_{out}}^{I_{in}} \frac{p_i(I)}{k_i I} dI. \quad (3.13)$$

This equation has an important interpretation. The first term on the right-hand side describes the relative contribution of species i to the total light absorption in the water column. The integral term describes how the absorbed light is converted into primary production. Hence, in total, this equation states which fraction of the total light absorbed by the entire community is captured by species i and subsequently converted into primary production.

We note from Lambert-Beer's law that $\sum k_j X_j + K_{bg} z = \ln(I_{in}) - \ln(I_{out})$. Hence, we may define a function $f_i(I_{out})$

$$f_i(I_{out}) = \frac{k_i}{\ln(I_{in}) - \ln(I_{out})} \int_{I_{out}}^{I_{in}} \frac{p_i(I)}{k_i I} dI, \quad (3.14)$$

such that the population dynamics of the competing species can be written as:

$$\frac{dX_i}{dt} = [f_i(I_{out}) - m_i] X_i. \quad (3.15)$$

This expression illustrates that each species will have one or more "critical light intensities", which are defined by the values of I_{out} at which $dX_i/dt = 0$. More specifically, if a species does not suffer from photoinhibition or if the Allee effect is weak, then this species will have a single critical light intensity $I_{out,i}^*$. It will increase if light availability exceeds its critical light intensity ($I_{out} > I_{out,i}^*$), while it will decrease if light availability is less than its critical light intensity ($I_{out} < I_{out,i}^*$). The species with the lowest critical light intensity will be the superior competitor for light, and will win the competition from all other species irrespective of the initial conditions (Huisman and Weissing, 1994; Huisman et al., 1999).

If a species suffers from photoinhibition with a strong Allee effect, then this species will have a subcritical light intensity $I_{out,i}^*$ and a supercritical light intensity $I_{out,i}^{**}$. These provide a lower and upper bound on the light conditions at which this species will be able to grow. That is, if light availability is either too low ($I_{out} < I_{out,i}^*$) or too high ($I_{out} > I_{out,i}^{**}$), the species will decrease. If light availability is within an intermediate range ($I_{out,i}^* < I_{out} < I_{out,i}^{**}$), this species will increase. Both critical light intensities can be measured in monoculture. The subcritical light intensity $I_{out,i}^*$ can be measured as the value of I_{out} at the stable monoculture equilibrium X_i^* and the supercritical light intensity $I_{out,i}^{**}$ can be measured as the value of $I_{out,i}^{**}$ at the unstable monoculture equilibrium X_i^{**} .

In competition, the species with the lowest subcritical light intensity is the superior competitor for light. However, if it suffers too much from photoinhibition, it may not be able to reach dominance and therefore may not win. The basic idea is

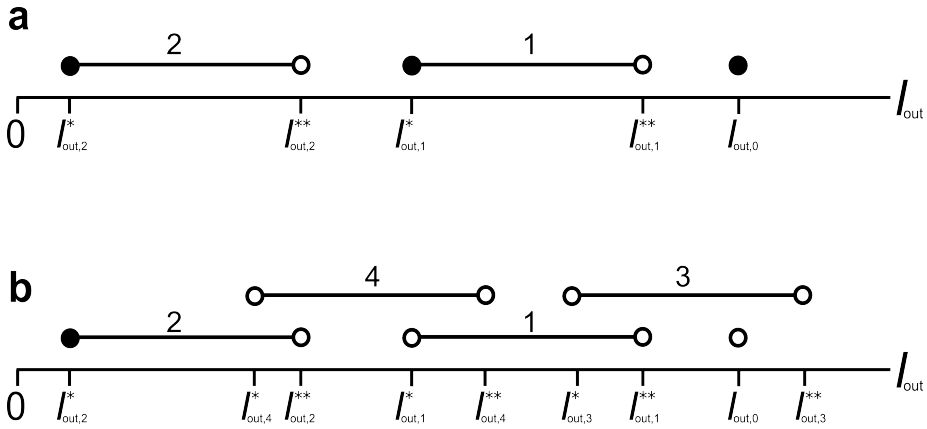
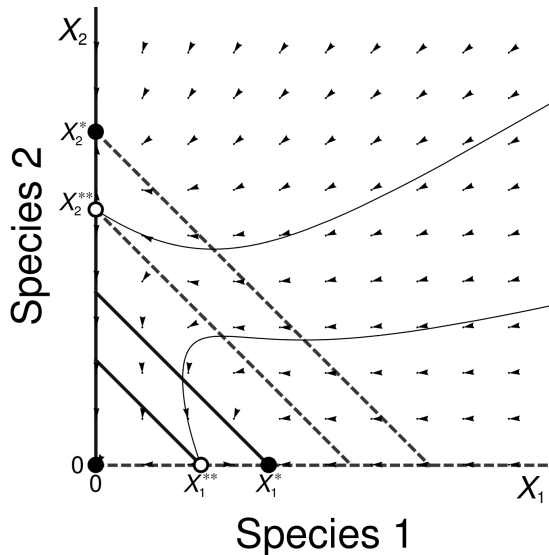


Figure 3.5. The intervals over which species have positive growth rates, plotted as function of the light availability I_{out} . The growth interval of each species ranges from its subcritical light intensity $I_{out,i}^*$ to its supercritical light intensity $I_{out,i}^{**}$. The point $I_{out,0}$ indicates the value of I_{out} in the absence of phytoplankton. Closed dots indicate stable equilibria, open dots unstable equilibria. (a) Two species with non-overlapping intervals. Since $I_{out,0}$ lies outside the growth intervals of the two species, the system has three alternative stable states (no phytoplankton, species 1 wins, or species 2 wins). (b) A four-species community with overlapping growth intervals. Species 1 and 2 are the same as in panel (a), but now they are facilitated by species 3 and 4, making the equilibrium of species 2 the global attractor. That is, species 2 has the lowest subcritical light intensity, and will ultimately win.

illustrated in figure 3.5. In figure 3.5a, species 2 has the lowest subcritical light intensity, but the growth intervals of the two species do not overlap. The subcritical light intensity of species 1 exceeds the supercritical light intensity of species 2. Hence, if species 1 attains its monoculture equilibrium, at $I_{out,1}^*$, then species 2 cannot invade because light availability is too high and species 1 will remain dominant. Conversely, if species 2 attains its monoculture equilibrium, at $I_{out,2}^*$, then species 1 cannot invade because light availability is too low and species 2 remains dominant. Accordingly, the outcome depends on the initial conditions. Another way to look at this example is by visualizing the competitive dynamics in phase space, where the population densities of the two species are plotted along the axes (figure 3.6). Each species has two zero isoclines in the interior of phase space, one corresponding with the set of population densities that yield its subcritical light intensity and the other corresponding with its supercritical light intensity. We note that all zero isoclines run parallel in phase space (Huisman and Weissing, 1994). This parallelism rules out coexistence, because the zero isoclines do not intersect.

In our example, the area in phase space where a species has positive growth (between its two isoclines) lies outside the area of positive growth of the other species (figure 3.6). Hence, assuming both species have a strong Allee effect, there are three alternative stable equilibria: a stable equilibrium in the origin, a stable monoculture

Figure 3.6. Phase plane with 3 alternative stable states. At the thick continuous zero growth isoclines species 1 has zero growth ($dX_1/dt = 0$), at the thick dashed zero isoclines species 2 has zero growth ($dX_2/dt = 0$). Closed dots indicate stable equilibria, open dots unstable equilibria. Arrows indicate the direction of the population dynamics. Thin curves are separatrices, separating the domains of attraction of the three alternative stable equilibria.



of species 1, and a stable monoculture of species 2. Which stable equilibrium will be reached depends on the initial population densities of the two species. The black curves in figure 3.6 indicate the separatrices, which separate the domains of attraction of each stable equilibrium. Note that the domain of attraction of the equilibrium in the origin extends to high population densities of species 1 and 2. Introducing both species together at high population densities may therefore lead to extinction of both species. The explanation for this counter-intuitive result is that when species 2 occurs at high population density, the population of species 1 declines rapidly due to competition. This increases light availability in the water column, so that the population growth rate of species 2 may turn negative as well due to photoinhibition. This increases light availability even further, aggravating the impact of photoinhibition on both species. As a consequence, both species eventually disappear due to photoinhibition (figure 3.6).

In figure 3.5 b, we added two more species, such that the growth intervals of the different species overlap. Now, if species 3 attains its monoculture equilibrium, at $I_{out,3}^*$, then species 1 can invade. Subsequently, species 1 may suppress light availability further and attain its monoculture equilibrium, at $I_{out,1}^*$, where species 4 may invade. Species 4 may continue to grow, casting even more shade, such that conditions become dark enough for species 2 to invade. In the end, species 2 will win, because it reduces light availability below the subcritical light intensities of all other species. It ultimately reaches dominance, after it has been facilitated by the shade cast by its competitors.

To assess which of these theoretical scenarios are likely to exist in real communities, we have assigned values to the model parameters according to empirically determined phytoplankton characteristics. These characteristics are such, that one

species performs better at low light, but is more sensitive to photoinhibition at high light than the other species. Such a trade-off has been observed between species or strains (e.g. Mur et al., 1977; Partensky et al., 1993) and also between populations of the same strain adapted to different light climates (e.g. Partensky et al., 1993; Callieri and Piscia, 2002).

Figure 3.7 contains a two-dimensional parameter diagram for these two species, analogous to the diagram in figure 3.4. The solid curves separate regions in the $I_{in}-m$ plane with different outcomes. The diagram is the superposition of the two single species diagrams, with an additional curve describing the transcritical bifurcation which separates the regions where species 1 can invade the equilibrium of species 2 and vice versa. Some interesting phenomena occur. For instance, in region c, species 2 cannot increase from low density when alone. However, species 1 can and as it does, it paves the way for invasion by species 2 and its own competitive exclusion. In region f, there are three alternative stable states, and the phase space in this region is qualitatively the same as in figure 3.6 .

3.4 Discussion

Alternative stable states and community assembly

We have shown that photoinhibition can cause alternative stable states in light-limited phytoplankton communities. In monoculture, a low population density may not cast sufficient shade to protect against photoinhibition, such that the population will ultimately go extinct. However, a high population density of the same species may create more turbid conditions to provide at least partial protection against the deleterious effects of photoinhibition, such that the population can establish itself (figure 3.2b). This configuration is called a strong Allee effect, because there is a threshold population density below which the population goes extinct (Taylor and Hastings, 2005a). When several species compete, there can be several alternative stable states. Each stable state contains at most one species, and sustained coexistence is therefore impossible. Which species will become dominant depends on the initial conditions.

The possible outcomes of competition are numerous and depend in complex ways on many parameters, even for just two species (figure 3.7). A full analysis, if feasible at all, is beyond the scope of the current study. However, we have studied the interactions of two species that differ in their photosynthesis parameters according to trade-offs observed in real organisms (e.g. Mur et al., 1977; Partensky et al., 1993). In this case, the outcome of the competitive interactions depends on light supply and the loss rates of the species. In figure 3.7, alternative stable states occur in regions d, e, f, g and h. Region f has even three alternative stable states (as in figure 3.6).

Although our results show that photoinhibition can cause alternative stable states in community composition, the order in which species arrive has no influence on the identity of the ultimate survivor if each species initially starts at low population

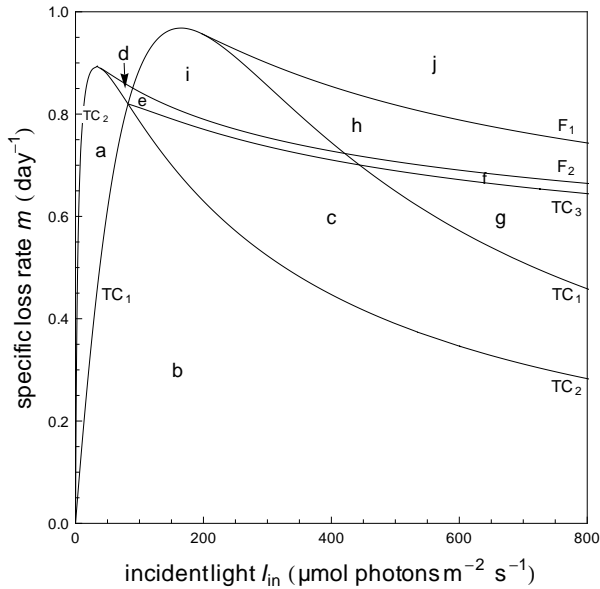


Figure 3.7. Two dimensional parameter diagram for two competing species, indicating regions with qualitatively different outcomes as function of the incident light intensity (I_{in}) and the specific loss rates (m). TC_1 and TC_2 indicate the transcritical bifurcations where species 1 and 2, respectively, can invade the empty system. F_1 and F_2 indicate the fold bifurcations where the stable and unstable equilibria of the corresponding species merge. TC_3 separates the two regions where species 1 can invade the equilibrium of species 2, and vice versa. In regions a-c, the equilibrium with only species 2 is the global attractor. In region a, species 1 cannot survive even when alone. In region b it can, but it is competitively excluded by species 2. In region c, species 2 has a strong Allee effect when alone, but its invasion is facilitated by species 1, which is competitively excluded. In region d, species 2 has a strong Allee effect and species 1 cannot survive even when alone. Region e has two alternative stable states: species 1 can invade the empty system and its equilibrium cannot be invaded by species 2, while species 2 has a strong Allee effect but its equilibrium cannot be invaded by species 1. Region f is similar to region e, but now species 1 also has a strong Allee effect, such that there are three alternative stable states. In region g, both species have a strong Allee effect, but species 2 can invade the equilibrium of species 1 and competitively exclude it. In region h, species 2 cannot survive even when alone, and species 1 has a strong Allee effect. In region i, species 2 cannot survive even when alone, while species 1 can invade the empty system. In region j, neither species can survive, irrespective of their initial population densities. Parameter values: $m_1 = m_2$, $p_{max,1} = 1 \text{ day}^{-1}$, $p_{max,2} = 0.9 \text{ day}^{-1}$, $I_{k,1} = 40 \text{ } \mu\text{mol photons m}^{-2} \text{ s}^{-1}$, $I_{k,2} = 0.02 \text{ } \mu\text{mol photons m}^{-2} \text{ s}^{-1}$, $I_{opt,1} = 100 \text{ } \mu\text{mol photons m}^{-2} \text{ s}^{-1}$, $I_{opt,2} = 20 \text{ } \mu\text{mol photons m}^{-2} \text{ s}^{-1}$, $K_{bg} = 1 \text{ m}^{-1}$ and $z_{max} = 1 \text{ m}$.

density. Consider, for instance, the hypothetical community in figure 3.5b but without species 4. In that case, there are two alternative stable states. Either species 1 or

species 2 will dominate. However, dominance by species 2 cannot be reached from low population densities, because there is a gap between the growth interval of species 2 and the other species. Instead, if community assembly proceeds through a series of species invasions, species 1 ultimately dominates irrespective of the order in which the species invade. In other words, the species with the lowest critical light intensity attainable from invasion will ultimately dominate the community. As such, the order of invasion does not result in alternative endpoints of community assembly.

Interestingly, when the number of species is increased, it becomes more likely that some species facilitate others and thereby suppress the potential for alternative stable states. For instance, suppose that we add species 4 to the scenario discussed above (figure 3.5b). The light requirements of species 4 bridge the gap between species 2 and the other species, such that reduction of light availability by species 4 paves the way for species 2 to invade. Hence, species 2 will ultimately become dominant in the community, irrespective of the initial conditions (figure 3.5b). Alternative stable states due to photoinhibition may thus be overcome in natural waters, if some of the species are sensitive to photoinhibition but others can facilitate their dominance.

Experimental tests of theoretical predictions

A key advantage of resource competition models is that the theoretical predictions can be experimentally tested in a straightforward manner. For instance, if one would measure the light response curves of different phytoplankton species, one can make predictions about the outcome of competition and test these predictions in chemostat experiments, along the same lines as in earlier experiments on competition for nutrients (e.g. Tilman, 1977; Sommer, 1985; Van Donk and Kilham, 1990; Grover, 1991) and competition for light (Huisman et al., 1999; Passarge et al., 2006; Agawin et al., 2007; Kardinaal et al., 2007). In chemostat experiments, the specific loss rates of the species are dominated by the dilution rate of the chemostat. Hence, by running monoculture and competition experiments inoculated with different initial population densities, across a range of different dilution rates and incident light intensities, one can easily test for the presence of alternative stable states predicted by our model.

In fact, some of these experiments have already been carried out. Mur et al. (1977) studied competition for light between the freshwater green alga *Scenedesmus protuberans* and the cyanobacterium *Planktothrix agardhii* (then named *Oscillatoria agardhii*). The latter species can produce microcystins, a family of toxins affecting the liver of higher organisms. Such harmful cyanobacteria become an increasing problem in many eutrophic waters (Chorus, 1999; Tonk et al., 2005; Paerl and Huisman, 2008). In Mur's experiments, *Planktothrix* had a higher specific growth rate at low light than *Scenedesmus*. However, *Planktothrix* suffered from photoinhibition at high light, whereas *Scenedesmus* was insensitive to high-light conditions. When both species were introduced simultaneously at low population densities, *Scenedesmus* steadily increased but *Planktothrix* quickly went extinct because the incident light was too strong. Once *Scenedesmus* established a dense monoculture, light intensity

had sufficiently decreased for *Planktothrix* to invade. Indeed, when *Planktothrix* was reintroduced several weeks later, its population did grow. And as it did, the population of *Scenedesmus* declined. In the end, *Planktothrix* dominated the experimental community and had replaced *Scenedesmus* (Mur et al., 1977). Accordingly, in this experiment, one species paved the way for invasion of the other species and, subsequently, its own competitive demise. Van Liere and Mur (1980) suggested that such facilitation is important for the invasion and ultimate dominance of the harmful cyanobacterium *Planktothrix agardhii* in eutrophic lakes.

Suggestions for further extensions

To what extent will our predictions be robust to changes in model structure? The model predictions do not depend on the exact way in which photoinhibition is modelled, because we made general assumptions about how photosynthetic rate depends on light intensity. Thus, qualitatively, our results should apply to a wide class of photoinhibition models (e.g. Steele, 1962; Peeters and Eilers, 1978; Platt et al., 1980). It would be interesting to replace our assumption of a static $p-I$ curve by a more dynamic $p-I$ curve, representative of photoadaptation (Ross et al., 2008) and the slow development of photoinhibition (Macedo et al., 1998; Han et al., 2000; Macedo and Duarte, 2006). Although a dynamic $p-I$ curve will change the quantitative predictions of our model, we do not expect that it will affect the predictions of our model in a qualitative manner as long as the $p-I$ curve remains hump-shaped (e.g. Partensky et al., 1993; Macedo et al., 1998; Callieri and Piscia, 2002). However, photoadaptation might affect our results qualitatively if it changes $p-I$ curves in such a way that photoinhibition is avoided (cf. Cullen and Lewis, 1988).

We expect profound differences between our model predictions and the outcome of competition between phytoplankton species of different colours. For instance, it has already been shown that competition between red and green phytoplankton species favours stable coexistence, because the species use different parts of the light spectrum (Stomp et al., 2004, 2007). It is conceivable that differently pigmented species are sensitive to high light in different parts of the light spectrum. Competition between species suffering from photoinhibition in different parts of the light spectrum may well lead to complex results with several alternative endpoints of community assembly.

We expect that incomplete mixing will also affect our model predictions, because it may enable species to avoid photoinhibition by growing deeper down in the water column. If water clarity is high and the system is shallow, it will be hard to escape from photoinhibition and many of our model predictions will probably still apply. However, species living in deeper or more turbid waters may escape more easily from photoinhibition, for instance by actively migrating away from the water surface (Ault, 2000; Whittington et al., 2000; Regel et al., 2004) or by growing in deeper parts of the water column such as the deep chlorophyll maximum (Moore and Chisholm, 1999; Modenutti et al., 2004; Six et al., 2008). It would be interesting to combine our present model analysis with earlier competition studies under incomplete mixing

(Huisman et al., 1999, 2004; Klausmeier and Litchman, 2001; Yoshiyama et al., 2009) to investigate how reduced vertical mixing may affect the impact of photoinhibition on community assembly.

Implications of photoinhibition in a food-web context could offer another promising avenue for further research. In many aquatic ecosystems, the phytoplankton spring bloom is followed by a distinct clearwater phase due to zooplankton grazing (Lampert et al., 1986; Straile and Adrian, 2000; Talling, 2003). This clearwater phase exposes phytoplankton to high light conditions. Theory predicts that an Allee effect in the prey, for instance due to photoinhibition, may cause sustained predator-prey cycles even in the absence of saturation of the predator. If the Allee effect is strong, these predator-prey cycles may drive the prey below its existence threshold, such that the food web collapses (Van Voorn et al., 2007). This suggests that photoinhibition could play an interesting role during the clearwater phase, affecting the community dynamics resulting from phytoplankton-zooplankton interactions.

Photoinhibition occurs not only in phytoplankton communities, but in other communities as well. For instance, experiments with a freshwater biofilm showed that it lost all of its chlorophyll-containing species under elevated light conditions (e.g. Lear et al., 2009). Likewise, some tree species cannot reestablish themselves in alpine vegetations due to inhibition by strong light (e.g. Bader et al., 2007). In these examples, strong Allee effects could play a role, and it is conceivable that these phototrophic organisms can reestablish themselves if a critical threshold density is overcome, or if they are facilitated by the shade cast by other species less sensitive to photoinhibition. Thus, although our model was specifically developed for phytoplankton communities, photoinhibition is a widespread phenomenon and the general implications of our findings are likely to be of relevance for many other communities as well.

Chapter 4

Effects of resources and predation on the predictability of community composition

Daan J. Gerla, Matthijs Vos, Bob W. Kooi and Wolf M. Mooij

Published in *Oikos* **118**:1044-1052 (2009)

Abstract. When does community assembly lead to a predictable species composition and when does this process depend on chance events, such as the timing of species arrivals? We studied the combined effects of enrichment and predation on the occurrence of priority effects, i.e. dependency on the timing of arrival, using a model of a small food web consisting of a predator, two competing prey and interference through allelopathy. Our analysis shows the conditions under which priority effects can occur. In the system we studied, the interfering species has to be the weaker resource exploiter of the two consumers, or it has to be more susceptible to predation. When it is the weaker resource exploiter, a minimum level of nutrient input is required for interference to be strong enough to cause a priority effect. When the interfering species is more susceptible to predation, a priority effect actually requires predation, which in itself also requires a minimum level of nutrient inflow. However, the priority effect disappears when predation pressure rises above a threshold value, also when the two competitors are equally preferred by the predator. This is so because predation reduces population densities and thereby the strength of interference. Our analyses make clear how the effects of resources and predation can combine to result in the absence or presence of priority effects during community assembly.

4.1 Introduction

When does the order in which species arrive to colonize a habitat matter for the composition of the community that develops in the long run? This is an important

question in community ecology (Chase, 2003) and restoration ecology (Young et al., 2005). If succession is deterministic in the sense that it repeatedly leads to the same eventual species composition given certain environmental conditions, its result is predictable. If community assembly is sensitive to the timing of species arrivals, it is not. When it is early arrival or high initial density that determines the establishment of a species in the community, we say there is a priority effect.

Because colonization is a stochastic event, priority effects may cause initially identical habitats to diverge in their species composition. This has for instance been shown for zooplankton communities in a set of experimental ponds with natural colonization (Jenkins and Buikema, 1998). Priority effects have been shown more rigorously by experimentally manipulating initial densities or the timing of introduction of species in a variety of systems. These include a toxin producing and a sensitive strain of the bacterium *Escherichia coli* (Chao and Levin, 1981), two species of flour beetles that predate upon each other (Neyman et al., 1956; Park, 1954; Park et al., 1965), a simple aquatic food web of ciliates and bacteria with intraguild predation (Price and Morin, 2004), cladoceran zooplankton species (Louette and De Meester, 2007) and pairs of competing algal species (Zhang and Zhang, 2007).

Quite a few mechanisms are known to cause priority effects. Most of them have in common that they enhance interspecific competition relative to intraspecific competition so that the competitive strength of a species increases with its own density. For instance, an Allee effect (a positive correlation between per capita growth rate and population size) can have this effect (Szathmari, 1991). Also competition for two resources with each of two species consuming more of the resource that limits its competitor's growth most can cause a priority effect (Tilman, 1980). Another example is intraguild predation, where one competitor predate upon the other (Holt and Polis 1997, Price and Morin 2004)(Holt and Polis, 1997; Price and Morin, 2004). Interference competition, in which one species directly interferes with the other for instance by hindering its feeding or by killing it, may also cause priority effects (Amarasekare 2002, Chao and Levin 1981, DeFreitas and Fredrickson 1978)(Amarasekare, 2002; Chao and Levin, 1981; DeFreitas and Fredrickson, 1978). Interference competition occurs among many species. In zooplankton communities it occurs both through physical contact (e.g Gilbert and Stemberger, 1985) and through the excretion of allelopathic chemicals that inhibit resource uptake (e.g. Conde-Porcuna, 1998; Matveev, 1993).

It has been shown previously that the occurrence of priority effects may depend on a minimal level of nutrient flow into the system (e.g. Chase 1999, Chase 2003b, Diehl and Feissel 2000, Mylius et al. 2001)(Chase, 1999; Diehl and Feissel, 2000; Mylius et al., 2001). However, the effect of an additional trophic level on the occurrence of priority effects has received less attention. In the present paper, we study a small food web model of one resource, two competing consumers, allelopathy and a shared top predator in a homogeneous environment. This system shows priority effects under certain conditions. We investigate how bottom-up control (limitation of resource input) and top-down control (predation intensity) affect the occurrence of priority effects by simultaneously varying enrichment and predation pressure. We show that strong predation pressure removes priority effects, both when the predator has no

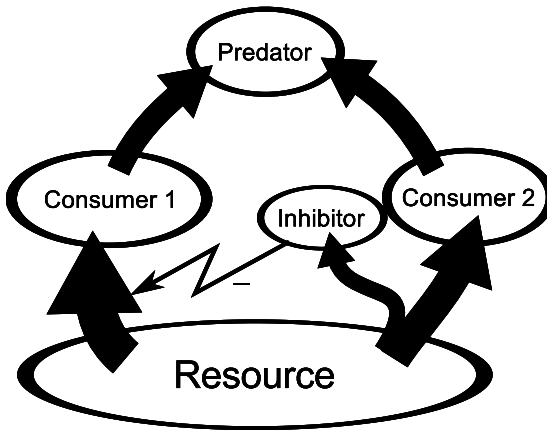


Figure 4.1. Structure of the model. Two consumers compete for a single resource. A predator predates potentially on both of these consumers. The thick arrows depict nutrient or energy flows. The thin arrow marked with a minus sign depicts the inhibitory effect of the compound excreted by consumer 2 (the interference competitor) on the resource intake rate of consumer 1.

preference for one of the consumers and when it does. We discuss when the assembly of this model community has a predictable outcome and when it is subject to priority effects, and thus contingent on colonization history and initial conditions.

4.2 Methods

The model

The model consists of a biotic basic resource (e.g. phytoplankton), two herbivorous consumer species competing for this resource (e.g. grazing zooplankton), and a top predator that eats both these consumer species (e.g. an invertebrate carnivore). One of the two competing consumer species interferes with the resource uptake of the other through the excretion of an allelopathic chemical. The structure of the model is depicted graphically in figure 4.1 and the meaning of the symbols used below is given in table 4.1.

We first introduce the functional response of consumer 1, the victim of interference. Its response is of Holling type II, modified to include inhibition. Thus, the per capita rate of resource uptake of consumer 1 depends both on resource density R and inhibitor concentration H :

$$f_1(R, H) = \frac{a_{C1}R}{(1 + a_{C1}h_{C1}R)(1 + sH)}, \quad (4.1)$$

where a_{C1} is the attack rate of consumer 1 on the resource and h_{C1} is its handling time for the resource. The sensitivity of consumer 1 to the inhibitor is determined by s . It is the reciprocal of the inhibitor concentration at which the consumption rate is half of what it would be in the absence of inhibition. This functional response is analogous to the Michaelis-Menten equation with non-competitive inhibition and has been used before in a model for microorganisms (DeFreitas and Fredrickson,

Table 4.1. Symbols for variables and parameters, their meaning, values and units of measurement. The values used in the construction of figures 4.2B and 4.3B are given between brackets if they deviate from the ones used in figures 4.2A and 4.3A.

symbol	meaning	value	units
variables			
R	density of basic resource		mg C L ⁻¹
C_i	density of grazer species i		mg C L ⁻¹
H	concentration of inhibitor		mg C L ⁻¹
P	density of predator		mg C L ⁻¹
t	time		day
parameters			
r	intrinsic growth rate of basic resource	0.275	day ⁻¹
K	carrying capacity of basic resource	varied	mg C L ⁻¹
e_{C1}	conversion efficiency of basic resource to grazer species 1	0.36	None
e_{C2}	conversion efficiency of basic resource to grazer species 2	0.30	mg C (mg C) ⁻¹
a_{C1}	attack rate of grazer species 1	0.77	L day ⁻¹ (mg C) ⁻¹
a_{C2}	attack rate of grazer species 2	0.77	L day ⁻¹ (mg C) ⁻¹
h_{C1}, h_{C2}	handling time of biotic resource by grazer species 1, 2	(1.1165) 0.5	day mg C (mg C) ⁻¹
s	sensitivity of species 1 for inhibitor	8.3	L (mg C) ⁻¹
d_{C1}, d_{C2}	background death rate of grazer 1, 2	0.17	day ⁻¹
e_H	conversion efficiency of biotic resource to inhibitor	0.06	mg C (mg C) ⁻¹
d_H	degradation rate of inhibitor	0.1	day ⁻¹
e_{P1}, e_{P2}	conversion efficiency of grazer 1, 2 to predator	0.5	mg C (mg C) ⁻¹
a_{P1}	attack rate on grazer 1 by predator	2.71	L day ⁻¹ (mg C) ⁻¹
a_{P2}	attack rate on grazer 2 by predator	2.71	L day ⁻¹ (mg C) ⁻¹
h_{P1}, h_{P2}	handling time of grazer 1, 2 by predator	(3.9295) 0.83	day mg C (mg C) ⁻¹
d_P	death rate of predator	varied	day ⁻¹

1978). It assumes that both attack rate and handling time are affected by the inhibitor. The effect of the inhibitor is saturating: at high levels of the inhibitor, adding more

has little effect. This is in accordance with studies on inhibition in zooplankton (Helgen, 1987; Matveev, 1993).

The resource uptake of consumer 2 is not inhibited and depends only on resource density:

$$f_2(R) = \frac{a_{C2}R}{1 + a_{C2}h_{C2}R}, \quad (4.2)$$

where a_{C2} and h_{C2} are the attack rate and handling time of consumer 2, respectively.

The basic resource, R , grows logistically in the absence of consumption. Its growth rate is

$$\frac{dR}{dt} = rR \left(1 - \frac{R}{K}\right) - C_1 f_1(R, H) - C_2 f_2(R), \quad (4.3)$$

where r is the intrinsic growth rate of the resource, K is its carrying capacity, and C_1 and C_2 are the densities of the consumers. Changes in population densities of the consumers are given by

$$\frac{dC_1}{dt} = C_1 \left(e_{C1} f_1(R, H) - d_{C1} - \frac{a_{P1}P}{1 + a_{P1}h_{P1}C_1 + a_{P2}h_{P2}C_2} \right), \quad (4.4)$$

$$\frac{dC_2}{dt} = C_2 \left(e_{C2} f_2(R) - d_{C2} - \frac{a_{P2}P}{1 + a_{P1}h_{P1}C_1 + a_{P2}h_{P2}C_2} \right), \quad (4.5)$$

where e_{Ci} denotes the efficiency with which consumer i converts consumed resource into new biomass, d_{Ci} its background death rate, a_{Pi} the attack rate of the top predator on consumer i , and h_{Pi} the handling time of the predator for species i . Consumer 2 excretes the inhibitor at a rate proportional to the rate at which it consumes the resource and produces new biomass:

$$\frac{dH}{dt} = e_H f_2(R) C_2 - d_H H, \quad (4.6)$$

where e_H denotes the yield of inhibitor per unit of consumed resource. The inhibitor degrades at a constant rate d_H . The predator's density P changes due to feeding on both consumers and due to a constant mortality rate d_P :

$$\frac{dP}{dt} = P \left(\frac{e_{P1}a_{P1}C_1 + e_{P2}a_{P2}C_2}{1 + a_{P1}h_{P1}C_1 + a_{P2}h_{P2}C_2} - d_P \right), \quad (4.7)$$

where e_{Pi} is the efficiency with which the predator converts consumer i into predator.

TWO SCENARIOS

In our basic scenario, consumer 1 and consumer 2 only differ in the efficiency e_{Ci} with which they convert consumed resource into biomass and in that only consumer 2 produces the inhibitor and only consumer 1 is sensitive to it. Here, consumer 1 is a more efficient resource exploiter (because $e_{C1} > e_{C2}$) and only consumer 2 interferes with its competitor's resource uptake. In a second scenario we added more differences between the two consumers. In this scenario of differential vulnerability

to predation, the attack rate of consumer 2 on the resource (a_{C2}) and the attack rate of the predator on consumer 2 (a_{P2}) are increased by 45%, making consumer 2 the stronger resource exploiter at the cost of a higher vulnerability to predation. The values we assigned to the parameters are as in table 4.1. These are largely based on realistic parameter estimates for a planktonic system (Vos et al. 2004a, Vos et al. 2004b).

ANALYSIS

We varied enrichment and predation pressure by varying the carrying capacity of the resource (K) and the death rate of the predator (d_p), respectively. We divided the K - d_p plane for both scenarios into regions of qualitatively different model behaviours, identifying those regions in parameter space where priority effects occur. This has resulted in the two-dimensional bifurcation diagrams of figure 4.2, where priority effects occur in the grey shaded region. To understand what happens in these diagrams, we additionally constructed two one-dimensional bifurcation diagrams in which K is held fixed at 1.6 mg C L^{-1} (figure 4.3A) and 1.4 mg C L^{-1} (figure 4.3B) and only d_p varies). In these diagrams the changes in equilibrium densities that lead to qualitative changes in model behaviour are depicted. The crossing points of a vertical line at $K = 1.6 \text{ mg C L}^{-1}$ (figure 4.2A) and at $K = 1.4 \text{ mg C L}^{-1}$ (figure 4.3B) with the curves in each two-dimensional bifurcation diagram correspond to the bifurcation points in the one-dimensional bifurcation diagrams (i.e. the d_p values where equilibria become stable or unstable, indicated by the vertical dotted lines in figures 4.3A and B).

The basic method for finding most curves that divide the K - d_p plane is invasion analysis, which is performed by determining when the per capita growth rate of a species that itself is absent (the invader) is positive or negative under the conditions set by the other species (the resident species). The values of K and d_p for which the growth rate of an invader is exactly zero define the invasion boundaries that divide the parameter space of figures 4.2A and B into regions with different possible community compositions. When the invasion analysis shows mutual non-invasibility of the two consumer species, this indicates a priority effect: when consumer 1 is present at a high initial density consumer 2 cannot invade, and vice versa. Mutual non-invasibility is a sufficient criterion for priority effects. Also, in this relatively simple food web there are no priority effects without mutual non-invasibility. However, a more complex criterion may be required in communities that have more species and more complex interactions.

We assumed that all species in the food web have the possibility to attempt invasion; we do not consider scenarios in which species are absent due to mere dispersal limitation. Using Mathematica, we found exact algebraic expressions for all curves in figure 4.2 that indicate thresholds for invasion of resident communities that exhibit stable (i.e. non-cyclic) dynamics, For the criteria for invasion in resident communities that show cyclic population densities, and of curves that separate stable and cyclic regimes we used numerical continuation (i.e. we used the software

packages LocBif and AUTO to determine for which pairs of K and d_p values the transcritical bifurcations for cyclic resident communities and the Hopf bifurcations occurred, respectively, see Kooi et al. 2002). We also used numerical continuation for locating the coexistence equilibrium of all four species in figures 4.3A and B, and for determining its stability.

4.3 Results

The model community shows a variety of qualitatively different behaviours, in terms of species composition, the presence of priority effects and the occurrence of either stable or cyclic population densities, as shown in figures 4.2A and B. In these figures, the carrying capacity K of the resource and the death rate d_p of the predator represent bottom-up and top-down controls and the lines and curves separate regions with different community compositions and dynamics. Symbols in each region indicate the set of species that can coexist at the particular K and d_p values, and that form a community that cannot be invaded by any of the other species when these are introduced at a low density. For instance, in the region marked " $R C_1$ " in figure 4.2, only the resource and consumer 1 can stably coexist.

We are particularly interested in the areas in which two distinct communities can resist invasion by other species, and where the initial densities of species determine which community becomes established. This is where there are priority effects. For instance, in the region " $R C_1$ or $R C_2$ " the resource can stably coexist with either consumer 1 or consumer 2, depending on the initial densities of these species. In figure 4.2, the regions with priority effects are shaded.

Equilibria may also be unstable in the sense that small deviations from these equilibria lead to sustained oscillations in species densities. These equilibria are marked with the word "cycles".

Scenario 1: no preferential predation

The case where the attack rates of the predator on the two consumers are equal is depicted in figure 4.2A. In the left most region of this figure, region " R ", only the basic resource can exist. This region is delimited on its right side by the existence boundary $K = R_{C_1}^*$, that is, the carrying capacity of the basic resource that equals the resource level at which the gains and losses of consumer 1 exactly balance – its R^* (Tilman 1982). To the right lies region " $R C_1$ " and further to the right region " $R C_1$ or $R C_2$ ". In this region, at high K , two equilibria are stable, so above a minimal productivity level there is a priority effect. Note that this minimal productivity level is not the R^* of consumer 2: consumer 2 can maintain a population at lower levels of productivity, however, there consumer 1 can invade and exclude consumer 2. Below " $R C_1$ " and " $R C_1$ or $R C_2$ ", at high K and low d_p values, the predator can establish a population feeding on consumer 1. At slightly higher K and lower d_p values the predator can also sustain itself feeding on consumer 2. In region " $R C_1 P$ or $R C_2$ ",

the system is sufficiently productive to sustain a predator population on consumer 1 (the more efficient resource exploiter), but not on consumer 2, so that a priority effect determines whether the predator can exist. If starting in region " $R C_1 P$ " or " $R C_2 P$ " predator mortality is decreased, the equilibrium with the resource, consumer 2 and the predator loses its stability against invasion by consumer 1. Thus, at high levels of predation the priority effect disappears.

To clarify the disappearance of the priority effect due to intense predation, we constructed figure 4.3 3, where we plotted equilibrium densities against predator mortality d_p , at a fixed value of carrying capacity $K = 1.6 \text{ mg C L}^{-1}$. At values below $d_p \hat{=} 0.067 \text{ day}^{-1}$ the density of consumer 1 at the equilibrium with coexistence of all species is negative, so here the coexistence equilibrium becomes unfeasible. This means there are no positive initial densities from which the system is attracted to the equilibrium with consumer 2 and the predator. The equilibrium with consumer 2 and the predator is now unstable and the equilibrium with consumer 1 and the predator becomes a global attractor: the priority effect has disappeared.

Because we assume in this scenario that the two consumers only differ in their resource conversion efficiencies e_{C_i} and the sensitivity to the inhibitor s , the inhibitor concentration at the coexistence equilibria with and without the predator (H_{coex}) is independent of predator mortality d_p (see appendix 4.5 and figure 4.3). It is also easy to see that when $d_p = 0$, the inhibitor concentration at the equilibrium of resource, consumer 2 and the predator ($H_{C_2}^{**}$) is zero and that when d_p is greater than zero, $H_{C_2}^{**}$ is greater than zero. This means that $H_{C_2}^{**}$ decreases to levels at which $H_{C_2}^{**} < H_{coex}$, if d_p is reduced far enough. As we show in appendix 4.5, invasion of the equilibrium with consumer 2 and the predator by consumer 1 is possible when $H_{C_2}^{**} < H_{coex}$. Thus, if predator mortality is reduced far enough, the priority effect, if present, disappears. (For a more exact argumentation, see appendix 4.5.)

In the right-most regions of figure 4.3A, at high system productivity, equilibria become unstable and densities fluctuate. This makes it more difficult for the predator to establish a population, because it needs a higher average prey density when prey have cyclic dynamics.

Scenario 2: preferential predation

A different scenario is depicted figure 4.2B. Here, consumer 2 is more vulnerable to predation but is also the more efficient resource exploiter (it has a lower R^*). In this case the predator enables the priority effect. However, there is still a region at low predator mortality at which consumer 1 outcompetes consumer 2 without a priority effect (region " $R C_1 P$ "). Figure 4.3B shows the equilibrium densities for a range of d_p values at a fixed value of $K = 1.4 \text{ mg C L}^{-1}$ for the scenario with differential predation. As can be seen, the loss of the priority effect with decreasing predator mortality is accompanied by a loss of feasibility of the coexistence equilibrium of the four species, as it is in figure 4.3. However, in the scenario with preferential predation, the coexistence equilibrium is also unfeasible at high predator mortalities (because C_2 and H become negative). There, in regions " $R C_2 P$ " and " $R C_2$ " consumer 2

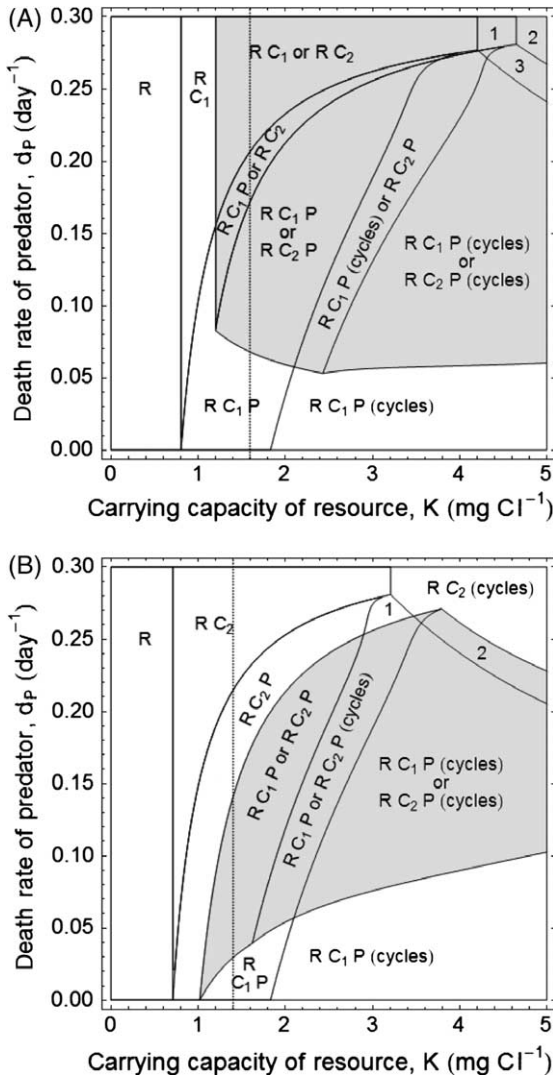


Figure 4.2. Regions in parameter space with qualitatively different model behaviours for (A) the scenario in which the interference competitor is the less efficient resource exploiter, but with no differences between the consumers with respect to the predator and (B) the scenario in which the interference competitor is the stronger resource competitor, but is more vulnerable to predation. Parameters are as in table 4.1. The symbols in each region indicate which species can coexist at the parameter values of that region. Sets of species marked with "cycles" show persistent oscillatory dynamics. In the shaded regions, there are two sets of coexisting species and a priority effect determines the outcome of community assembly. The dotted vertical lines in (A) and (B) indicate the K -values used in figure 4.3A and B, respectively. Region 1: R_{C_1} (cycles) or R_{C_2} ; region 2: R_{C_1} (cycles) or R_{C_2} P (cycles); region 3: R_{C_1} (cycles) or R_{C_2} P (cycles). (B) Region 1: $R_{C_2} P$ (cycles); region 2: $R_{C_1} P$ (cycles) or R_{C_2} (cycles).

always excludes consumer 1, which in this scenario is the lesser resource exploiter. In the other regions in figure 3B at least one equilibrium is unstable in the sense that densities oscillate. The effect of these density fluctuations on the possibility of existence of the predator is similar to those in figure 4.2. However, since existence of the predator is a prerequisite for a priority effect in the scenario with differential predation, cycles reduce the region where a priority effect occurs, especially when both the carrying capacity is high and predator mortality is low.

We also performed a more elaborate numerical analysis for the case in which the

two consumer species are not nearly identical, following the methods presented in Kooi et al. (2002), but these results are beyond the scope of this paper. The main lesson we learned from that analysis concerns the importance of certain parameters, such as s , the sensitivity to the inhibitor which has to have a minimal or threshold value for priority effects to occur.

4.4 Discussion

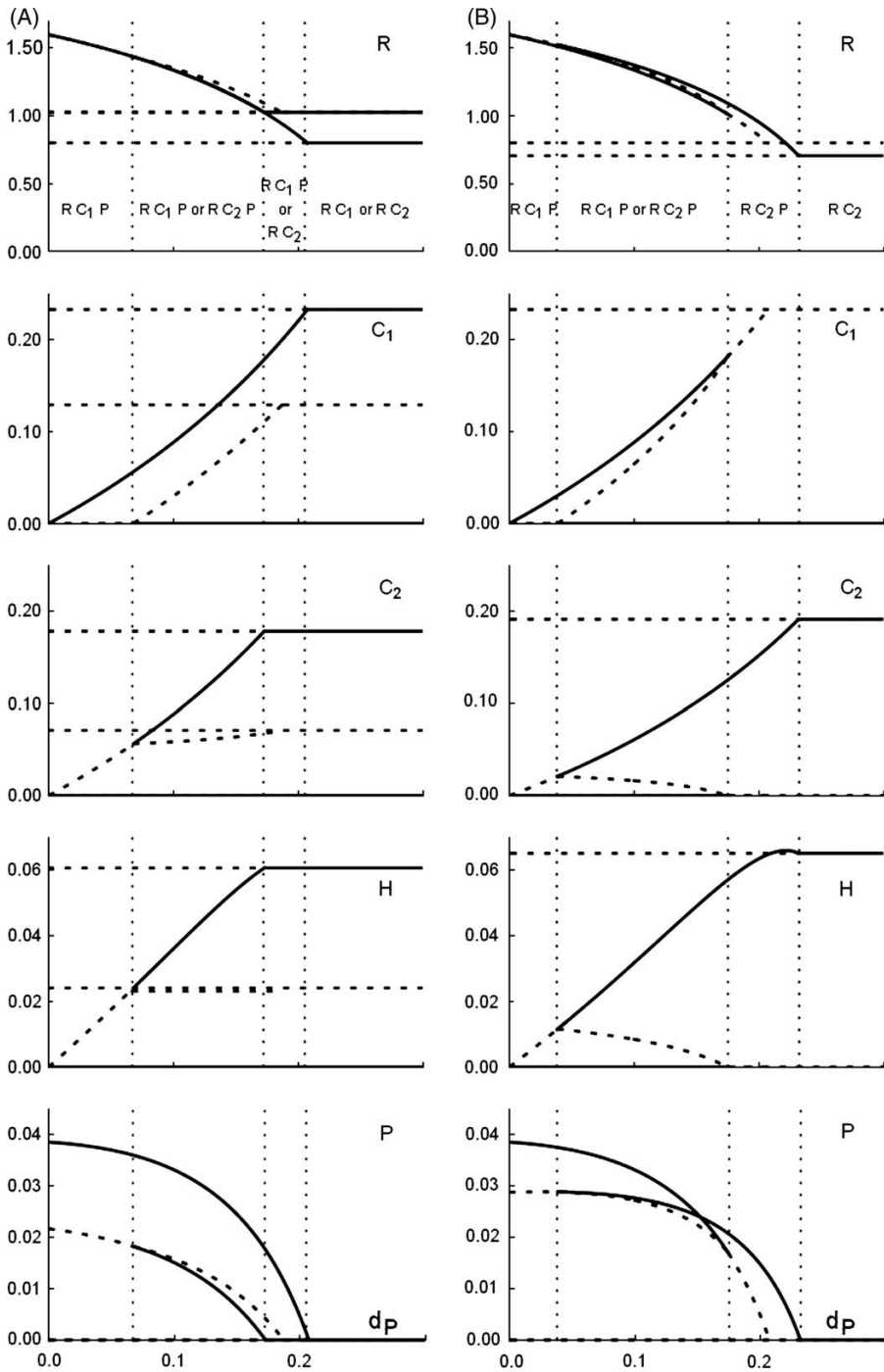
When do the combined forces of bottom-up and top-down control allow priority effects to occur during community assembly? For interference to cause a priority effect there needs to be a minimum level of productivity, because only then population levels or levels of excretory compounds are sufficiently high for interference to be strong enough. However, our results show that if predation pressure is strong, the priority effect disappears because it reduces interference between the competitors, even if the two competitors are equally vulnerable to predation (figures 4.2 and 4.3 and appendix 4.5). Also when the interfering species is the stronger resource exploiter but is more vulnerable to predation, high predation pressure prevents the occurrence of a priority effect (figure 4.2B). However, in this case the predator in fact enables a priority effect at intermediate predation pressures: in all areas with a priority effect the predator is present, in contrast with the findings shown in figure 4.2A. It should be noted that the occurrence of the priority effect does not only depend on resource carrying capacity and predation pressure, but also on for instance whether sensitivity s to inhibitor is large enough.

We will now discuss in more detail the bottom-up effects on the occurrence of priority effects for both the scenario with and without predator preference. Then we will discuss top-down effects for both scenarios.

Bottom-up effects

When each of the consumers cannot invade a population of the other, there is a priority effect. When consumer 2 (the interference competitor) is invading, the

Figure 4.3 (facing page). Equilibrium densities plotted against predator mortality d_p (A) for the scenario without preferential predation and (B) for the scenario with preferential predation. Parameters as in table 4.1, with $K = 1.6 \text{ mg } C L^{-1}$ in (A) and $1.4 \text{ mg } C L^{-1}$ in (B). Solid lines indicate densities at stable equilibria, dashed lines indicate densities at unstable equilibria. The vertical dotted lines separate ranges of d_p values for which the model has qualitatively different outcomes; these outcomes are indicated in the top panels with letter symbols as in figure 4.2. Equilibrium densities have only been plotted for the range in which an equilibrium is biologically feasible (i.e. for which all densities at that equilibrium are all non-zero). The inhibitor concentration at the equilibrium with all species present has been slightly shifted down for clarity. More than one stable equilibrium in a plot implies a priority effect. All densities are measured in $\text{mg } C L^{-1}$, d_p is measured in day^{-1} .



environment contains little or no inhibitor. If consumer 1 is a more efficient resource exploiter than the interference competitor, the resource level in this environment is too low for the interference competitor to grow. So, one criterion for the occurrence of a priority effect is that the interference competitor is the weaker resource exploiter. An empirical example in which this requirement is met is a pair of copepod species, with the weaker grazer of the two producing a compound that reduces the filtering rate of the other (Folt and Goldman 1981). Being the weaker resource exploiter, species 2 has a higher R^* (Tilman 1982). This R^* does not depend on the productivity of the system. Whether the first consumer can invade a population of the interference competitor depends on the resource density and inhibitor level in the environment that is set by the interference competitor. The resource level set by the interference competitor does not depend on system productivity either, but the level of inhibitor does: it increases with increasing productivity. So there is a value of K above which the growth rate of the invading consumer is negative: the system needs to be sufficiently productive for a priority effect to occur. If it is not, the level of inhibitor in a population of the interference competitor is insufficient to keep the more efficient resource competitor out. This is the situation at the top of figure 4.2A, where predator mortality is too high for the predator to exist. In the top part of figure 4.2B, there is no priority effect, because here consumer 2 is both the interference competitor as well as the stronger resource exploiter and there is no predation.

Top-down effects

In the presence of a predator, things are quite different. In this case, whether a priority effect occurs, does not only depend on the productivity of the system, but also on the exact strength of predation pressure. If it is too strong, as in the regions at the bottom of figure 4.2A, there is no priority effect. This is because the population density of the interference competitor, which is controlled by the predator, is kept at such a low level that the inhibitor concentration is insufficient to keep the stronger resource exploiter out (see figure 4.3 and appendix 4.5).

In the scenario of figure 4.2A, the attack rate of the predator is the same on each of the two consumers, and the same is true for the attack rates of each of the consumers on the resource. In some cases this may be a good approximation and slight deviations from equality do not alter the picture much (as evident from results obtained with slightly altered parameter sets; results not shown). However, sometimes the more efficient resource exploiter is also the stronger interference competitor. For instance, in some aquatic communities both resource exploitation efficiency (Gliwicz 1990), strength of interspecific interference (Burns 2000) and vulnerability to predation (Brooks and Dodson 1965) correlate positively with body size. We have adapted attack rates to reflect this in the scenario of figure 4.2B. Here, a priority effect only occurs when the predator exists, because the interference competitor is now the stronger resource exploiter and thus has a double advantage in the absence of the predator. However, there is still –again– a region at high predation pressures, where the priority effect is lost (figures 4.2B and 4.3B). This loss is now not only caused by

decreased interference, but also by apparent competition (i.e. by interaction through the shared predator).

In both scenarios, oscillations in consumer densities make it more difficult for the predator to exist. This results from the saturating (Holling type II) functional responses of the consumers and the predators (Armstrong and McGehee 1980). In the scenario of figure 4.2 this had very little effect on the occurrence of priority effects. However, in the scenario of figure 4.2B, where predation enables the priority effect, the region where a priority effect occurs is reduced by the fluctuations of the population densities. The amplitude of the oscillations increases as productivity increases (Rosenzweig 1971), thus the bottom-up effect of resource carrying capacity reduces the top-down effect of predation on the occurrence of priority effects. In this second scenario priority effects therefore disappear when productivity is too high.

General discussion

The results from either scenario show that there is a minimum level of productivity below which a priority effect cannot occur. This is not just true for the system we considered here. With a chemostat model of microbial growth of two species on one resource, with one species excreting an inhibitor that affects the other species, DeFreitas and Frederickson (1978) showed that if nutrient input is sufficiently high, a priority effect may occur. Studies of intraguild predation have also found that a minimal level of nutrient input is required for a priority effect to occur (Diehl and Feissel 2000, Mylius et al. 2001). This not surprising: intraguild predation can cause a priority effect if the conversion efficiency of intraguild prey to intraguild predator is low (Amarasekare 2002, Holt and Polis 1997) so that intraguild predation resembles interference competition through killing. Competition between two species in which one has a size refuge against predation also requires a minimal nutrient input to cause a priority effect (Chase 1999, Chase 2003b). In all of these cases, it was the more efficient resource exploiter that excluded its competitor at low nutrient inputs.

The effect of additional trophic levels has been studied only to a limited extent. However, in an experimental study with zooplankton, the addition of predators prevented a priority effect between two species, apparently because they were both outcompeted by a third species that was better equipped to resist predation (Louette and De Meester 2007). In a study of a multispecies Lotka–Volterra competition model, the addition of a higher trophic level reduced the number of alternative attractors (van Nes and Scheffer 2004). In an experimental study, E.S. Bakker et al. (unpublished) showed that the exclusion of herbivores increased the between-plot variation in plant community composition of otherwise identical plots. In an aquatic system, Morin (1984) showed that priority effects occurred only in the absence of predatory fish. Our result suggests a reason for the results of the latter three studies: predation suppresses competing populations to levels at which the interaction between these populations is not strong enough to cause a priority effect. Jiang and Patel (2008) suspected a similar effect in a study with bacteria and ciliates, where disturbance in the form of indiscriminate density-independent mortality promoted convergence

of communities of which the arrival times of species were experimentally varied. Besides removing priority effects, mild predation and interference can, as we have shown, also cause priority effects if there is differential vulnerability to predation. A similar result has been obtained by Vance (1978) who modelled interference in a phenomenological, Lotka-Volterra manner. Also without interference, predation can cause a priority effect if there is a trade-off between exploitation and predation and if the better resource exploiter has a lower density when in equilibrium with the predator (Grover and Holt 1998, Holt et al. 1994).

Although in our system of interference competition the priority effect implies the loss of one or the other species, diversity may still be maintained regionally if different competitors arrive first in different places. However, if local populations go extinct by disturbance, priority effects are not enough to cause regional coexistence (e.g. Shurin et al. 2004, Yu and Wilson 2001). Regional coexistence then requires that each species has places in the region where it is competitively dominant, irrespective of initial densities (Shurin et al. 2004). For a variety of mechanisms that cause priority effects this could be achieved through varying the productivity between patches, with the superior resource exploiter being dominant in patches with a low productivity and the other species being dominant in patches with a high productivity, with a priority effect at intermediate levels. In the model communities we studied, this only happens when there is predation and differential vulnerability to predation (figure 4.2B, at e.g. $d_p = 0.05$ or 0.25 day^{-1}).

Our results may also be relevant for mechanisms other than allelopathy that cause priority effects. Especially our result that priority effects disappear if predation is too strong is likely to apply to other systems as well, because high predation intensity reduces population densities and thereby the interaction between the species that are preyed upon, irrespective of how exactly they interact.

Ecology is faced with the task to predict when community (re-)assembly after environmental disturbance leads to a predictable community composition. Our results contribute to understanding how bottom-up and top-down controls determine when the outcome of community assembly is predictable as opposed to when it depends on history and initial conditions.

4.5 Appendix: Disappearance of the priority effect due to predation

Consumer 1 can invade an equilibrium community of the resource, consumer 2 and predator if its per capita growth rate, evaluated at that equilibrium, is greater than zero:

$$\frac{dC_1}{C_1 dt} > 0. \quad (4.8)$$

Because at an equilibrium with $C_2 > 0$, $\frac{dC_2}{C_2 dt} = 0$, condition (4.8) is equivalent to

$$\frac{dC_1}{C_1 dt} > \frac{dC_2}{C_2 dt}. \quad (4.9)$$

Using equations (4.2), (4.2), (4.4) and (4.5), we can write (4.9) as

$$e_{C_1} f_1(R_{C_2}^{**}) - d_C - g P_{C_2}^{**} > \frac{e_{C_2} f_1(R_{C_2}^{**})}{1 + s H_{C_2}^{**}} - d_C - g P_{C_2}^{**}, \quad (4.10)$$

where $d_c = d_{c_1} = d_{c_2}$ and $g = \frac{a_{C_1}}{1 + a_{P_1} h_{P_1} C_1 + a_{P_2} h_{P_2} C_2} = \frac{a_{C_2}}{1 + a_{P_1} h_{P_1} C_1 + a_{P_2} h_{P_2} C_2}$, and the double stars and C_2 in the subscript of R , H and P indicate values at the equilibrium of resource, consumer 2 and the predator. Solving inequality (4.10) for $H_{C_2}^{**}$ yields the condition for which consumer 2 can invade:

$$H_{C_2}^{**} < \frac{e_{C_1} - e_{C_2}}{e_{C_2} s}. \quad (4.11)$$

The right hand side of inequality (4.11) is the inhibitor level at the coexistence equilibria of consumer 1 and 2 with and without the predator. It is independent of d_P . $H_{C_2}^{**}$ does depend on d_P . Using Mathematica, we found an expression for the $H_{C_2}^{**}$ by solving for equilibrium densities of the subsystem with consumer 1 left out. Also with Mathematica, we found, assuming positive values for the parameters, that $\frac{\partial H_{C_2}^{**}}{\partial d_P} > 0$ reduces to

$$r > \frac{4 d_P a_{C_2}}{a_{P_2} (2 + K a_{C_2} h_{C_2}) (e_{P_2} - d_P h_{P_2})} \quad (4.12)$$

for $e_{P_2} - d_P h_{P_2} > 0$. This last inequality is always satisfied if the predator can exist at all feeding on consumer 2. Condition (4.12) is true for the parameter values used in figure 4.2 in the range of d_P values for which the predator can exist. If d_P is chosen small enough, this condition is true for all biologically feasible parameter values. This means that if predator mortality is reduced far enough the priority effect, if present, disappears.

Chapter 5

Alternative states and population crashes in a resource-susceptible-infected model for planktonic parasites and hosts

Daan J. Gerla, Alena Gsell, Bob W. Kooi, Bas W. Ibelings, Ellen van Donk and Wolf M. Mooij

Accepted for publication in *Freshwater Biology* (with minor revisions)

Abstract. There is an increasing awareness that parasites can regulate phytoplankton communities to the same degree as resource competition or predation by grazers. However, only few models have been developed that specifically include parasitism in phytoplankton ecology or aquatic food web studies. Here we provide a susceptible-infected model for a diatom-chytrid host-parasite system that explicitly includes nutrients, infected and uninfected hosts, reproduction of the parasite on the hosts, and free-living infective stages. A distinguishing feature of the model is that parasite reproduction on hosts increases with nutrient availability to the infected host. Published experiments have corroborated this assumption, both in a diatom-chytrid system as well as in several bacterium-virus systems. Thus, the model is likely to have a broad applicability to the epidemiology of plankton communities. It follows from this assumption that the parasite's basic reproduction number, R_0 , increases with nutrient concentration, because at higher nutrient concentrations infected hosts consume more nutrient, which is used for the reproduction of the parasite. Another important result is that under certain conditions, there may be an Allee effect in the parasite population (i.e. a decreased per capita reproduction of the parasite with decreasing parasite density) due to the parasite suppressing the host population, which increases nutrient availability to the remaining host population, which in turn increases the growth rate of the parasite. A strong Allee effect may result in two alternative states to which the densities may converge: one with only the host and one with host and parasite co-existing. Which of these two states is attained, depends on the initial nutrient concentration and densities of host and parasite. The parasite

can then only invade a host population if it is introduced above a threshold density. Finally, the model shows a strong tendency for host-parasite cycles, which may be chaotic. These may lead to a Paradox of Enrichment, i.e. a collapse of the system due to nutrient enrichment causing cycles of increasing amplitude which leads to host or parasite population extinction due to stochastic fluctuations during periods of low population density. A collapse of the parasite population is especially likely if alternative stable states and cycles co-occur. Then, increased population cycle amplitude due to nutrient enrichment may drive the parasite below its threshold density for successful invasion, causing a "deterministic Paradox of Enrichment". Published results confirm that host-parasite cycles and collapse of host-parasite systems may occur in real plankton communities. Our results underline that ecological detail in host-parasite models may have consequences for disease dynamics which may be overlooked when ecological interactions between environment, host and parasite are not explicitly taken into account.

5.1 Introduction

Traditionally, phytoplankton populations are considered to be regulated by resource availability and grazing (Sommer et al., 1986). However, there is an increasing awareness that microparasites can be at times similarly important in regulating phytoplankton populations (Lund, 1957; Canter and Lund, 1969; Van Donk and Ringelberg, 1983; Ebert et al., 2000; Gons et al., 2002; Ibelings et al., 2004; Brussaard et al., 2008; Gachon et al., 2010). In lakes these plankton parasites include viruses, bacteria, and fungi. They can have a strong impact on the abundance and diversity of hosts and the distribution of resources within food webs. For instance, selective parasitism on a species may abruptly terminate phytoplankton blooms and favour the development of other species competing for the same resources (Canter and Lund, 1951; Ibelings et al., 2004). Parasites may also change food web topology (Marcogliese, 2001). For instance, aquatic microparasites, which have a free-living stage that is vulnerable to predation, can transfer nutrients of large inedible hosts to higher trophic levels (Kagami et al., 2007). Furthermore, viral-induced lysis of host cells may divert nutrients and organic carbon away from higher trophic levels towards the pool of dissolved nutrients and organic matter (Wilhelm and Suttle, 1999). Thus, parasitism in lakes cannot be neglected and should be included in food web studies.

Despite the importance of parasites, models of plankton communities that include parasitism remain relatively rare, although some models have been developed for phytoplankton and their parasites, especially viruses. Although it has been shown that resource availability to infected hosts has a strong impact on parasite reproduction (e.g. Bruning, 1991*a*; Middelboe, 2000; Hall et al., 2009), often these models do not include nutrient competition explicitly. Nevertheless, in many of these models the density of infected hosts does negatively affect the growth of uninfected hosts, even though infected hosts do not reproduce (e.g. Beltrami and Carroll, 1994; Beretta and Kuang, 1998; Siekmann et al., 2008). For instance, Siekmann et al. (2008) model

virus reproduction within infected hosts, but keep this reproduction independent of competition between hosts. Weitz and Dushoff (2008) do model a direct effect of host growth rate on virus reproduction, by making the rate at which host cells lyse to release new virus particles decline as the host population gets closer to its carrying capacity. Despite these models being simple, they are hard to interpret because they do not model the mechanisms behind the phenomena. Recently, progress has been made by addressing the role of nutrients explicitly by including parasitism into standard nutrient-phytoplankton models (e.g. Chattopadhyay et al., 2003; Fuhrman et al., 2011) or nutrient-phytoplankton-zooplankton models (e.g. Rhodes and Martin, 2010). Fuhrman et al. (2011) even have variable nutrient quota, although in their model the rate at which viruses are produced does not depend on the nutritional state of the host cell.

Besides the effects of resource competition between hosts, researchers also have to make a choice on how to model parasite transmission from host to host. The options range from simple linear mass-action terms to more complex, non-linear transmission functions (McCallum et al., 2001). Also, infection may occur through contact with infective particles or free-living infective stages, rather than through direct contact between susceptible and infected hosts. How host-parasite interaction is modelled may have a profound impact on host-parasite dynamics. For instance, a saturating transmission function may lead to sustained host-parasite cycles. However, most models of these host-parasite interactions assume simple linear interaction terms (e.g. Miki et al., 2011). Although simplification has the advantage of keeping models tractable, the weight of evidence is that the resulting models often do not describe the host-parasite systems adequately (McCallum et al., 2001). Thus, it is necessary to investigate the consequences of relaxing these assumptions.

In the present paper, we address the above two issues, i.e. the effects of resources and of the complexity of parasite transmission on host-parasite dynamics. We do so by introducing explicit nutrient dynamics, free-living infective stages and reproduction of the parasite on the host into a susceptible-infected model, drawing upon both the disciplines of epidemiology and of plankton community ecology. The resulting eco-epidemiological model is based on a specific host-parasite system, namely the freshwater diatom *Asterionella formosa* Hassall and its virulent fungal parasite, the chytrid *Zygorhizidium planktonicum* Canter. In this system, infection by the parasite prohibits reproduction of the host and leads to its death (Canter and Lund, 1951). The infective life stage of the parasite is a motile, flagellated zoospore that actively searches for host cells and depends entirely on its internal energy storage during dispersal (Holfeld, 2000). When successfully infecting, the zoospore attaches itself to the host and becomes a sporangium. It then forms a germ tube which invades the host cell and by which it extracts nutrients from the host, ultimately killing the host (Canter and Lund, 1953; Van Donk and Ringelberg, 1983). The attached zoospore then ripens into a mature sporangium which produces new zoospores by mitosis. These zoospores are released when the sporangium bursts. Until maturation, the sporangium depends on the host cell for sustenance and is dependent on the nutrient condition of the host and its further fate. Moreover, the production of zoospores

per sporangium increases with increasing resource availability to the host (Bruning, 1991*a,c*). This system (or systems of closely related species) has been studied extensively both in the field (e.g. Canter and Lund, 1948; Van Donk and Ringelberg, 1983; Holfeld, 2000; Ibelings et al., 2011) and in the laboratory (e.g. Bruning, 1991*b,a,c*; De Bruin et al., 2004; Kagami et al., 2007).

The model we present here takes these characteristics of the host-parasite system and its resource dependence into account by making the rate of zoospore production an increasing function of ambient nutrient concentration. Furthermore, the model keeps track of the number of infected hosts, zoospores contained within sporangia as well as free-living zoospores. Although developed for a specific host-parasite system (*Asterionella* and its chytrid parasite), it shares many features with other systems such as lytic viral infections i.e., with a life cycle in which the host cell bursts releasing new virus particles). We thus expect that the model has a broad applicability. It may be used to make predictions on the dynamics of the host-parasite system, interpret field observations and develop components of larger food web models.

5.2 Methods

Summary of model assumptions

We assume that the system is limited by a single nutrient, phosphorus, which appeared as the limiting nutrient for host growth during spring chytrid epidemics in the Dutch Lake Maarsveen I (Van Donk and Ringelberg, 1983). The limiting nutrient is consumed by the host and via the infected host by the parasite. The host population is divided into two compartments: susceptible (uninfected) and infected hosts. Infection occurs according to the law of mass-action, that is, at a rate proportional to the densities of susceptible hosts and free-living zoospores. It is important to note that this is different from assuming mass-action of susceptible hosts and infected hosts. For each infection event one susceptible host becomes an infected host, and one zoospore is removed from the population of free-living zoospores. For simplicity, we assume that a host can only be infected once, so that the number of infected equals the number of sporangia. Both susceptible and infected hosts consume the nutrient. Nutrient consumed by susceptible hosts is used for the reproduction of susceptible hosts. However, nutrient consumed by infected hosts is used for the production of zoospores in sporangia attached to hosts. Sporangia burst at a constant rate releasing their zoospores in a process called dehiscence and the zoospores become free-living zoospores. The host then dies and the nutrients leftover within it and within the empty sporangium are lost by sedimentation.

By assuming a constant phosphorus content of host cells, we limit the complexity of the model. We focus instead on how nutrients are divided over the different parasite stages i.e. sporangia, zoospores contained within sporangia and free-living zoospores). The assumption that resource consumed by infected hosts is allocated to the production of zoospores is supported by the observation that the number of

zoospores per sporangium is roughly a linearly increasing function of the specific growth rate of uninfected hosts, both for phosphorus-limited (Bruning, 1991a) and light-limited hosts (Bruning, 1991c). Bruning (1991a,c) also observed that the development time of sporangia is only very weakly affected by resource availability, supporting the assumption of a constant rate of dehiscence.

Model equations

The above mentioned assumptions guide us to formulate the following model. Nutrient concentration, N , follows semi-chemostat dynamics (Persson et al., 1998), which is commonly used to model nutrient dynamics. Nutrient is consumed by infected and susceptible hosts.

$$\frac{dN}{dt} = D(N_{in} - N) - c\mu(N)(S + I), \quad (5.1)$$

where t denotes time, N is the nutrient concentration, D is the chemostat dilution rate, N_{in} is the nutrient concentration in the inflow, c is the nutrient content of the host, $\mu(N)$ is the specific growth rate of the host, S is the density of susceptible hosts, and I is the density of infected hosts. For a summary of the symbols, their meaning and units of measurement, see table 5.1. The population growth rate of susceptible hosts is given by

$$\frac{dS}{dt} = \mu(N)S - dS - \beta SZ, \quad (5.2)$$

where d is the per capita loss rate of the host (not including losses related to parasitism), β is the infectivity constant, which measures how efficiently zoospores infect hosts, and Z is the density of free-living zoospores. The population growth rate of infected hosts, or equivalently, of sporangia, is given by

$$\frac{dI}{dt} = \beta SZ - dI - \gamma I, \quad (5.3)$$

where γ is the rate at which sporangia release zoospores, which is the inverse of sporangium maturation time. The total density of zoospores contained within sporangia (attached zoospores), Y , is given by

$$\frac{dY}{dt} = b\mu(N)I - dY - \gamma Y, \quad (5.4)$$

where b is the ratio of nutrient content of zoospores to the nutrient content of hosts, which is the number of zoospores that can be produced from the amount nutrient required to produce exactly one new host cell. The population growth rate of the free-living zoospores is given by

$$\frac{dZ}{dt} = \gamma Y - \delta Z - \beta SZ, \quad (5.5)$$

where δ is the per capita loss rate of free-living zoospores, which is the inverse of their infective life-time. The specific growth rate $\mu(N)$ of the host is given by

$$\mu(N) = \frac{\mu_{max}N}{N + K}, \quad (5.6)$$

where μ_{max} is the maximum specific growth rate and K is the half-saturation constant for growth.

Table 5.1. Symbols, their meaning, standard values, and units of measurement.

symbol	meaning	value	units
variables			
t	time		days
N	concentration of free nutrient		$\mu\text{g P L}^{-1}$
S	density of susceptible, uninfected hosts		cells L^{-1}
I	density of infected hosts		cells L^{-1}
Y	density of zoospores contained within sporangia attached to hosts		cells L^{-1}
Z	density of free-living zoospores		cells L^{-1}
parameters			
D	dilution rate	0.1	day^{-1}
K	half-saturation constant	0.5 ^(a)	$\mu\text{g P L}^{-1}$
N_{in}	resource concentration in inflow	varied ^(b)	$\mu\text{g P L}^{-1}$
b	ratio of resource content of zoospores to that of hosts	8 ^(c)	cells cell^{-1}
c	resource content of host	$10^{-6(d)}$	$\mu\text{g P cell}^{-1}$
d	specific loss rate of host	varied ^(e)	day^{-1}
β	infectivity	$10^{-6(f)}$	$\text{L cell}^{-1} \text{day}^{-1}$
γ	bursting rate	0.6 ^(g)	day^{-1}
δ	specific loss rate of free-living zoospores	0.4 ^(h)	day^{-1}
μ	specific growth rate of susceptible hosts		day^{-1}
μ_{max}	maximum specific growth rate of susceptible hosts	1.0 ⁽ⁱ⁾	day^{-1}

(a) 0.62 at 20°C (Tilman and Kilham, 1976); 0.62 to 1.1 at 5 to 20°C (Van Donk and Kilham, 1990). (b) In Lake Maarsveen: depth-averaged total phosphorus: circa 5 to circa 20, time average: circa 12 (Lingeman et al., 1987). (c) Under high ambient phosphorus concentrations: 4.08 (Kagami et al., 2007); estimate from Bruning (1991a): circa 11. (d) Minimum: $2.3 \cdot 10^{-7}$ to $2.9 \cdot 10^{-7}$ (Van Donk and Kilham, 1990); under high ambient phosphorus concentrations: $9.8 \cdot 10^{-6}$ (Kagami et al., 2007). (e) Hard to estimate and hence varied. (f) Under constant light and low turbulence (see Methods) at 16°C: circa $2.5 \cdot 10^{-6}$ to circa $5 \cdot 10^{-6}$ (Bruning, 1991a). (g) circa 0.6 at 16°C (Bruning, 1991a); on light limited hosts: 0.05 at 2°C to 0.5 at 21°C (Bruning, 1991b). (h) 0.09 at 4°C to 0.33 at 19°C (Bruning, 1991b) (i) 0.88 at 20°C (Tilman and Kilham, 1976); 0.44 at 5°C to 0.80 at 20°C (Van Donk and Kilham, 1990); 0.95 at 16°C (Bruning, 1991a).

Methods of analysis

We analyse the model through bifurcation analysis (see e.g. Kuznetsov, 2004), which shows how the long term model behaviour changes as model parameters are varied. At certain parameter values the change may be qualitative instead of just quantitative. Such change is called a bifurcation. We thus identify regions of parameter values for which certain model behaviours occur. Some bifurcations can be determined directly, for instance invasion criteria for host and for parasite as illustrated in figure 5.1. The bifurcations are depicted in parameter diagrams (figures 5.2, 5.3 and 5.4). Such diagrams tell us how robust model outcomes are against variation in parameters, and how system behaviour changes with the parameters.

We have done most of the bifurcation analysis in a numerical manner, because of the complexity of the model. To this end, we have parameterized the model with realistic values that are similar to those reported in the literature for *A. Formosa* and *Z. planktonicum*, and then varied one or two parameters (see table 5.1 and the references at the bottom of the table). We probably have reliable estimates of the upper bound of infectivity constant β (Bruning, 1991*a*). However the infectivity constant varies with turbulence and infection ceases in the dark (Canter and Jaworski, 1981). Therefore, we have chosen an infectivity constant that is substantially lower than under optimal conditions.

For construction of the two dimensional parameter diagram (figure 5.2, where we varied two parameters), we used the software package AUTO-07p (Doedel and Oldemans, 2007, homoclinic connections can be calculated using the HomCont part of AUTO-07p). The one dimensional parameter diagrams (see figures 5.3 en 5.4) were constructed through simulation. The parameter N_{in} was increased in steps of $0.001 \mu\text{g P L}^{-1}$. For each step, a simulation was run for 2000 days (figure 5.3) or 10000 days (figure 5.4) and the local minima and maxima of nutrient concentration and of the population densities in the last 1000 days (figure 5.3) or 5000 days (figure 5.4) were plotted as individual dots in the graph. The final densities of one simulation (at $t = 2000$ days (figure 5.3) or at $t = 10000$ days (figure 5.4)) served as initial densities for the next simulation.

5.3 Results

Invasion of the nutrient-phytoplankton system by the parasite

Some relevant insights can be derived from the basic reproduction number, denoted R_0 . The basic reproduction number is defined as "the expected number of secondary cases produced by at typical infected individual during its entire infectious period, in a population of susceptibles only" (Heesterbeek and Dietz, 1996). If $R_0 < 1$, a small parasite population invading a population of susceptible hosts is expected to die out. If $R_0 > 1$, invasion is expected to be successful and an initially small parasite population will grow. Thus, R_0 gives a criterion for invasion of the parasite.

We calculate R_0 from equations (5.3-5.5) as follows:

$$\begin{aligned}
 R_0 &= \begin{array}{l} \text{infections} \\ \text{per zoospore} \\ \text{per unit time} \end{array} \times \begin{array}{l} \text{infective} \\ \text{life time} \\ \text{zoospores} \end{array} \times \begin{array}{l} \text{zoospores produced} \\ \text{per sporangium} \\ \text{per unit time} \end{array} \\
 &\quad \times \begin{array}{l} \text{life time} \\ \text{infected} \end{array} \times \begin{array}{l} \text{fraction of infected} \\ \text{that survives till} \\ \text{sporangium bursts} \end{array} \quad (5.7) \\
 &= \beta S^* \times \frac{1}{\delta + \beta S^*} \times b\mu(N^*) \times \frac{1}{d + \gamma} \times \frac{\gamma}{d + \gamma} \\
 &= \frac{\beta S^*}{\delta + \beta S^*} \times \frac{b\mu_{\max} N^*}{N^* + K} \times \frac{\gamma}{(d + \gamma)^2},
 \end{aligned}$$

where N^* and S^* denote nutrient concentration and host density at equilibrium in absence of the parasite. (For a more rigorous derivation of the invasion criterion, based on linear stability analysis, see appendix 5.5). Thus, R_0 increases with the density of susceptible individuals as well as with nutrient concentration and these saturate as susceptible host density or nutrient concentration become high. We have depicted the dependence of R_0 on susceptible host density and nutrient concentration for various values of nutrient supply N_{in} and host loss rate d (figure 5.1). In this figure, R_0 is greater than 1 in the grey shaded areas, that is, for higher susceptible and nutrient densities. The curve at which $R_0 = 1$ has two asymptotes parallel to the axes (the grey dashed lines), which means that there are low nutrient densities for which R_0 cannot be greater than one, no matter how high the density of susceptible hosts is, and similarly that there are low densities of susceptible hosts for which there are no nutrient concentrations that give $R_0 > 1$.

Thus, whether the R_0 is greater than one depends on whether the nutrient concentration and susceptible host density at the disease-free equilibrium fall within the grey shaded areas of figure 5.1. To determine this, we have also plotted in figure 5.1 the zero growth isoclines of the nutrient and the susceptible host (see legend of figure 5.1). At these isoclines, $dN/dt = 0$ and $dS/dt = 0$, and their intersection marks the nutrient concentration and susceptible host density at the disease-free equilibrium, i.e. N^* and S^* . N^* is the nutrient concentration at which the uninfected host can reproduce just fast enough to make up for its losses, that is $\mu(N^*) = d$. As N_{in} increases, the position of the vertical isocline at which $dS/dt = 0$ does not change. Thus, N^* does not depend on N_{in} . Also, the area for which R_0 is greater than one does not change with N_{in} (see also equation 5.7). However, the isocline at which $dN/dt = 0$ does change with nutrient supply. At high host loss rate and very low nutrient supply this isocline does not intersect the isocline of the host and the host cannot persist (figure 5.1a). At a higher nutrient supply, N_{in} exceeds N^* and the isoclines do intersect. So then the host can establish a population. However, the intersection does not fall in grey shaded area, so we still have $R_0 < 1$ (figure 5.1b). As nutrient supply increases further, S^* increases along the black dotted host isocline. In figure

5.11c, N^* and S^* do fall within the grey shaded area and thus there the parasite can invade a population of the host.

In figure 5.1d-f, host loss rate is much lower. Here, the asymptotes of the curve $R_0 = 1$ have shifted towards the axes and the area for which $R_0 > 1$ is larger due to reduced losses of infected hosts (see equation 5.7). (Note that the S -axis in figure 5.1f extends to a larger density.) This in itself facilitates invasion by the parasite, however, the susceptible, uninfected host has become a much more effective nutrient consumer due to the reduced loss rate, and now has much lower N^* . In fact, the isocline of the host now lies to the left of the vertical asymptote of the curve $R_0 = 1$. Thus, even though S^* increases with nutrient supply, the disease-free equilibrium will never fall within the area for which $R_0 > 1$ and parasite invasion is impossible no matter how many susceptible hosts there are.

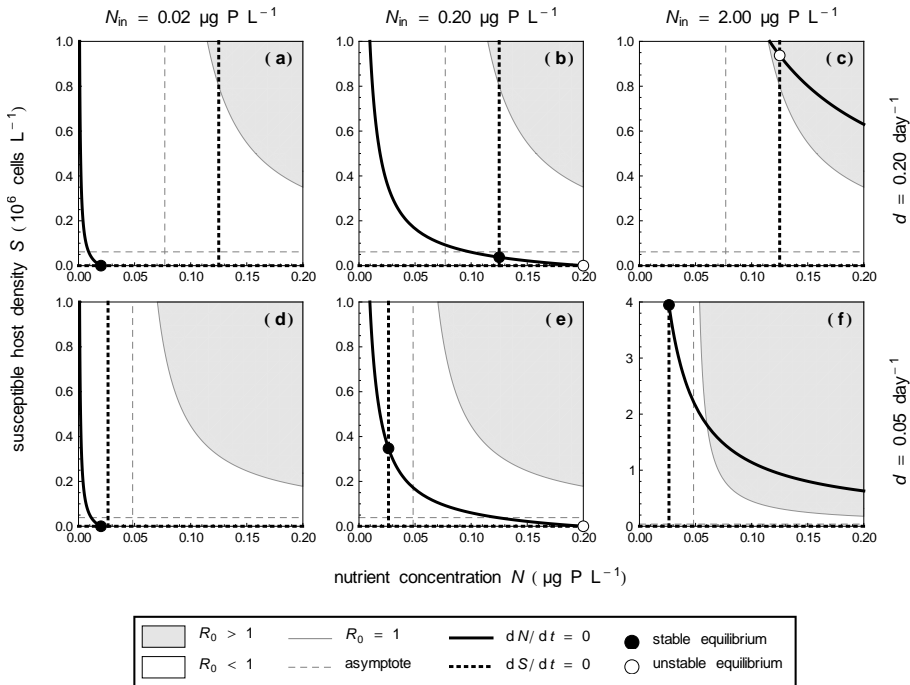


Figure 5.1. The dependence of the basic reproduction number, R_0 , on the density of susceptible hosts, S , and nutrient concentration, N , for various values of nutrient supply N_{in} and host loss rate d . Other parameter values are as in table 5.1. Note that the S -axis in (f) extends to a higher density than in the other panels.

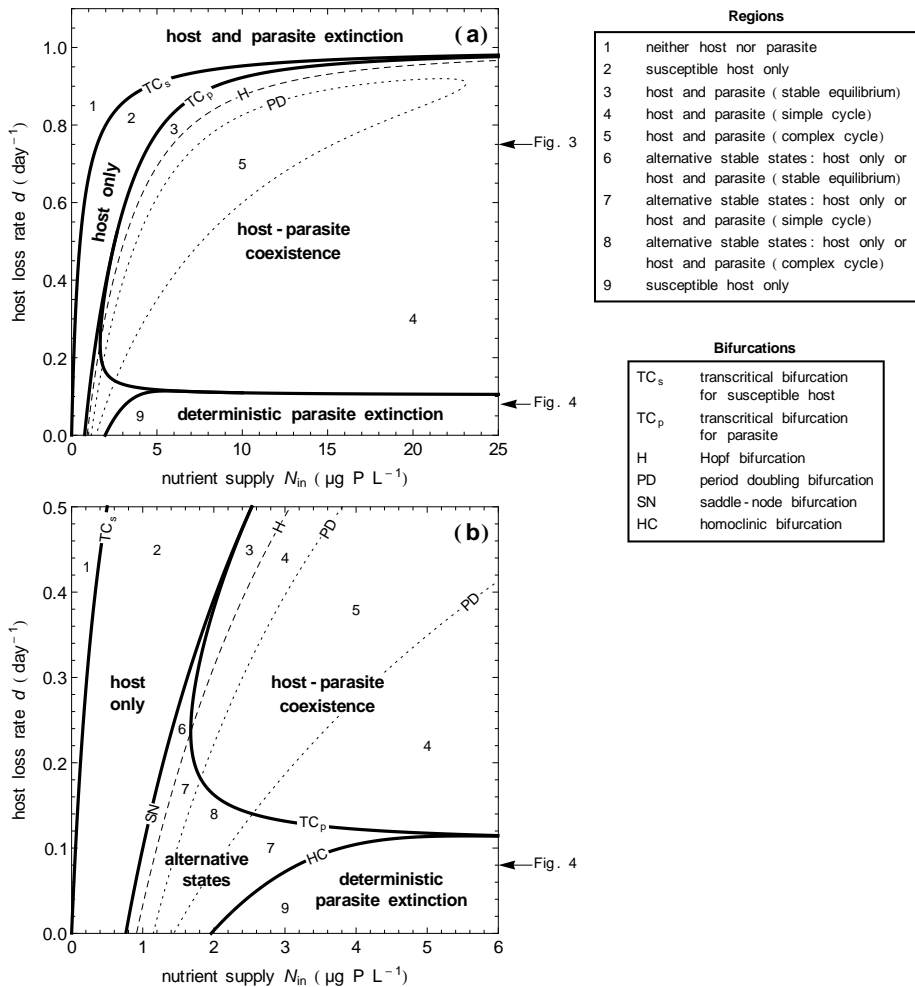


Figure 5.2. Two dimensional parameter diagram indicating regions of nutrient supply (N_{in}) and host loss rate (d) with qualitatively different dynamical attractors. (b) is a magnification of the bottom-left of (a). Thick solid curves separate regions where different species persist, dashed or dotted curves separate regions with different dynamical regimes. The arrows at $d = 0.75 \mu\text{g P L}^{-1}$ and $d = 0.08 \mu\text{g P L}^{-1}$ indicate the host loss rate used in figure 5.3 and 5.4, respectively. Other parameter values are given in table 5.1.

Dependence of host-parasite coexistence on nutrient supply and host loss rate

R_0 tells us whether the parasite can invade a host population from low density. However, it does not tell us what happens after the parasite population has started to grow and reached appreciable densities. Furthermore, in principle it may be possible

for the parasite population to grow when introduced at a higher density, even when it cannot invade when introduced at a low density. To investigate this further, we have constructed the parameter diagram of figure 5.2. In this diagram, we vary nutrient supply N_{in} and host loss rate d along the axes, and divide the N_{in} - d plane into regions with qualitatively different attractors. By attractor we mean the dynamical behaviour the model tends to when time gets large. Qualitatively different attractors differ in the absence and presence of species and the type of population dynamics. The solid curves in figure 5.2 separate regions where different species persist: in region 1 ("host and parasite extinction"), neither host nor parasite survives; in region 2 ("host only"), only the host survives; in region 3-4-5 ("host-parasite coexistence"), host and parasite coexist; in region 6-7-8 ("alternative states"), either only the host survives, or host and parasite coexist, depending on the initial population densities and nutrient concentration; in region 9 ("deterministic parasite extinction"), only the host survives in the long run. The dashed curve in figure 5.2 separates regions where the dynamics of host and parasite converge to a stable equilibrium and regions where host-parasite cycles persist. The dotted curve encloses a region where the host-parasite cycles are complex or chaotic. In the next paragraph we will explain what this means.

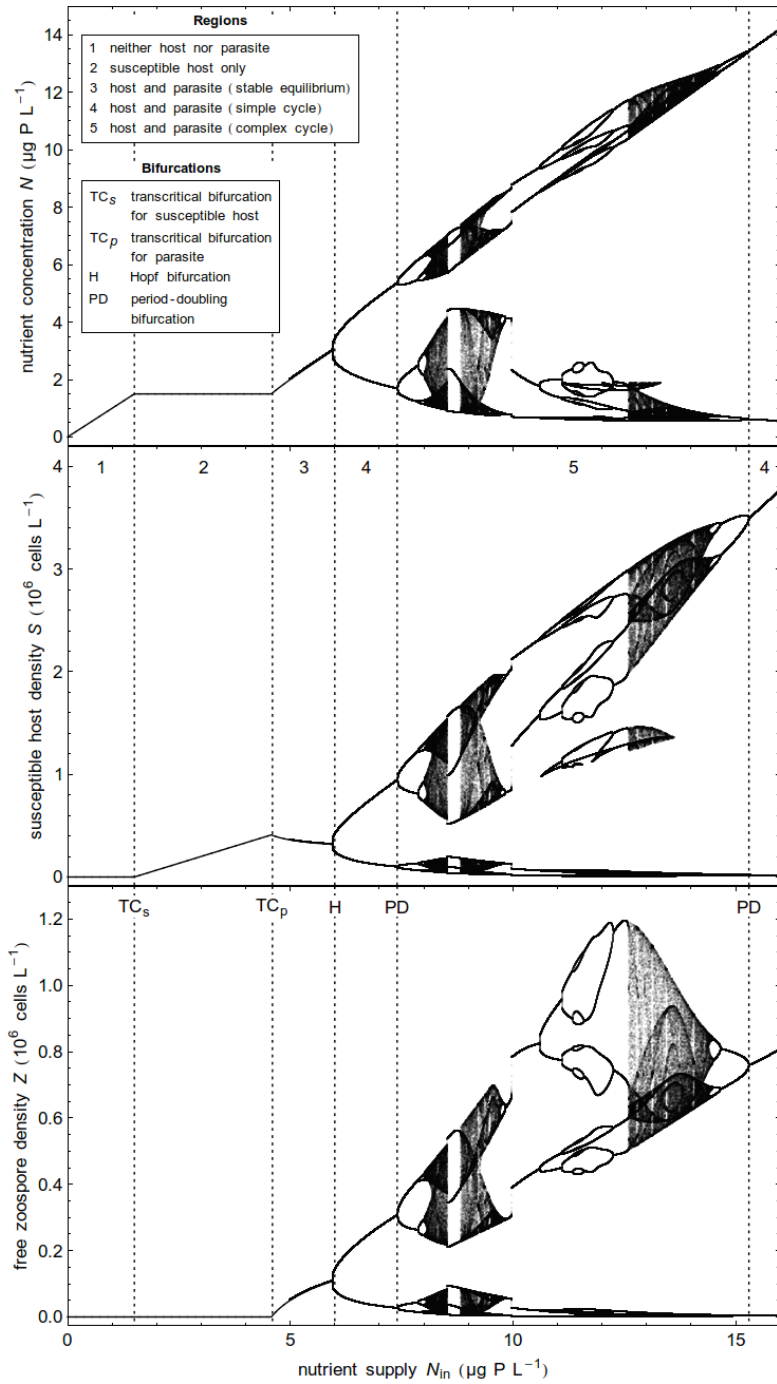
In the one dimensional parameter diagram of figure 5.3, we have plotted for a range of nutrient supplies (but with host loss rate fixed at $d = 0.75 \text{ day}^{-1}$) the local minima and maxima of nutrient, susceptible host and free zoospore density between $t = 1000$ days and $t = 2000$ days, as determined from simulations. The plots for infected hosts and attached zoospores (not shown) look very similar to the plot for free zoospores. The arrow at $d = 0.75 \text{ day}^{-1}$ in figure 5.2 indicates the host loss rate used in figure 5.3. As N_{in} increases, the dynamics change quantitatively and qualitatively as N_{in} passes through the different regions of figure 5.2 and the system undergoes several different bifurcations. At low N_{in} , resource supply is too low for the host to persist and nutrient concentration settles at $N = N_{in}$ (region 1). At $N_{in} = N^* = 1.5 \mu\text{g P L}^{-1}$, a transcritical bifurcation occurs (TC_s) and for larger N_{in} the host persists and nutrient concentration remains constant as long as susceptible density is too low for the parasite to invade (region 2). However, if N_{in} increases further, another transcritical bifurcation occurs at which $R_0 = 1$ (TC_p). From that point on, the parasite can invade. Now, nutrient concentration and parasite density increase with N_{in} and susceptible density decreases (region 3). Further increasing N_{in} leads to a Hopf bifurcation (H) at which the coexistence equilibrium becomes unstable and nutrient concentration, host density, and parasite density start to oscillate at a limit cycle. Hence, from the Hopf bifurcation onwards, the minima and maxima are distinct. First the cycle is a simple cycle, that is, each cycle has one maximum and one minimum (region 4). As N_{in} increases further, the number of maxima and minima doubles at a period doubling bifurcation (PD), and the cycle becomes complex (region 5). Further increases in nutrient supply cause a cascade of period doublings en route to chaos. Thus, eventually, the dynamics become chaotic. Increasing N_{in} even further leads to more period doublings, periodic (non-chaotic) windows within the chaotic regions and period halvings (note that the sudden jumps of the minima and maxima at N_{in} of circa $8.6 \mu\text{g P L}^{-1}$ and N_{in} of circa $10.0 \mu\text{g P L}^{-1}$ are due to the sudden disappearance

of one of two alternative stable cycles). Finally, at high nutrient supply, the cycle becomes a simple cycle again (region 4).

We have constructed another parameter diagram similar to figure 5.3, but with $d = 0.08 \text{ day}^{-1}$ (figure 5.4). Here, for part of the nutrient supply range, the system exhibits alternative stable states, where in one state only the host is present, and in the other state host and parasite coexist (region 6-7-8-7). In these parameter regions, persistence of the parasite depends on the initial densities of nutrient, host and parasite. All initial densities from which the system converges to one or the other stable state are called the attractor's domain of attraction. As nutrient supply increases from low values in figure 5.4, we first encounter the transcritical bifurcation from beyond which the host can persist (TC_s). As nutrient supply increases further, we encounter a saddle-node bifurcation (SN). At the saddle-node bifurcation, a stable equilibrium and a saddle (not stable) equilibrium originate. (The saddle equilibrium is not shown in figure 5.4.) Following the stable equilibrium we encounter the Hopf bifurcation (H), where the equilibrium becomes unstable and a stable limit cycle originates (note that for N_{in} between approximately $2.5 \mu\text{g P L}^{-1}$ and $3.2 \mu\text{g P L}^{-1}$ free zoospore density has two minima and maxima in one cycle, while for the same range of N_{in} nutrient concentration and susceptible host density have only one). As N_{in} increases, the amplitude of the cycle increases (undergoing a period doubling and halving at the PD's) and as we approach the homoclinic bifurcation (HC), the orbit of the limit cycle passes nearer and nearer to the saddle equilibrium. This saddle equilibrium lies at the border of the domain of attraction of the limit cycle. Therefore, at the homoclinic bifurcation, the domain of attraction disappears together with the limit cycle itself. At the homoclinic bifurcation, the cycle has become a homoclinic orbit connecting the saddle equilibrium with itself. Beyond this bifurcation, populations starting close to the unstable equilibrium (the one from which the limit cycle originated), end up, after a number of oscillations, in the disease-free, stable, equilibrium. Note that, when following the homoclinic bifurcation by increasing both N_{in} and d in figure 5.2, it merges with the transcritical bifurcation for the parasite (TC_p).

Thus, to summarize, at high host loss rates (figure 5.3), host-parasite coexistence requires a minimum nutrient supply. At this nutrient supply (at TC_p), the basic reproduction number of the parasite turns greater than 1, and from then on, the parasite can invade a population of susceptible hosts from low density. However, at high nutrient supply, the amplitude of the limit cycle is very large and the population densities periodically become very small, at which times one or both populations may go extinct due to stochastic fluctuations. This phenomenon is called the Paradox of

Figure 5.3 (facing page). One dimensional parameter diagram with local minima and maxima of nutrient concentration N , susceptible density S , and free zoospore density Z , as determined by simulation, for a range of nutrient supplies, N_{in} and host loss rate fixed at $d = 0.75 \text{ day}^{-1}$. For each value of N_{in} , a point is plotted for each minimum and maximum between $t = 1000$ days and $t = 2000$ days. The bifurcations and numbers for regions correspond to those in figure 5.2. Other parameter values are given in table 5.1.



Enrichment: increasing nutrient supply leads to a collapse of the system (Rosenzweig, 1971).

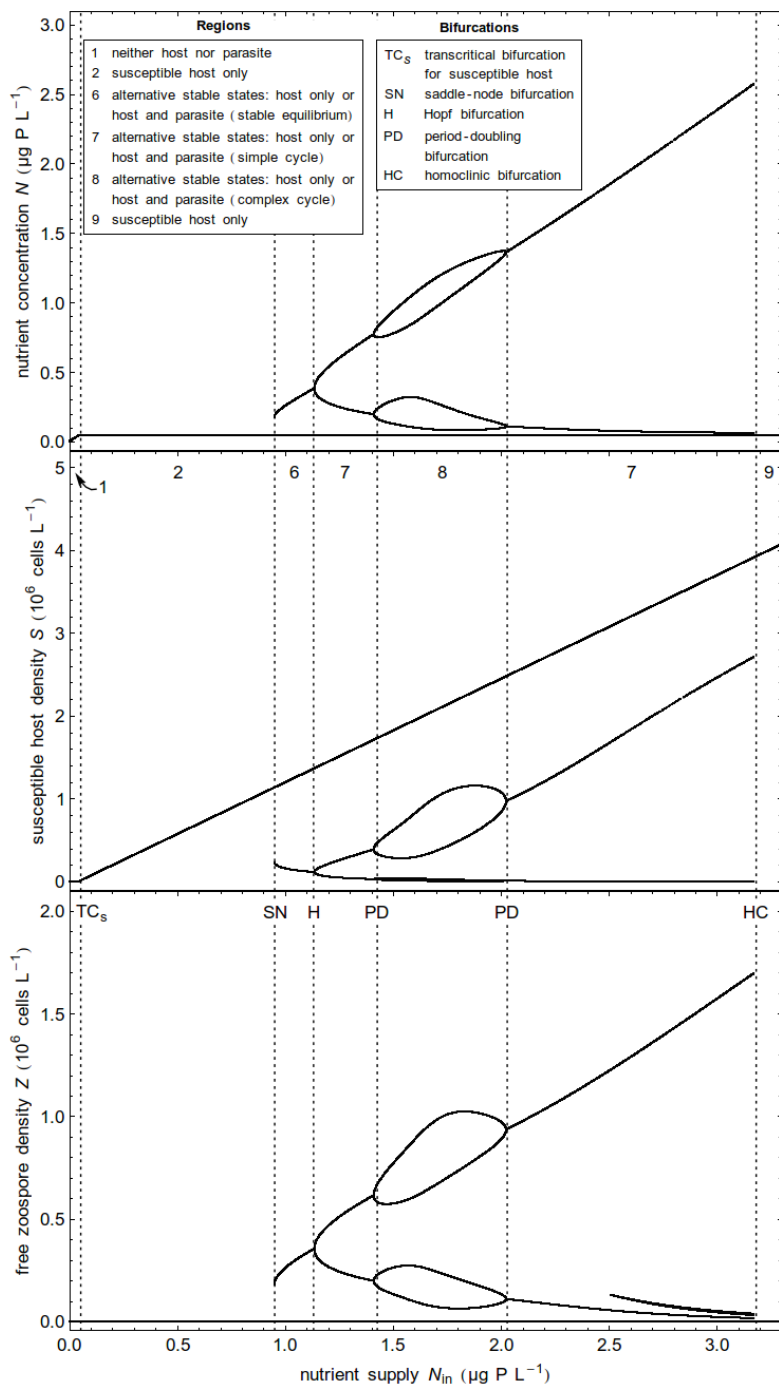
In contrast, at low host loss rates (figure 5.4), the basic reproduction number is less than 1 for all nutrient supplies (as in figure 5.1-d-f). Nonetheless, for a minimum nutrient supply (at SN), the parasite may invade a population of susceptible hosts if introduced at high enough density. Thus, for a range of nutrient supplies, there are alternative stable states, with survival of the parasite depending on initial population densities. The state with host and parasite coexisting need not be a stable equilibrium, instead, population densities may oscillate. As nutrient supply increases, the amplitude of the oscillation increases and from some nutrient supply (at HC) onwards, densities cycle, as it were, into the domain of attraction of the host-only equilibrium. Thus, for large nutrient supplies, the parasite goes extinct independent of initial densities, even in the absence of population stochasticity. Therefore, this phenomenon may be termed the deterministic Paradox of Enrichment.

The deterministic extinction of the parasite in this Paradox is illustrated in figure 5.5, where nutrient concentration and population densities are plotted as a function of time. Initially, nutrient concentration is high. When susceptible hosts and zoospores are introduced at $t = 0$ days, susceptible hosts quickly increase, followed by the parasite. Then, the susceptible host population declines while the infected host population, the attached spores and the free zoospores increase, leading to an eruption of disease and a collapse of the host population. During this collapse, the parasite goes extinct deterministically, because it falls below its threshold density for successful invasion. Also, the density of the susceptible host becomes very low (staying below 1 cell L^{-1} for circa 9 days), making the host vulnerable to stochastic extinction. In our deterministic model, however, the host eventually recovers.

5.4 Discussion

Despite the high abundances and strong impact of parasites in aquatic ecosystems, their role in shaping food webs has been little studied when compared to the roles of herbivores and predators (Kagami et al., 2007; Gachon et al., 2010). Food web models often do not include parasites (Marcogliese and Cone, 1997). In the present paper, we proposed a model of a food web module (*sensu* Holt, 1997) consisting of an algal host and a parasite with a free-living infective stage. The model keeps track of both the number of free-living parasites, as well as the number of parasites contained

Figure 5.4 (facing page). One dimensional parameter diagram with local minima and maxima of nutrient concentration N , susceptible density S , and free-living zoospore density Z , as determined by simulation, for a range of nutrient supplies, N_{in} , and host loss rate fixed at $d = 0.08 \text{ day}^{-1}$. For each value of N_{in} , a point is plotted for each minimum and maximum between $t = 5000$ days and $t = 10000$ days. The bifurcations and numbers for regions correspond to those in figure 5.2. Other parameter values are given in table 5.1.



on the host. By explicitly modelling both infected hosts and individual parasites our model forms an alternative to standard epidemiological models in which the rate at which new infections occur follows mass-action, i.e. is proportional to the densities of susceptible and infected hosts. Furthermore, our model accounts for resource consumed by infected hosts by making the production of new parasites proportional to resource uptake by infected hosts. This assumption is in accordance with the observation of (Bruning, 1991*a*) that the amount of zoospores per sporangium increases with the specific growth rate of uninfected hosts in phosphorus-limited cultures. The same observation has been made with light-limited cultures (Bruning, 1991*c*). It is also a reasonable assumption for other host-parasite systems, such as algae and their viral parasites, that parasite reproduction in or on hosts increases when hosts consume more of the limiting resource. For instance, Bratbak et al. (1998) showed a thirty-fold increase in the number of viruses produced per host in exponentially growing, nutrient replete algal cultures as opposed to nutrient depleted or light-limited cultures. Also, Middelboe (2000) observed an increased number of viruses per host in algal cultures in chemostats at increased nutrient concentrations and increased specific growth rates of the host. Furthermore, parasite production has also been shown to increase in *Daphnia* hosts as ambient food levels increase (Hall et al., 2009).

One of the consequences of the assumption that parasite reproduction depends on the rate of resource supply to the host becomes clear in the basic reproduction number, R_0 . As can be seen from equation (5.7), R_0 increases with susceptible host density. This is expected, because a higher density of susceptible hosts makes it easier for the parasite to find a host (e.g. Anderson and May, 1979; May and Anderson, 1979). An additional result, however, is that R_0 also increases with nutrient concentration. This is so because resource taken up by infected hosts is used for parasite reproduction. This results in more zoospores per sporangium, because sporangium maturation time is not affected by nutrient concentration. This is why the parasite cannot invade from low density when host loss rate is low: then, the host in absence of the parasite can reduce nutrient concentrations to very low levels, because low nutrient levels are sufficient for the host to maintain itself (compare figure 5.1*a-c* with figure 5.1*d-f* and figure 5.3 with figure 5.4). This makes that infected hosts produce simply too few spores for the parasite to spread. Figure 5.1 illustrates that invasion from low density by the parasite of a susceptible population, i.e. $R_0 > 1$, requires both a minimum host density as well as a minimum resource density.

One of our most striking results is the strong tendency of the model to produce sustained host-parasite cycles. The possibility for sustained population cycles has been shown before in models with free-living infective stages (May and Anderson, 1979). A large area in the parameter diagram of figure 5.2 contains host-parasite cycles, thus for a wide range of parameter values these cycles occur. This is also clear from the parameter diagram of figure 5.3: starting from the nutrient supply marked with "H" (for Hopf bifurcation) the minima and maxima of the population densities are distinct, meaning that there are population cycles. It is perhaps more surprising that these cycles can be complex and even chaotic. With complex cycles we mean

that the cycles have a periodicity higher than one and population densities have more than one minimum and maximum per cycle. In figure 5.3, this happens between nutrient supplies marked with "PD" (for period doubling bifurcation). In parts of this range, the number of minima and maxima is so large, that the plot in figure 5.3 becomes grey with dots. In this area we speak of chaos. Chaos implies that densities at a future time depend very sensitively on the current densities, that is, there is a strong sensitivity to initial conditions. This sensitivity has important consequences for the predictability of the population dynamics, because approximate knowledge of the current state is not enough to predict the approximate densities at some future time, even if the exact mechanisms, parameter values, etc. are known.

Another interesting result is that for some parameter values, there are two alternative states to which the densities may converge, one with only the host, and one with host and parasite co-existing. Which of these two states is attained, depends on the initial nutrient concentration and host and parasite densities. This is the case in the region marked with "alternative states" in figure 5.2, i.e. at low host loss rates. An intuitive explanation could be the following. At low levels of infection and at low host loss rates, a low nutrient concentration is sufficient for the host to maintain itself, allowing the host population to reduce the nutrient concentration to low levels (Tilman's R^* rule (Tilman, 1982), figure 5.1d-f and figure 5.3). This impairs parasite reproduction because infected hosts can produce only few parasites due to lack of nutrients. This causes the level of infection to drop even further. However, a parasite that is already at high population density suppresses the host population through increased host mortality and decreased host reproduction. Although a reduced host population by itself is detrimental to the parasite because it impairs transmission, suppressed host densities increase nutrient availability, increasing nutrient uptake by infected hosts, which in turn increases parasite reproduction per infected host. If the net effect is positive, the per capita growth rate of the parasite increases with increasing parasite density, enabling the parasite to persist.

The existence of such alternative stable states limits the usefulness of the basic reproduction number as an indicator of whether the parasite can persist. Often, it is assumed that if the parasite cannot invade from low density, the parasite cannot persist under any circumstances. However, as in our case, the parasite may be able to persist if it is introduced above a threshold density. In population biology, such an effect is called a strong Allee effect (Stephens et al., 1999; Taylor and Hastings, 2005a). Allee effects and alternative stable states in parasite populations have been observed before in eco-epidemiological models (Regoes et al., 2002; Weitz and Dushoff, 2008), which suggests that Allee effects may be more common in host-parasite systems. Especially the model of Weitz and Dushoff (2008) is interesting, because they include a direct effect of host growth rate on the rate at which parasites reproduce, even though they do not model nutrients explicitly. Their bifurcation diagram is strikingly similar to our figure 5.2, the main difference being that Weitz and Dushoff (2008) did not find sustained host-parasite cycles.

The combination of host-parasite cycles and alternative states gives rise to yet another result: the deterministic extinction of the parasite population at high nutrient

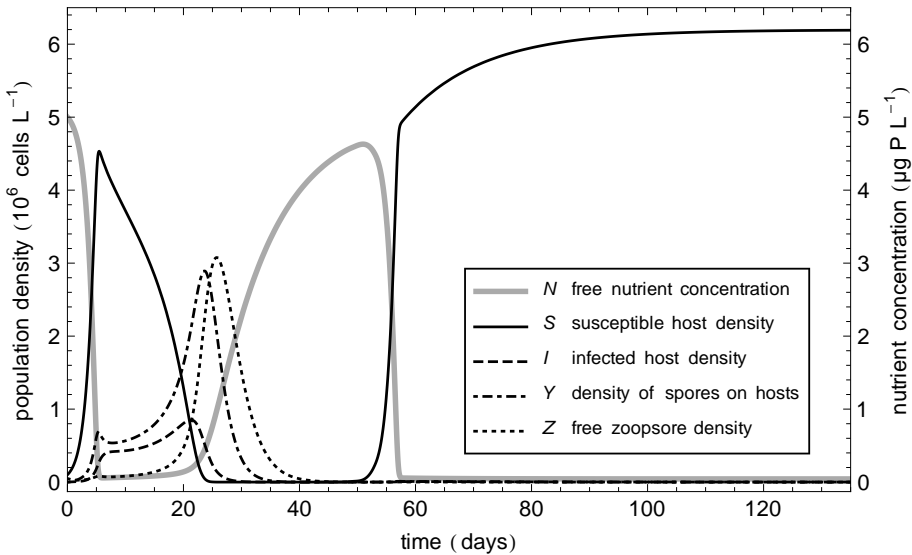


Figure 5.5. Nutrient concentration and cell densities plotted as function of time, illustrating deterministic extinction of the parasite. Parameters are as in table 5.1, with $d = 0.08 \text{ day}^{-1}$ and $N_{\text{in}} = 5.0 \text{ } \mu\text{g P L}^{-1}$. Initial densities: $N(0) = N_{\text{in}}$, $S(0) = 10^5 \text{ cells L}^{-1}$, $I(0) = 0 \text{ cells L}^{-1}$, $Y(0) = 0 \text{ cells L}^{-1}$, $Z(0) = 5 \times 10^4 \text{ cells L}^{-1}$

supply and low host loss rates (region 9 in figure 5.2 and 5.4). Here, only the host survives in the long run, like it does in region 2. The difference is that in region 2 host density is too low for the parasite to reproduce. In region 9, the host can reproduce, however, the host-parasite cycles are of such amplitude that the densities get close enough to the equilibrium at which the parasite is absent for this equilibrium to become the only attractor. Here, we have a type of Paradox of Enrichment: increasing nutrient supply leads to a collapse of the system. The difference from the classical Paradox of Enrichment (Rosenzweig, 1971), is that the parasite population goes extinct even if population densities can become arbitrarily small. The collapse may be very sudden: for some nutrient supply, the population densities stay well away from zero, for a slightly larger nutrient supply, the host-parasite system collapses and the parasite goes extinct. Thus, here, parasite extinction is not due to population stochasticity. Hence, this phenomenon may be termed the "deterministic Paradox of Enrichment". Deterministic extinction of the parasite is illustrated in figure 5.5, where the parasite can initially invade, but fails to recover after the host-parasite system crashes, whereas the host does recover. Deterministic extinction of parasite or host and parasite were also found in a plankton model that included fish predation (Hall et al., 2005). A similar phenomenon was also studied by Kooijman et al. (2004), in a model for a grazer-alga system with a varying biomass composition of the algae.

Thus, one of our key results is that host-parasite cycles may be a prominent

feature in plankton communities. Such cycles may lead to parasite extinction or the collapse of an entire host-parasite system. This is true even if host and parasite can invade from arbitrarily low densities as in figure 5.3, because the minimum densities of host or parasite may be so low that one or the other goes extinct due to stochastic fluctuations, as in the classical Paradox of Enrichment (Rosenzweig, 1971). In figure 5.5, the host is prone to such extinction during the period in which its density is very low. Some empirical evidence has suggested the existence of host parasite cycles in lakes. For instance, time series of the densities of *A. formosa* and its chytrid parasites in a Dutch lake showed some alternating peaks in the density of uninfected and infected hosts, often ending in the demise of the host-parasite system (Ibelings et al., 2011; Gsell et al., 2012). Also, cyanobacterial populations have been shown to collapse due to virus induced cell lysis in continuously enriched cultures (Gons et al., 2002; Simis et al., 2005).

Of course, the situation in real lakes is considerably more complicated than in our model. An obvious difference is that in lakes many more species interact. It would therefore be reasonable to extend the model with more species. For instance, the host *A. formosa* has a number of resource competitors, such as the diatoms *Stephanodiscus hantzschii* Grunow and *Fragilaria crotonensis* Kitton (Van Donk and Kilham, 1990). Adding more diatom species to the model is interesting, not only because they compete for limiting resources with *Asterionella*, but also because the presence of non-host diatoms may interfere with the ability of zoospores to find a suitable hosts (due to dilution effects, see e.g. Keesing et al., 2006). *A. formosa* is itself not vulnerable to grazing by zooplankton, however, zooplankton may consume the free-living zoospores of *Z. Planktonicum* (Kagami et al., 2007). Theoretically, this predation can lead to a "food web mutualism" between *A. formosa* and its competitors (Miki et al., 2011). Another interesting extension of the model would be to include seasonality. In temperate lakes, build-up and breakdown of stratification drives seasonal variance in nutrient supply. Such variance can lead to chaos in plankton community models (Beltrami and Carroll, 1994; Huppert et al., 2005; Dakos et al., 2009). This effect may be reduced by climate warming, which may increase the stability of thermal stratification in lakes (Livingstone, 2003).

Models of aquatic communities have neglected parasites for a long time, and when they have included parasitism, they have often neglected the ecological details of the interaction between host and parasite. For many host-parasite systems it is plausible – and has indeed been shown experimentally – that parasite reproduction increases not only with host availability, but also with the availability of resource to the host. As we have shown, such detail may have unexpected consequences, such as a sudden collapse of the parasite population and chaos. Thus, in order to make predictions based on model results, such ecological detail should be explicitly acknowledged.

5.5 Appendix: Analysis of the disease-free system and derivation of the invasion criterion

The disease-free system reads:

$$\frac{dN}{dt} = D(N_{in} - N) - c\mu(N)S \quad (5.8)$$

$$\frac{dS}{dt} = \mu(N)S - dS \quad (5.9)$$

with

$$\mu(R) = \frac{\mu_{max}N}{N+K}. \quad (5.10)$$

The non-trivial equilibrium values denoted by N^* and S^* read:

$$N^* = \frac{dK}{\mu_{max} - d} S^* = \frac{D(N_{in} - N^*)}{c\mu(N^*)}. \quad (5.11)$$

Hence $S^* > 0$ when $N_{in} > N^*$ and the latter condition holds for a positive equilibrium.

$$J = \begin{pmatrix} -D - \frac{c\mu_{max}S^*}{K+N^*} + \frac{c\mu_{max}N^*S^*}{(K+N^*)^2} & -\frac{c\mu_{max}N^*}{K+N^*} \\ \frac{\mu_{max}S^*}{K+N^*} - \frac{\mu_{max}N^*S^*}{(K+N^*)^2} & \frac{\mu_{max}N^*}{K+N^*} - d \end{pmatrix} \quad (5.12)$$

Evaluated at the trivial solution $S = 0$ and $N = N_{in}$ we have

$$J = \begin{pmatrix} -D & -\frac{c\mu_{max}N_{in}}{K+N_{in}} \\ 0 & \frac{\mu_{max}N_{in}}{K+N_{in}} - d \end{pmatrix} \quad (5.13)$$

and therefore the two eigenvalues are $-D$ and $\frac{\mu_{max}N_{in}}{K+N_{in}} - d$. Thus the trivial solution is unstable when $\frac{\mu_{max}N_{in}}{K+N_{in}} > d$. The equality fixes the transcritical bifurcation. We assume that the positive solution, which obviously exists when the criterion is met, is stable so that invasion by the susceptible population leads to a stable equilibrium. Now we consider the complete system (equations 1-5) and derive in a similar way the invasion criterion (5.7). We consider the invasion of the N, S system where $S^* > 0$, $N_{in} > N^*$, $I = 0$, $Y = 0$, $Z = 0$. The Jacobian matrix evaluated at that point reads

$$J = \begin{pmatrix} -D - \frac{c\mu_{max}S^*}{K+N^*} + \frac{c\mu_{max}N^*S^*}{(K+N^*)^2} & -\frac{c\mu_{max}N^*}{K+N^*} & -\frac{c\mu_{max}N^*}{K+N^*} & 0 & 0 \\ \frac{\mu_{max}S^*}{K+N^*} - \frac{\mu_{max}N^*S^*}{(K+N^*)^2} & \frac{\mu_{max}N^*}{K+N^*} - d & 0 & 0 & -\beta S^* \\ 0 & 0 & -\gamma - d & 0 & \beta S^* \\ 0 & 0 & \frac{b\mu_{max}N^*}{K+N^*} & -\gamma - d & 0 \\ 0 & 0 & 0 & \gamma & -\delta - \beta S^* \end{pmatrix} \quad (5.14)$$

Due to the zero 3-by-2 lower-left matrix the 3-dimensional I, Y, Z system is decoupled from the 2-dimensional N, S system. The real parts of the eigenvalues of the 2-by-2

upper-left diagonal matrix are those of the disease-free system and have a negative real part because that equilibrium is stable. The remaining three eigenvalues are those of the lower-right diagonal matrix. In order to derive the invasion criterion we require that $\det(J) = 0$. This gives

$$\lambda_1 = b\beta\gamma\mu(N^*)S^* - (d + \gamma)^2(\delta + \beta S^*) \quad (5.15)$$

or equivalently

$$\frac{b\beta\gamma\mu(N^*)S^*}{(d + \gamma)^2(\delta + \beta S^*)} = 1 = R_0. \quad (5.16)$$

This is condition (5.7). When $R_0 > 1$ at least one eigenvalue is positive and the equilibrium $(N^*, S^*, 0, 0, 0)$ is unstable. Besides the zero eigenvalue there are two eigenvalues:

$$\lambda_1 = 0 \quad (5.17)$$

$$\lambda_{2,3} = -\gamma - d - \frac{1}{2}\delta - \frac{1}{2}\beta S^* \pm \frac{1}{2}\sqrt{(\delta + \beta S^*)^2 - 4(\delta + \beta S^*)(\gamma + d)}. \quad (5.18)$$

Since $\lambda_{2,3} < 0$ or $\text{Re } \lambda_{2,3} < 0$ the sign of the eigenvalue $\lambda_{2,3} = b\beta\gamma\mu(N^*)S^* - (d - \gamma)^2(\delta - \beta S^*)$ determines the stability of the equilibrium.

Chapter 6

Synthesis

6.1 Priority effects

When does the outcome of species interactions depend on the order and timing of species arrivals? Or: when do priority effects determine the outcome? Much of this thesis is centred around this question. As argued in the introductory chapter (chapter 1) and in chapter 2, the answer to this question depends on how one exactly defines priority effects, and on how communities are assembled. The definition of priority effect given in the General Introduction (on page 3) defines a priority effect in terms of the effect on species abundances, without mention of when this effect is to be determined. Obviously, abundances differ for at least some time if one species arrives before another in stead of the other species arriving first. In this thesis, however, I have dealt with the asymptotic behaviour of species communities, meaning the state the dynamical system converges to as time gets large (more precisely: the attractor the system converges to). In a way, the community state is to be determined after an infinite amount of time. Thus, in this thesis, a priority effect implies alternative stable states (or coexisting attractors).

Often community assembly models make the following simplifying assumptions on how communities are assembled (e.g. Drake, 1990; Luh and Pimm, 1993; Law and Morton, 1993; Capitan and Cuesta, 2011):

1. Species are introduced at low density only.
2. A new species is introduced only when the resident community has reached an attractor.

Of course, what one calls low density is rather arbitrary. The models assume that a species can only invade if the long-term low-density growth rate of the invader is positive. The long term low density growth rate is the time-averaged population growth rate in the limit of low density, where the time to be averaged over runs from the time of introduction to infinity. Besides the assumptions on how the community

assembles, one also has to decide how the species community is characterised when determining the effect of arrival times. There are two possibilities: (1) the community is characterised by the density or abundance of each species, or (2) the community is characterised merely by the absence or presence of species. The first option is used in the definition of priority effects given in the General Introduction (the definition of Fukami and Nakajima (2011), section 1.1).

I will now discuss what the the previous four chapters tell us about the occurrence of priority effects, with the outcome of species interactions determined as the asymptotic behaviour of the system. I will do this either with assumption 2 (about the timing of species introductions) in effect or with this assumption relaxed, and with either option 1 or option 2 above applied.

In the model of chapter 2, the regional species pool consisted of two species, which interact positively or negatively, depending on their population densities. Positive and negative interactions were modelled in a very simple and abstract way, which allowed for general conclusions (at least general in the same way that conclusions derived from the Lotka-Volterra two species competition model are general; see the conclusions about priority effects in the Lotka-Volterra model in section 1.2). Perhaps the most interesting result of chapter 2 is given in inequality (2.12). This inequality, together with its analogue, for the other species states the condition for mutual non-invasibility, in the case both species have a positive intrinsic growth rate. Mutual non-invasibility means that neither species can invade (here: increase from low density) when the resident species is at its attractor. The mutual non-invasibility criterion of chapter 2 may be phrased informally as follows: in the case that each species can establish a population from low density when alone, mutual non-invasibility becomes more likely when each species facilitates its own species more relative to the other species or inhibits the other species more relative to its own species. It is the balance of these two effects that determines whether the resident can keep the invader out. This condition nicely complements the condition for mutual non-invasibility in the Lotka-Volterra competition model, which states that interspecific competition (inhibition) must exceed intraspecific competition (inhibition). See section 1.2. The conditions for mutual non-invasibility in the Lotka-Volterra model and in the model of chapter 2 reflect the notion that priority effects are caused by positive feedback of relative density on relative fitness, i.e. an increase of the per capita population growth rate of the one species relative to the per capita population growth rate of the other species, with an increase in its population density relative to the population density of the other.

Whether mutual non-invasibility is a necessary or sufficient criterion for a priority effect, depends on how the community is characterised. Assuming that the resident community (the one resisting invasion) is reachable through community assembly, mutual non-invasibility is a sufficient criterion for a priority effect. If communities are characterised only by the absence or presence of species, it is also a necessary condition. However, if we consider not just the presence or absence of species, but also their densities, priority effects are possible even when mutual non-invasibility does not occur, and the criterion is merely sufficient. This is the case in figure 2.4e.

Here, each species can invade the single species equilibrium of the other, however, each invasion leads to another stable equilibrium. Thus, here there is a priority effect without mutual non-invasibility, at least if we characterise the community by species densities. If we characterise the community merely by the presence of species, there is no priority effect because each of the two alternative stable states has the same species present in it. Let us now abandon the assumption that the single species equilibria are reachable through community assembly. This is for instance the case when species are introduced only at low density and the empty community is stable against invasions from low density, as in figure 2.2c. In this figure, there is also mutual non-invasibility, but because the the single species equilibria are unreachable, there is no priority effect. The same is true for the phase plane with alternative stable states of chapter 3 (figure 3.6).

The number of endstates of community assembly may also be determined by how often invasion attempts are made. This is the case in figure 2.2e. Here, if new invasion attempts are only made after the resident has reached its attractor, the coexistence equilibrium is unreachable. A priority effect still occurs, but only decides between survival of one species or the other, coexistence being excluded from the possibilities.

Photoinhibition (chapter 3) causes per capita growth rates to increase with increasing population density for low population densities because the shade the population casts on itself protects against damaging high levels of irradiance. This mechanism of positive feedback of population density on per capita population growth causes an Allee effect, which may lead to alternative stable states and hysteresis in single species populations, as is illustrated by figure 3.3. This has recently found experimental verification in phytoplankton laboratory cultures (Veraart et al., 2012). With multiple species, there are more alternative stable states possible. In the model of chapter 3, there may be one stable state for each species plus one stable state at which none of the species is present. An example of this is given in the phase plane of figure 3.6. In this figure, two species compete and there are three alternative stable states. However, if the community is assembled by species invasions from low density starting from an empty community, the single species equilibria are unreachable, and community assembly begins and ends with the empty community. It is possible for one species to facilitate another. For instance, a species sensitive to photoinhibition may be unable to invade an empty system because of a strong Allee effect caused by high levels of irradiance. Another species, less sensitive to photoinhibition may be able to invade, and as its population grows it reduces the light levels, facilitating the invasion of the first species. Coexistence is impossible and this invasion will lead to the exclusion of the first species. This scenario is supported by the the experiments of Mur et al. (1977). Community assembly thus again leads to a single endstate independent of the order in which species are introduced. This scenario in which alternative stable states become unstable by including more species in the species pool is illustrated in figure 3.5. Thus, photoinhibition may cause alternative stable states, but not alternative endpoints of community assembly if species are introduced at low density only.

Chapter 4 dealt with a model of two prey species competing for a single resource

(food) and sharing a predator. One of the two produces a chemical that decreases the food ingestion rate of the other (this may be regarded as a form of interference competition). This may cause either the first or the second species to exclude the other due to a priority effect through mutual non-invasibility. Mutual non-invasibility occurs here because one species is a stronger resource competitor and reduces the resource to a level that is too low for the other species to grow. However, the second species, the interference competitor, can, if it arrives a sufficiently long time before the first, build up high concentration of the inhibiting chemical. The amount of resource in a population of the interference competitor would be high enough to allow invasion of the stronger resource competitor, were it not for the inhibitor. However, whether this priority effect actually occurs depends on environmental conditions. For interference to be strong enough to cause a priority effect, there must be a large enough population of the interference competitor. This requires a sufficient supply of the resource. However, if predation is too strong, the priority effect disappears because predation suppresses populations, reducing the strength of interference. These effects of nutrient enrichment (food supply) and predation are illustrated in the parameter diagram of figure . An important message here is that including additional trophic layers may have a strong influence on the occurrence of priority effects.

The model for the planktonic host-parasite system of chapter 5 exhibits alternative stable states but no alternative endstates of community assembly, if community assembly proceeds through invasions from low density. The alternative states are a host-only equilibrium and a state of host-parasite coexistence. In a model of a similar system, Weitz and Dushoff (2008) also found such alternative states, and argued that the timing of parasite (virus) addition while the host is approaching its carrying capacity, determines whether the parasite persists. The phase plane for their model is depicted in figure 6.1. In the phase plane it is clear that it is easy to find introduction densities for which this effect of timing is absent. Importantly, for a sufficiently small initial parasite density, the timing effect disappears. Thus, the presence of a priority effect depends critically on the condition that the parasite is added at a high enough density (but not a density that is too high). The same is true for the more complicated host-parasite model of chapter 5. Furthermore, in this model nutrient enrichment may lead to a stable host-parasite cycle, and further enrichment leads to the disappearance of this cycle, so that parasite extinction is inevitable and not dependent on initial densities or timing of arrival.

6.2 A principle of community assembly

What limits the number of alternative endstates of community assembly? Is there a general principle that allows us to determine the maximum number of endstates for a given community?

Consumer-resource theory gives us the R^* -rule (Tilman, 1982), which states (loosely speaking) that when species compete for a single resource, the species which

reduces the resource concentration to the lowest level, that is, the species with the lowest resource concentration at equilibrium when grown alone (the lowest R^*), will competitively exclude all other species when grown together. Since only one species can have the lowest R^* , only one species will persist and the rest will be excluded. This rule is most often regarded as setting a limit to the number of species that exist on a single resource (namely, only one). However, it also sets a limit to the number of alternative endstates of community assembly, which is also just one: the community state with the species with the lowest R^* at equilibrium. Thus, in the situation that the R^* -rule limits the number of coexisting resource competitors, it also limits the number of endstates.

The R^* -rule is related to the competitive exclusion principle, which states, loosely speaking, that if species interact solely through resource competition, no more species can coexist at equilibrium than there are resources they compete for (see e.g. Armstrong and McGehee, 1980). The relatedness with the R^* -rule suggests that there is a similar principle that limits the number of endstates of community assembly. This principle would relate the maximum number of endstates to the number of resources species compete for. For the case of a single resource, the community assembly

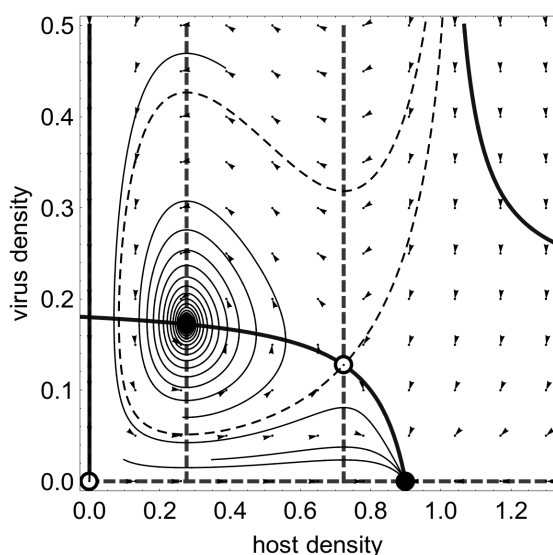


Figure 6.1. Phase plane and zero growth isoclines for the host-virus model of Weitz and Dushoff (2008). Their non-dimensionalized model reads $\frac{dN}{dt} = N(1-N) - \phi NV(1-N) - dN$, $\frac{dV}{dt} = \phi NV(1-N) - mV$, where N denotes rescaled host density and V denotes rescaled virus density. Parameter values: $\phi = 5$, $m = 1$, $d = 0.1$. For more details, I refer to the original paper of Weitz and Dushoff (2008). The thick continuous curves indicate the zero growth isoclines of the host population, the thick dashed curves those of the virus population. The dashed thin black curve indicates a separatrix. The continuous thin black curves indicate trajectories that serve as examples. The open dots indicate unstable equilibria, the closed dots indicate stable equilibria (one of which is in the centre of the spiral trajectory). The arrows indicate the direction of flow of trajectories

principle follows from the R^* -rule. For two species, we may deduce the principle as follows. If the outcome of competition between two species depends on their initial densities, and each of the coexisting attractors is reachable from low density, there is a separatrix starting at the origin of species space. Since there are only two species, this separatrix is a single trajectory in species space. In any reasonable model this trajectory is bounded in both species densities, because population growth cannot be sustained for ever. This suggests that this trajectory that is the separatrix ends (in the limit of large time) on a limit set. Let this limit set be a single point, i.e. an equilibrium. This equilibrium is an unstable equilibrium (a saddle point), however, this does not prevent the competitive exclusion principle from applying. Thus, if the alternative endstates require the (unstable) equilibrium coexistence of the two species, they require that the species compete for at least two resources. In this case, the resources define the niches of the species. More generally, one might say the number of niches limit the number of endstates of community assembly.

This result, if verified in more formal manner and generalized to more species and resources would connect consumer-resource theory to community assembly theory and would represent a major step forward in understanding when priority effects and alternative endstates of community assembly occur. This would in turn contribute to more complete understanding of regional biodiversity and may find applications in restoration ecology.

Bibliography

- Agawin, N. S. R., S. Rabouille, M. J. W. Veldhuis, L. Servatius, S. Hol, H. M. J. van Overzee, and J. Huisman. 2007. Competition and facilitation between unicellular nitrogen-fixing cyanobacteria and non-nitrogen-fixing phytoplankton species. *Limnology and Oceanography* **52**:2233–2248.
- Allee, W. C. 1931. *Animal Aggregations: A Study in General Sociology*. University of Chicago Press, Chicago.
- Amarasekare, P. 2002. Interference competition and species coexistence. *Proceedings of the Royal Society of London Series B-Biological Sciences* **269**:2541–2550.
- Anderson, R. M., and R. M. May. 1979. Population biology of infectious diseases: Part I. *Nature* **280**:361–367.
- Armstrong, R. A., and R. McGehee. 1980. Competitive-Exclusion. *American Naturalist* **115**:151–170.
- Ault, T. R. 2000. Vertical migration by the marine dinoflagellate *Prorocentrum triestinum* maximises photosynthetic yield. *Oecologia* **125**:466–475.
- Bader, M. Y., I. van Geloof, and M. Rietkerk. 2007. High solar radiation hinders tree regeneration above the alpine treeline in northern Ecuador. *Plant Ecology* **191**:33–45.
- Belay, A. 1981. An experimental investigation of inhibition of phytoplankton photosynthesis at lake surfaces. *New Phytologist* **89**:61–74.
- Beltrami, E., and T. O. Carroll. 1994. Modeling the role of viral disease in recurrent phytoplankton blooms. *Journal of Mathematical Biology* **32**:857–863.
- Beretta, E., and Y. Kuang. 1998. Modeling and analysis of a marine bacteriophage infection. *Mathematical Biosciences* **149**:57–76.
- Bertness, M. D., and R. Callaway. 1994. Positive interactions in communities. *Trends in Ecology & Evolution* **9**:191–193.
- Bertness, M. D., and S. M. Yeh. 1994. Cooperative and competitive interactions in the recruitment of marsh elders. *Ecology* **75**:2416–2429.
- Boukal, D. S., and L. Berec. 2002. Single species models of the Allee effect: extinction boundaries, sex ratios and mate encounters. *Journal of Theoretical Biology* **218**:375–394.
- Bratbak, G., A. Jacobsen, M. Heldal, K. Nagasaki, and F. Thingstad. 1998. Virus production in *Phaeocystis pouchetii* and its relation to host cell growth and nutrition. *Aquatic Microbial Ecology* **16**:1–9.
- Bruning, K. 1991a. Effects of phosphorus limitation on the epidemiology of a chytrid phytoplankton parasite. *Freshwater Biology* **25**:409–417.
- Bruning, K. 1991b. Effects of temperature and light on the population-dynamics of the *Asterionella rhizophydium* association. *Journal Of Plankton Research* **13**:707–719.
- Bruning, K. 1991c. Infection of the diatom *Asterionella* by a chytrid 1. Effects of light on

- reproduction and infectivity of the parasite. *Journal of Plankton Research* **13**:103–117.
- Bruno, J. F., J. J. Stachowicz, and M. D. Bertness. 2003. Inclusion of facilitation into ecological theory. *Trends in Ecology & Evolution* **18**:119–125.
- Brussaard, C. P. D., S. W. Wilhelm, F. Thingstad, M. G. Weinbauer, G. Bratbak, M. Heldal, S. A. Kimmance, M. Middelboe, K. Nagasaki, J. H. Paul, D. C. Schroeder, C. A. Suttle, D. Vaque, and K. E. Wommack. 2008. Global-scale processes with a nanoscale drive: the role of marine viruses. *ISME Journal* **2**:575–578.
- Callieri, C., and R. Piscia. 2002. Photosynthetic efficiency and seasonality of autotrophic picoplankton in Lago Maggiore after its recovery. *Freshwater Biology* **47**:941–956.
- Canter, H. M., and G. H. M. Jaworski. 1981. The effect of light and darkness upon infection of *Asterionella-formosa* Hassall by the chytrid *Rhizophyidium-planktonicum* Canter emend. *Annals of Botany* **47**:13–30.
- Canter, H. M., and J. Lund. 1953. Studies on plankton parasites II. The parasitism of diatoms with special reference to lakes in the English Lake District. *Transactions of the British Mycological Society* **36**:13–37.
- Canter, H. M., and J. W. G. Lund. 1948. Studies on plankton parasites I. Fluctuations in the numbers of *Asterionella formosa* Hass. in relation to fungal epidemics. *New Phytologist* **47**:238–261.
- Canter, H. M., and J. W. G. Lund. 1951. Studies on plankton parasites III. Examples of the interaction between parasitism and other factors determining the growth of diatoms. *Annals of Botany* **15**:359–&.
- Canter, H. M., and J. W. G. Lund. 1969. Parasitism of planktonic desmids by fungi. *Österreichische Botanische Zeitschrift* **116**:351–377.
- Capitan, J. A., and J. A. Cuesta. 2011. Species assembly in model ecosystems I: Analysis of the population model and the invasion dynamics. *Journal of Theoretical Biology* **269**:330–343.
- Chao, L., and B. R. Levin. 1981. Structured habitats and the evolution of anticompetitor toxins in bacteria. *Proceedings of the National Academy of Sciences of the United States of America-Biological Sciences* **78**:6324–6328.
- Chase, J. M. 1999. Food web effects of prey size refugia: variable interactions and alternative stable equilibria. *American Naturalist* **154**:570.
- Chase, J. M. 2003. Community assembly: when should history matter? *Oecologia* **136**:489–498.
- Chattopadhyay, J., R. R. Sarkar, and S. Pal. 2003. Dynamics of nutrient-phytoplankton interaction in the presence of viral infection. *Biosystems* **68**:5–17.
- Chorus, J., I Bartram. 1999. Toxic cyanobacteria in water: a guide to their public health consequences, monitoring and management. Spon, London.
- Conde-Porcuna, J. M. 1998. Chemical interference by *Daphnia* on *Keratella*: a life table experiment. *Journal of Plankton Research* **20**:1637–1644.
- Courchamp, F. 1999. Population dynamics of obligate cooperators. *Proceedings of the Royal Society B: Biological Sciences* **266**:557–563.
- Cullen, J. J., and M. R. Lewis. 1988. The kinetics of algal photoadaptation in the context of vertical mixing. *Journal of Plankton Research* **10**:1039–1063.
- Dakos, V., E. Beninca, E. H. van Nes, C. J. M. Philippart, M. Scheffer, and J. Huisman. 2009. Interannual variability in species composition explained as seasonally entrained chaos. *Proceedings of The Royal Society B-Biological Sciences* **276**:2871–2880.
- De Bruin, A., B. W. Ibelings, M. Rijkeboer, M. Brehm, and E. van Donk. 2004. Genetic variation in *Asterionella formosa* (Bacillariophyceae): Is it linked to frequent epidemics of host-

- specific parasitic fungi? *Journal of Phycology* **40**:823–830.
- DeFreitas, M. J., and A. G. Fredrickson. 1978. Inhibition as a factor in maintenance of diversity of microbial ecosystems. *Journal of General Microbiology* **106**:307–320.
- Diehl, S., and M. Feissel. 2000. Effects of enrichment on three-level food chains with omnivory. *American Naturalist* **155**:200–218.
- Doedel, E. J., and B. Oldemans. 2007. AUOTO07P: Continuation and Bifurcation Software for Ordinary Differential Equations. Concordia University, Montreal.
- Drake, J. A. 1990. The mechanics of community assembly and succession. *Journal of Theoretical Biology* **147**:213–233.
- Ebert, D., M. Lipsitch, and K. L. Mangin. 2000. The effect of parasites on host population density and extinction: Experimental epidemiology with *Daphnia* and six microparasites. *American Naturalist* **156**:459–477.
- Eilers, P. H. C., and J. C. H. Peeters. 1988. A model for the relationship between light-intensity and the rate of photosynthesis in phytoplankton. *Ecological Modeling* **42**:199–215.
- Fajardo, A., and E. J. B. McIntire. 2011. Under strong niche overlap conspecifics do not compete but help each other to survive: facilitation at the intraspecific level. *Journal of Ecology* **99**:642–650.
- Ferdy, J.-B., and J. Molofsky. 2002. Allee effect, spatial structure and species coexistence. *Journal of Theoretical Biology* **217**:413 – 424.
- Fuhrman, K. M., G. A. Pinter, and J. A. Berges. 2011. Dynamics of a virus-host model with an intrinsic quota. *Mathematical And Computer Modelling* **53**:716–730.
- Fukami, T., I. A. Dickie, J. P. Wilkie, B. C. Paulus, D. Park, A. Roberts, P. K. Buchanan, and R. B. Allen. 2010. Assembly history dictates ecosystem functioning: evidence from wood decomposer communities. *Ecology Letters* **13**:675–684.
- Fukami, T., and M. Nakajima. 2011. Community assembly: alternative stable states or alternative transient states? *Ecology Letters* **14**:973–984.
- Gachon, C. M. M., T. Sime-Ngando, M. Strittmatter, A. Chambouvet, and G. H. Kim. 2010. Algal diseases: spotlight on a black box. *Trends In Plant Science* **15**:633–640.
- Gause, G. F. 1934. *The struggle for existence*. William & Wilkins, Baltimore.
- Gerla, D. J., W. M. Mooij, and J. Huisman. 2011. Photoinhibition and the assembly of light-limited phytoplankton communities. *Oikos* **120**:359–368.
- Gilbert, J. J., and R. S. Stemberger. 1985. Control of *Keratella* populations by interference competition from *Daphnia*. *Limnology and Oceanography* **30**:180–188.
- Gons, H. J., J. Ebert, H. L. Hoogveld, L. van den Hove, R. Pel, W. Takkenberg, and C. J. Woldringh. 2002. Observations on cyanobacterial population collapse in eutrophic lake water. *Antonie Van Leeuwenhoek International Journal of General and Molecular Microbiology* **81**:319–326.
- Grover, J. P. 1991. Dynamics of competition among microalgae in variable environments - experimental tests of alternative models. *Oikos* **62**:231–243.
- Grover, J. P., and J. H. Lawton. 1994. Experimental studies on community convergence and alternative stable states: comments on a paper by Drake et al. *Journal of Animal Ecology* **63**:pp. 484–487.
- Gsell, A. S., L. De Senerpont Domis, S. M. H. Naus-Wiezer, N. R. Helmsing, E. Van Donk, and B. W. Ibelings, 2012. Spatio-temporal variation in the distribution of chytrid parasites in diatom host populations. In press.
- Gyllenberg, M., J. Hemminki, and T. Tammaru. 1999. Allee effects can both conserve and create spatial heterogeneity in population densities. *Theoretical Population Biology*

- 56:231 – 242.
- Hall, S. R., M. A. Duffy, and C. E. Cáceres. 2005. Selective predation and productivity jointly drive complex behavior in host-parasite systems. *American Naturalist* **165**:70–81.
- Hall, S. R., J. L. Simonis, R. M. Nisbet, A. J. Tessier, and C. E. Cáceres. 2009. Resource ecology of virulence in a planktonic host-parasite system: an explanation using dynamic energy budgets. *American Naturalist* **174**:149–162.
- Han, B. P., M. Virtanen, J. Koponen, and M. Straskraba. 2000. Effect of photoinhibition on algal photosynthesis: a dynamic model. *Journal of Plankton Research* **22**:865–885.
- Heesterbeek, J. A. P., and K. Dietz. 1996. The concept of R_0 in epidemic theory. *Statistica Neerlandica* **50**:89–110.
- Helbling, E. W., A. G. J. Buma, W. van de Poll, M. V. Fernandez Zenoff, and V. E. Villafane. 2008. UVR-induced photosynthetic inhibition dominates over DNA damage in marine dinoflagellates exposed to fluctuating solar radiation regimes. *Journal of Experimental Marine Biology and Ecology* **365**:96–102.
- Helgen, J. C. 1987. Feeding rate inhibition in crowded *Daphnia pulex*. *Hydrobiologia* **154**:113–119.
- Henley, W. J. 1993. Measurement and interpretation of photosynthetic light-response curves in algae in the context of photoinhibition and diel changes. *Journal of Phycology* **29**:729–739.
- Holfeld, H. 2000. Relative abundance, rate of increase, and fungal infections of freshwater phytoplankton. *Journal of Plankton Research* **22**:987–995.
- Holt, R. D., 1997. Community modules. Pages 333–350 in Gange, AC and Brown, VK, editor. *Multitrophic Interactions in Terrestrial Systems*.
- Holt, R. D., and G. A. Polis. 1997. A theoretical framework for intraguild predation. *American Naturalist* **149**:745–764.
- Huisman, J., 1997. The Struggle for Light. Ph.D. thesis, Rijksuniversiteit Groningen.
- Huisman, J., R. R. Jonker, C. Zonneveld, and F. J. Weissing. 1999. Competition for light between phytoplankton species: experimental tests of mechanistic theory. *Ecology* **80**:211–222.
- Huisman, J., J. Sharples, J. M. Stroom, P. M. Visser, W. E. A. Kardinaal, J. M. H. Verspagen, and B. Sommeijer. 2004. Changes in turbulent mixing shift competition for light between phytoplankton species. *Ecology* **85**:2960–2970.
- Huisman, J., N. N. P. Thi, D. M. Karl, and B. Sommeijer. 2006. Reduced mixing generates oscillations and chaos in the oceanic deep chlorophyll maximum. *Nature* **439**:322–325.
- Huisman, J., P. van Oostveen, and F. J. Weissing. 1999. Species dynamics in phytoplankton blooms: Incomplete mixing and competition for light. *American Naturalist* **154**:46–68.
- Huisman, J., and F. J. Weissing. 1994. Light-limited growth and competition for light in well-mixed aquatic environments - an elementary model. *Ecology* **75**:507–520.
- Huisman, J., and F. J. Weissing. 1995. Competition for nutrients and light in a mixed water column - a theoretical analysis. *American Naturalist* **146**:536–564.
- Huppert, A., B. Blasius, R. Olinky, and L. Stone. 2005. A model for seasonal phytoplankton blooms. *Journal of Theoretical Biology* **236**:276–290.
- Hutchinson, G. E. 1947. A note on the theory of competition between two social species. *Ecology* **28**:319–321.
- Ibelings, B. W., A. De Bruin, M. Kagami, M. Rijkeboer, M. Brehm, and E. van Donk. 2004. Host parasite interactions between freshwater phytoplankton and chytrid fungi (Chytridiomycota). *Journal of Phycology* **40**:437–453.
- Ibelings, B. W., A. S. Gsell, W. M. Mooij, E. van Donk, S. van den Wyngaert, and L. N. d. S. Domis.

2011. Chytrid infections and diatom spring blooms: paradoxical effects of climate warming on fungal epidemics in lakes. *Freshwater Biology* **56**:754–766.
- Jenkins, D. G., and A. L. Buikema. 1998. Do similar communities develop in similar sites? A test with zooplankton structure and function. *Ecological Monographs* **68**:421–443.
- Kagami, M., E. von Elert, B. W. Ibelings, A. de Bruin, and E. Van Donk. 2007. The parasitic chytrid, *Zygorhizidium*, facilitates the growth of the cladoceran zooplankton, *Daphnia*, in cultures of the inedible alga, *Asterionella*. *Proceedings of The Royal Society B-Biological Sciences* **274**:1561–1566.
- Kardinaal, W. E. A., L. Tonk, I. Janse, S. Hol, P. Slot, J. Huisman, and P. M. Visser. 2007. Competition for light between toxic and nontoxic strains of the harmful cyanobacterium *Microcystis*. *Applied and Environmental Microbiology* **73**:2939–2946.
- Keesing, F., R. D. Holt, and R. S. Ostfeld. 2006. Effects of species diversity on disease risk. *Ecology Letters* **9**:485–498.
- Kirk, J. T. O. 1994. Light and photosynthesis in aquatic ecosystems. Cambridge University Press, Cambridge.
- Klausmeier, C. A., and E. Litchman. 2001. Algal games: The vertical distribution of phytoplankton in poorly mixed water columns. *Limnology and Oceanography* **46**:1998–2007.
- Kooijman, S. A. L. M., T. Andersen, and B. W. Kooi. 2004. Dynamic energy budget representations of stoichiometric constraints on population dynamics. *Ecology* **85**:1230–1243.
- Kostitzin, V. A. 1940. Sur la loi logistique et ses généralisations. *Acta Biotheoretica* **5**:155–159.
- Kuznetsov, Y. A. 2004. *Elements of Applied Bifurcation Theory*. Springer, New York.
- Lampert, W., W. Fleckner, H. Rai, and B. E. Taylor. 1986. Phytoplankton control by grazing zooplankton: a study on the spring clear-water phase. *Limnology and Oceanography* **31**:478–490.
- Law, R., and R. D. Morton. 1993. Alternative permanent states of ecological communities. *Ecology* **74**:1347–1361.
- Law, R., and R. D. Morton. 1996. Permanence and the assembly of ecological communities. *Ecology* **77**:762–775.
- Law, R. D., 1999. Theoretical aspects of community assembly. Pages 143–170 in M. J., editor. *Advanced Ecological Theory: Principles and Applications*. Blackwell Science.
- Lear, G., S. J. Turner, and G. D. Lewis. 2009. Effect of light regimes on the utilisation of an exogenous carbon source by freshwater biofilm bacterial communities. *Aquatic Ecology* **43**:207–220.
- Lingeman, R., F. Heinis, and A. Veen. 1987. Time series of physical, chemical and plankton parameters in Lake Maarsseveen I: 1980-1986. *Hydrobiological Bulletin* **21**:25–38.
- Livingstone, D. M. 2003. Impact of secular climate change on the thermal structure of a large temperate central European lake. *Climatic Change* **57**:205–225.
- Long, S. P., S. Humphries, and P. G. Falkowski. 1994. Photoinhibition of photosynthesis in nature. *Annual Review of Plant Physiology and Plant Molecular Biology* **45**:633–662.
- Lotka, A. J. 1925. *Elements of Physical Biology*. Williams & Wilkins, Baltimore.
- Lotka, A. J. 1932. The growth of mixed populations: two species competing for a common food supply. *Washington Academy of Sciences* **22**:461–469.
- Louette, G., and L. De Meester. 2007. Predation and priority effects in experimental zooplankton communities. *Oikos* **116**:419–426.
- Luh, H. K., and S. L. Pimm. 1993. The assembly of ecological communities - a minimalist approach. *Journal of Animal Ecology* **62**:749–765.
- Lund, J. W. G., 1957. Fungal diseases of plankton algae. in C. Horton-Smith, editor. *Biological*

- Aspects of the Transmission of Disease. Oliver and Boyd, Edinburgh.
- Macedo, M. F., and P. Duarte. 2006. Phytoplankton production modelling in three marine ecosystems - static versus dynamic approach. *Ecological Modelling* **190**:299–316.
- Macedo, M. F., J. G. Ferreira, and P. Duarte. 1998. Dynamic behaviour of photosynthesis-irradiance curves determined from oxygen production during variable incubation periods. *Marine Ecology-Progress Series* **165**:31–43.
- Maestre, F. T., S. Bautista, and J. Cortina. 2003. Positive, negative, and net effects in grass-shrub interactions in mediterranean semiarid grasslands. *Ecology* **84**:3186–3197.
- Marcogliese, D. J. 2001. Pursuing parasites up the food chain: implications of food web structure and function on parasite communities in aquatic systems. *Acta Parasitologica* **46**:82–93.
- Marcogliese, D. J., and D. K. Cone. 1997. Food webs: A plea for parasites. *Trends In Ecology & Evolution* **12**:394.
- Matveev, V. 1993. An investigation of allelopathic effects of *Daphnia*. *Freshwater Biology* **29**:99–105.
- May, R. M., 1976. Models for two interacting populations. Pages 49–70 in R. M. May, editor. *Theoretical Ecology: Principles and Applications*. Blackwell Scientific Publications, Oxford.
- May, R. M., and R. M. Anderson. 1979. Population biology of infectious diseases: Part II. *Nature* **280**:455–461.
- McCallum, H., N. Barlow, and J. Hone. 2001. How should pathogen transmission be modelled? *Trends In Ecology & Evolution* **16**:295–300.
- Middelboe, M. 2000. Bacterial growth rate and marine virus-host dynamics. *Microbial Ecology* **40**:114–124.
- Miki, T., G. Takimoto, and M. Kagami. 2011. Roles of parasitic fungi in aquatic food webs: a theoretical approach. *Freshwater Biology* **56**:1173–1183.
- Modenutti, B., E. Balseiro, C. Callieri, C. Queimalinos, and R. Bertoni. 2004. Increase in photosynthetic efficiency as a strategy of planktonic organisms exploiting deep lake layers. *Freshwater Biology* **49**:160–169.
- Moore, L. R., and S. W. Chisholm. 1999. Photophysiology of the marine cyanobacterium *Prochlorococcus*: ecotypic differences among cultured isolates. *Limnology and Oceanography* **44**:628–638.
- Morin, P. J. 1999. *Community Ecology*. Blackwell Science, Massachusetts.
- Morton, R. D., and R. Law. 1997. Regional species pools and the assembly of local ecological communities. *Journal of Theoretical Biology* **187**:321–331.
- Moser, M., C. Callieri, and T. Weisse. 2009. Photosynthetic and growth response of freshwater picocyanobacteria are strain-specific and sensitive to photoacclimation. *Journal of Plankton Research* **31**:349–357.
- Mur, L., H. Gons, and L. Van Liere. 1977. Some experiments on competition between green-algae and blue-green bacteria in light-limited environments. *FEMS Microbiology Letters* **1**:335–338.
- Mylius, S. D., K. Klumpers, A. M. de Roos, and L. Persson. 2001. Impact of intraguild predation and stage structure on simple communities along a productivity gradient. *American Naturalist* **158**:259–276.
- Neyman, J., T. Park, and E. L. Scott. 1956. Struggle for existence. The *Tribolium* model: Biological and statistical aspects. *Proceedings of the Third Berkeley Symposium on Mathematical Statistics Probability* **4**:41–79.

- Paerl, H. W., and J. Huisman. 2008. Blooms like it hot. *Science* **320**:57–58.
- Park, T. 1954. Experimental studies of interspecies competition 2. Temperature, humidity, and competition in 2 species of *Tribolium*. *Physiological Zoology* **27**:177–238.
- Park, T., D. B. Mertz, Grodzins.W, and T. Prus. 1965. Cannibalistic predation in populations of flour beetles. *Physiological Zoology* **38**:289–&.
- Partensky, E., N. Hoepffner, W. K. W. Li, O. Ulloa, and D. Vaultot. 1993. Photoacclimation of *Pritochlorococcus* sp. (Prochlorophyta) strains Isolated from the North Atlantic and the Mediterranean Sea. *Plant Physiology* **101**:285–296.
- Passarge, J., S. Hol, M. Escher, and J. Huisman. 2006. Competition for nutrients and light: Stable coexistence, alternative stable states, or competitive exclusion? *Ecological Monographs* **76**:57–72.
- Peeters, J. C. H., and P. H. C. Eilers. 1978. The relationship between light intensity and photosynthesis - a simple mathematical model. *Hydrobiological Bulletin* **12**:134–136.
- Persson, L., K. Leonardsson, A. M. de Roos, M. Gyllenberg, and B. Christensen. 1998. Ontogenetic scaling of foraging rates and the dynamics of a size-structured consumer-resource model. *Theoretical Population Biology* **54**:270–293.
- Platt, T., C. L. Gallegos, and W. G. Harrison. 1980. Photoinhibition of photosynthesis in natural assemblages of marine-phytoplankton. *Journal of Marine Research* **38**:687–701.
- Price, J. E., and P. J. Morin. 2004. Colonization history determines alternate community states in a food web of intraguild predators. *Ecology* **85**:1017–1028.
- Regel, R. H., J. D. Brookes, and G. G. Ganf. 2004. Vertical migration, entrainment and photosynthesis of the freshwater dinoflagellate *Peridinium cinctum* in a shallow urban lake. *Journal of Plankton Research* **26**:143–157.
- Regoes, R., D. Ebert, and S. Bonhoeffer. 2002. Dose-dependent infection rates of parasites produce the Allee effect in epidemiology. *Proceedings of The Royal Society of London Series B-Biological Sciences* **269**:271–279.
- Rhodes, C. J., and A. P. Martin. 2010. The influence of viral infection on a plankton ecosystem undergoing nutrient enrichment. *Journal of Theoretical Biology* **265**:225–237.
- Rosenzweig, M. L. 1971. Paradox of enrichment - destabilization of exploitation ecosystems in ecological time. *Science* **171**:385–&.
- Ross, O. N., C. M. Moore, D. J. Suggett, H. L. MacIntyre, and R. J. Geider. 2008. A model of photosynthesis and photo-protection based on reaction center damage and repair. *Limnology and Oceanography* **53**:1835–1852.
- Shurin, J. B., P. Amarasekare, J. M. Chase, R. D. Holt, M. F. Hoopes, and M. A. Leibold. 2004. Alternative stable states and regional community structure. *Journal of Theoretical Biology* **227**:359–368.
- Siekmann, I., H. Malchow, and E. Venturino. 2008. An extension of the Beretta-Kuang model of viral diseases. *Mathematical Biosciences and Engineering* **5**:549–565.
- Simis, S. G. H., M. Tjeldens, H. L. Hoogveld, and H. J. Gons. 2005. Optical changes associated with cyanobacterial bloom termination by viral lysis. *Journal of Plankton research* **27**:937–949.
- Six, C., Z. V. Finkel, F. Rodriguez, D. Marie, F. Partensky, and D. A. Campbell. 2008. Contrasting photoacclimation costs in ecotypes of the marine eukaryotic picoplankter *Ostreococcus*. *Limnology and Oceanography* **53**:255–265.
- Sommer, U. 1985. Comparison between steady-state and non-steady state competition - experiments with natural phytoplankton. *Limnology And Oceanography* **30**:335–346.
- Sommer, U., Z. M. Gliwicz, W. Lampert, and A. Duncan. 1986. The PEG-model of seasonal

- succession of planktonic events in fresh waters. *Archiv für Hydrobiologie* **106**:433–471.
- Stachowicz, J. 2001. Mutualism, facilitation, and the structure of ecological communities. *BioScience* **51**:235–246.
- Steele, J. H. 1962. Environmental control of photosynthesis in the sea. *Limnology and Oceanography* **7**:137–150.
- Stephens, P. A., W. J. Sutherland, and R. P. Freckleton. 1999. What is the Allee effect? *Oikos* **87**:185.
- Stomp, M., J. Huisman, F. de Jongh, A. J. Veraart, D. Gerla, M. Rijkeboer, B. W. Ibelings, U. I. A. Wollenzien, and L. J. Stal. 2004. Adaptive divergence in pigment composition promotes phytoplankton biodiversity. *Nature* **432**:104–107.
- Stomp, M., J. Huisman, L. Voros, F. R. Pick, M. Laamanen, T. Haverkamp, and L. J. Stal. 2007. Colourful coexistence of red and green picocyanobacteria in lakes and seas. *Ecology Letters* **10**:290–298.
- Straile, D., and R. Adrian. 2000. The North Atlantic Oscillation and plankton dynamics in two European lakes - two variations on a general theme. *Global Change Biology* **6**:663–670.
- Suding, K. N., K. L. Gross, and G. R. Houseman. 2004. Alternative states and positive feedbacks in restoration ecology. *Trends in Ecology & Evolution* **19**:46–53.
- Szathmary, E. 1991. Simple growth laws and selection consequences. *Trends in Ecology & Evolution* **6**:366–370.
- Takahashi, S., and N. Murata. 2008. How do environmental stresses accelerate photoinhibition? *Trends in Plant Science* **13**:178–182.
- Talling, J. F. 2003. Phytoplankton-zooplankton seasonal timing and the ‘clear-water phase’ in some English lakes. *Freshwater Biology* **48**:39–52.
- Taylor, C., and A. Hastings. 2005a. Allee effects in biological invasions. *Ecology Letters* **8**:895–908.
- Taylor, C. M., and A. Hastings. 2005b. Allee effects in biological invasions. *Ecology Letters* **8**:895–908.
- Tilman, D. 1977. Resource competition between planktonic algae - experimental and theoretical approach. *Ecology* **58**:338–348.
- Tilman, D. 1980. Resources - a graphical-mechanistic approach to competition and predation. *American Naturalist* **116**:362–393.
- Tilman, D. 1982. Resource competition and community structure. Princeton University Press, Princeton; Guildford.
- Tilman, D., and S. S. Kilham. 1976. Phosphate and silicate growth and uptake kinetics of diatoms *Asterionella formosa* and *Cyclotella meneghiniana* in batch and semicontinuous culture. *Journal of Phycology* **12**:375–383.
- Tonk, L., P. M. Visser, G. Christiansen, E. Dittmann, E. O. F. M. Snelder, C. Wiedner, L. R. Mur, and J. Huisman. 2005. The microcystin composition of the cyanobacterium *Planktothrix agardhii* changes toward a more toxic variant with increasing light intensity. *Applied and Environmental Microbiology* **71**:5177–5181.
- Urban, M. C., and L. De Meester. 2009. Community monopolization: local adaptation enhances priority effects in an evolving metacommunity. *Proceedings of the Royal Society B-Biological Sciences* **276**:4129–4138.
- Van Donk, E., and S. S. Kilham. 1990. Temperature effects on silicon-limited and phosphorus-limited growth and competitive interactions among three diatoms. *Journal of Phycology* **26**:40–50.
- Van Donk, E., and J. Ringelberg. 1983. The effect of fungal parasitism on the succession of

- diatoms in lake Maarsseveen-I (The Netherlands). *Freshwater Biology* **13**:241–251.
- Van Liere, L., and L. R. Mur. 1980. Occurrence of *Oscillatoria agardhii* and some related species: a survey. in L. R. Barcia, J. Mur, editor. Hypertrophic ecosystems. Junk, The Hague.
- Van Voorn, G. A. K., L. Hemerik, M. P. Boer, and B. W. Kooi. 2007. Heteroclinic orbits indicate overexploitation in predator-prey systems with a strong Allee effect. *Mathematical Biosciences* **209**:451–469.
- Vandermeer, J. H. 1973. Generalized models of two species interactions: a graphical analysis. *Ecology* **54**:809–818.
- Veraart, A. J., E. J. Faassen, V. Dakos, E. H. van Nes, M. Lurling, and M. Scheffer. 2012. Recovery rates reflect distance to a tipping point in a living system. *Nature* **481**:357–359.
- Volterra, V. 1926. Fluctuations in the abundance of a species considered mathematically. *Nature* **118**:558–560.
- Volterra, V. 1931. Leçons sur la théorie mathématique de la lutte pour la vie. Gauthier-Villars, Paris.
- Volterra, V. 1938. Population growth, equilibria, and extinction under specified breeding conditions: a development and extension of the theory of the logistic curve. *Human Biology* **10**:1–11.
- Wang, G., X. Liang, and F. Wang. 1999. The competitive dynamics of populations subject to an Allee effect. *Ecological Modelling* **124**:183–192.
- Wang, M.-H., and M. Kot. 2001. Speeds of invasion in a model with strong or weak Allee effects. *Mathematical Biosciences* **171**:83–97.
- Warren, P. H., R. Law, and A. J. Weatherby. 2003. Mapping the assembly of protist communities in microcosms. *Ecology* **84**:1001–1011.
- Weissing, F. J., and J. Huisman. 1994. Growth and competition in a light gradient. *Journal of Theoretical Biology* **168**:323–336.
- Weitz, J., and J. Dushoff. 2008. Alternative stable states in host-phage dynamics. *Theoretical Ecology* **1**:13–19.
- Whittington, J., B. Sherman, D. Green, and R. L. Oliver. 2000. Growth of *Ceratium hirundinella* in a subtropical Australian reservoir: the role of vertical migration. *Journal of Plankton Research* **22**:1025–1045.
- Wilhelm, S. W., and C. A. Suttle. 1999. Viruses and nutrient cycles in the sea - Viruses play critical roles in the structure and function of aquatic food webs. *Bioscience* **49**:781–788.
- Yoshiyama, K., J. P. Mellard, E. Litchman, and C. A. Klausmeier. 2009. Phytoplankton competition for nutrients and light in a stratified water column. *American Naturalist* **174**:190–203.
- Young, T. P., D. A. Petersen, and J. J. Clary. 2005. The ecology of restoration: historical links, emerging issues and unexplored realms. *Ecology Letters* **8**:662–673.
- Zhang, B., Z. Zhang, Z. Li, and Y. Tao. 2007. Stability analysis of a two-species model with transitions between population interactions. *Journal of Theoretical Biology* **248**:145 – 153.
- Zhang, Q. G., and D. Y. Zhang. 2007. Colonization sequence influences selection and complementarity effects on biomass production in experimental algal microcosms. *Oikos* **116**:1748–1758.
- Zhang, Z. 2003. Mutualism or cooperation among competitors promotes coexistence and competitive ability. *Ecological Modelling* **164**:271 – 282.

Summary

Under some circumstances, the eventual population densities in a species community depend on the initial densities or the times at which species are introduced. If the timing of arrival determines the species composition, a priority effect has occurred. Priority effects may occur if the species community exhibits alternative stable states. Alternative stable states (and other forms of coexisting attractors) are in general caused by positive feedback of population density on the reproduction of individuals. This thesis studies four model communities of mostly plankton species that exhibit such positive feedback.

The first model is an abstract model in which two species either stimulate or inhibit, depending on population densities, the population growth of the own or the other species. An example of this situation is found in communities of plants that compete for scarce resources and at the same time ameliorate harsh conditions. In the model, a priority effect is more likely if the species compete more strongly with the own species than with the other species, or if they help the own species more than the other species (given that each species can establish a population when introduced at low density). The reachability of a community state may be limited by the density at which species are introduced during community assembly and on how often introductions occur.

The second model models the growth of light-limited phytoplankton populations that suffer from photoinhibition, meaning that their photosynthetic rate decreases with increasing light if light is strong. In a single population, photoinhibition may lead to alternative stable states where in one state the population is extinct, and another in which it survives. If several species grow together, there may be several alternative stable states, with at most one species at each state. Species that are less sensitive to photoinhibition may facilitate the establishment of those that are. However, sustained coexistence is not possible. Furthermore, if populations start off only at low density, the community species composition does not depend on the arrival times of species.

The third model is of a community of two zooplankton prey species competing for a single resource (food) and sharing a predator. One competitor interferes with the feeding of the other, but is more vulnerable to predation. Given the right trade-offs, a priority effect occurs if food supply is sufficient, and if predation pressure is not too strong.

The fourth model models a planktonic host-parasite system, where nutrient consumed by infected hosts is used for the reproduction of the parasite. Alternative stable states, where persistence of the parasite depends on a high enough initial density, arise if nutrient supply is sufficient and host loss rate not too high. Increasing nutrient supply and decreasing host loss rate lead to host-parasite cycles and extinction of the parasite through a deterministic Paradox of Enrichment.

In all these cases, the occurrence of alternative stable states and priority effects depends on environmental conditions such as resource supply and loss rates. One should realise however, that not all alternative stable states may be reachable if species communities are assembled with species starting off at low density only. If communities are assembled in this way, the number of alternative stable states that can be reached may be limited by the number of niches the environment harbours.

Samenvatting

Soms hangen de uiteindelijke populatiedichtheden in een soortengemeenschap af van de initiële dichtheden of van de tijdstippen waarop soorten worden geïntroduceerd. Als het tijdstip waarop een soort arriveert de soortensamenstelling van een gemeenschap bepaalt, heeft er een prioriteitseffect plaats gevonden. Prioriteitseffecten kunnen optreden als de soortengemeenschap alternatieve stabiele toestanden heeft. Alternatieve stabiele toestanden (en andere vormen van coëxisterende attractoren) worden in het algemeen veroorzaakt door positieve terugkoppeling van de populatiedichtheid op de reproductie van individuen. Dit proefschrift bestudeert vier modelgemeenschappen van met name planktonsoorten die zulke terugkoppeling vertonen.

Het eerste model is een abstract model waarin twee soorten hun eigen populatiegroei of de populatiegroei van de ander stimuleren of remmen, afhankelijk van hun populatiedichtheden. Een voorbeeld van een dergelijke situatie vindt men in gemeenschappen van planten die concurreren om schaarse hulpbronnen en tegelijkertijd moeilijke omstandigheden verzachten. In het model neemt de kans op een prioriteitseffect toe als de soorten meer met de eigen soort concurreren dan met de andere soort, of als ze de eigen soort meer helpen dan de andere soort (gegeven dat elke soort zich kan vestigen wanneer hij geïntroduceerd wordt in een lage dichtheid). De bereikbaarheid van een gemeenschapstoestand kan beperkt worden door de dichtheid en frequentie waarmee soorten worden geïntroduceerd tijdens de opbouw van een gemeenschap.

Het tweede model beschrijft de groei van licht-gelimiteerde fytoplanktonpopulaties die last hebben van fotoinhibitie, dat wil zeggen dat in sterk licht hun fotosynthesesnelheid afneemt met toenemende lichtsterkte. In een enkele populatie kan fotoinhibitie leiden tot alternatieve stabiele toestanden waarbij in één toestand de populatie is uitgestorven en in de andere toestand de populatie overleeft. Als er meerdere soorten zijn, kunnen er meerdere alternatieve stabiele toestanden zijn met op zijn hoogst één soort per toestand. Soorten die minder gevoelig zijn voor fotoinhibitie kunnen de vestiging van soorten die wel gevoelig zijn faciliteren. Duurzame coëxistentie is echter niet mogelijk. Verder is het zo dat als populaties alleen op een lage dichtheid beginnen, de soortensamenstelling van de gemeenschap niet afhangt van de tijdstippen waarop soorten aankomen.

Het derde model is van een gemeenschap van twee zoöplankton-prooi-soorten

die concurreren om een enkele hulpbron (voedsel) en die een gemeenschappelijke predator hebben. Één van de twee concurrenten hindert de ander bij het foerageren maar is kwetsbaarder voor predatie. Gegeven de juiste trade-offs, is er een prioriteitseffect als de toevoer van voedsel voldoende is en als predatiedruk niet te sterk is.

Het vierde model beschrijft een planktonisch gastheer-parasietsysteem waarbij door geïnfekteerde gastheren geconsumeerde nutriënten worden gebruikt voor de reproductie van de parasiet. Alternatieve stabiele toestanden, waarbij persistentie van de parasiet afhangt van een introductiedichtheid die hoog genoeg is, ontstaan als de nutriënttoevoer voldoende is en de verliezen van de gastheer niet te hoog zijn. Een toenemende nutriënttoevoer en afnemende verliezen van de gastheer leiden tot gastheer-parasiet cycli en uitsterven van de parasiet door een deterministische Paradox van de Verrijking.

In al deze gevallen hangt het optreden van alternatieve stabiele toestanden en prioriteitseffecten af van omgevingsfactoren zoals de toevoer van hulpbronnen en verliezen van organismen. Men moet zich er echter van bewust zijn dat niet alle alternatieve toestanden bereikbaar zijn als de opbouw van de gemeenschap uitsluitend plaats vindt door middel van introductie van soorten op lage dichtheid. Als de gemeenschapsopbouw op deze manier plaats vindt, wordt het aantal alternatieve stabiele toestanden dat bereikt kan worden wellicht beperkt door het aantal niches dat de omgeving herbergt.

About the author

The author of this thesis, Daan Gerla, was born May 31, 1977 in The Hague, The Netherlands. In The Hague, he attended Eerste Vrijzinnig Christelijk Lyceum, obtaining a Gymnasium diploma in 1996. From 1997 to 2001 he studied at the University of Amsterdam, obtaining a Bachelor degree in biology. From 2002 to 2006, Daan followed the Master curriculum General Biology at the same university, studying mainly topics in ecology and evolution. During this period, he participated in a research project on competition for light at the Aquatic Microbiology department of the University of Amsterdam and in a research project on experimental evolution of yeast populations at the Department of Genetics of the Wageningen University. After graduating *cum laude*, Daan was employed as a PhD candidate at the Netherlands Institute of Ecology, working in what later became the Department of Aquatic Ecology. The result of his work there lies before you. Currently, Daan is employed as a post-doctoral researcher at the Institute of Marine Resources and Ecosystem Studies, Wageningen UR.

Publications

Gerla D.J., A. Gsell, B.W. Kooi, B.W. Ibelings, E. van Donk, and W.M. Mooij. In press. Alternative states and population crashes in a resource-susceptible-infected model for planktonic parasites and hosts. *Freshwater biology*.

Gerla, D.J., W.M. Mooij, and J. Huisman. 2011. Photoinhibition and the assembly of light-limited phytoplankton. *Oikos* **120**:359-368.

Gerla, D.J., M. Vos, B.W. Kooi and W.M. Mooij. 2009. Effects of resources and predation on the predictability of community. *Oikos* **118**:1044-1052.

Wloch-Salamon, D.M., D. Gerla, R. F. Hoekstra and J.A.G.M. de Visser. 2008. Effect of dispersal and nutrient availability on the competitive ability of toxin-producing yeast. *Proceedings of the Royal Society B-Biological Sciences* **275**:535-541.

Stomp, M., J. Huisman, F. de Jongh, A.J. Veraart, D. Gerla, M. Rijkeboer, B.W. Ibelings, U.I.A. Wollenzien, and L.J. Stal. 2004. Adaptive divergence in pigment composition promotes phytoplankton biodiversity. *Nature* **432**:104-107.

Acknowledgements

This thesis has come about with contributions of several people who deserve special mention. First of all, my supervisor Wolf Mooij, for his guidance, encouragement and support. It has been great to have a supervisor who has been so readily available for help and advice. Ellen van Donk has had an important contribution by 'keeping me down to earth', among other things by suggesting a research topic founded in the biology of a well studied system (the host-parasite system of chapter 5). Also, Bob Kooi has had an invaluable contribution with his infectious enthusiasm for the mathematics of dynamical systems. Matthijs Vos important contributions include pointing out some consequences of the topics of my research within the 'bigger picture' of ecology.

Further gratitude goes to the members of the European Science Foundation project BIOPOOL, led by Luc de Meester, which my research was part of. The regular meetings with the participating researchers of this project were stimulating and fun as well.

Also stimulating was the environment at the institute where I conducted my research, the Netherlands Institute of Ecology, thanks to my colleagues there.

Last but not least I thank the reviewers and editors of the journals *Oikos* and *Freshwater Biology* for comments on draft versions of manuscripts submitted for publication in these journals, which serve as chapters in this thesis.